Self-Anchored Suspension Bridges

Part II:
Structural behaviour
&
Main span possibilities

David van Goolen
April 2007

Iv-Infra

TU Delft
Delft University of Technology

Self-Anchored Suspension Bridges

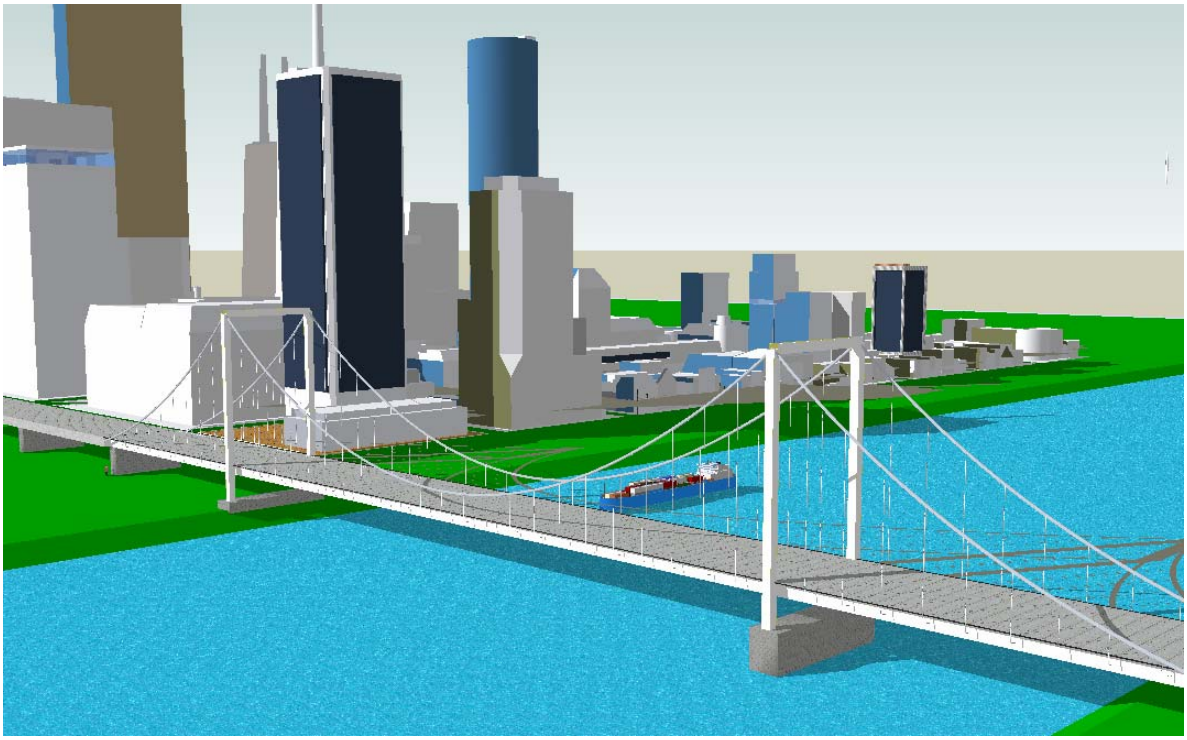

Project: **Master of Science Final Thesis**
Start date: **September 2006**
Document: **Part II**: **Main Study**

Name: **David van Goolen**
Student nr.: **1040596**

Civil Engineering & Geosciences
Delft University of Technology

Final Thesis Project

Topic:	Self-Anchored Suspension bridges	
Document:	Part II: Main study	
Name:	David van Goolen	
Student number:	1040596	
University:	Delft University of Technology	
	Faculty of Civil Engineering	
Examining board:	Prof. Ir. F.S.K. Bijlaard	Delft University of Technology
	Dr. A. Romeijn	Delft University of Technology
	Dr.ir. C. van der Veen	Delft University of Technology
	Ir. L.J.M. Houben	Delft University of Technology
	Ir. W.P.J. Langedijk	Engineering office Iv-Infra B.V.

Preface

The first phase of this final thesis project has been presented earlier by means of part I: literature survey captured in a report:
'Structural behaviour of self-anchored suspension bridges: Literature Survey

This partial document part II presents the second phase of this final thesis; the main study. In the main study the structural behaviour is researched. First part is a parameter study. Second part is increasing the span length and trying to find a limit. The third part is erection aspects of a self-anchored suspension bridge at Nijmegen.

I would like to express my gratitude to Engineering office Iv-Infra, they offered me the possibility to execute this study at their office and enabled me to fill in this study completely according to my personal interpretations. Iv-Infra gave me the opportunity to make use of their facilities and experience in bridge engineering. Especially I would like to thank my daily supervisor at Iv-Infra, Mr. Walter Langedijk for providing me information, help and guidance throughout the entire final thesis project. His experience helped me a lot with generating ideas and tackling this thesis project.
Further more I would like to thank the other examining board members for offering guidance, help and discussing the progress of my final thesis:

Prof. Ir. F.S.K. Bijlaard	Delft University of Technology
Dr. A. Romeijn	Delft University of Technology
Dr.ir. C. van der Veen	Delft University of Technology
Ir. L.J.M. Houben	Delft University of Technology

David van Goolen

Delft University of Technology
Faculty of Civil Engineering

Delft 2007

The Netherlands

Summary

Since 1870, only about 25 highway bridges have been executed as a self-anchored suspension bridge. The rise of the cable stayed bridge since 1955 made this suspension type an obsolete alternative for a long period of time. The largest existing main span for a self-anchored suspension bridge is 300 metres and dates from 1999. Main difficulties for this bridge type to reach spans over 300 metres can be blamed on erection problems and the buckling stability of the girder. Erecting the deck structure prior to the main cable makes this bridge technically and economically less attractive than for instance the cable stayed bridge.
A dimensional inventory has shown that the deck slenderness is limited to about $\lambda = 1/95$ and the sag ratio varies between 1/5-1/8. The deck slenderness is related to the required bending stiffness to have sufficient resistance against buckling. Also the relatively high sag ratios, compared to conventional suspension bridges, are mainly chosen to reduce the normal force in the deck that is imposed by the main cable.
A parameter study into the structural behaviour has revealed that the most important bridge parameters are the bending stiffness EI_{deck} of the deck and the axial stiffness $EA_{main\ cable}$ of the main cable. A well chosen ratio between the EI_{deck} and $EA_{main\ cable}$ influences the maximum bending moments and the deflections in the girder. In the pre-design process of a suspension bridge type it is favourable to consider:

-A slender stiffening girder, to reduce the maximum bending moment in the girder
-A stiff main cable, to increase the global stiffness of the bridge and to reduce the maximum bending moment in the girder
-A high sag to span ratio, to reduce the normal force in the deck and the maximum bending moment in the deck.

A study to the static strength, stiffness, frequency behaviour and the buckling stability of the box girder, revealed that a deck slenderness of the box girder of $\lambda = 1/100$ and even more slender is very well feasible.
Exploring the main span possibilities of this bridge type, this study has shown that a span length of 500 metres is very well possible and even beyond that. The on before hand expected limitation on the global buckling stability of the girder has turned out to be feasible. With an increasing main span the buckling phenomena does become more critical but still of acceptable level.
A difference is visible in buckling of the main span and the side span. The upward buckling mode of the side span is decisive over the downward buckling mode of the main span. But at least up to 500 metres a deck slenderness of $\lambda = 1/100$ and beyond that is very well possible regarding all important design criteria.
The most limiting factor for the self-anchored suspension bridge, to reach a large main span and apply a very slender deck, is the erection stage. The number of temporary supports in the main span determines a decisive stress condition for erecting the deck. Erecting with temporary stays is an option but remains a laborious method.
It is almost inevitable that for the erection stage some significant provisions have to be made in the cross section of the deck regarding the shear and bending conditions or else a much less slender deck should be applied.

So it has been shown that it is structural feasible to reach more competitive main span lengths up to at least 500 metres but that the erection stage can determine decisive conditions for designing the deck.

Introduction

The total research of this M.Sc. study is presented in two parts to fulfil the requirements of the degree of Master of Science obtained at Delft University, faculty of Civil Engineering.
This document presents part II; the main study of my final thesis project. The objective of part II is to research the structural behaviour of a self-anchored suspension bridge. A reference model is designed and used to investigate the influence of the main bridge parameters on the structural behaviour of a self-anchored suspension bridge.
The first chapter presents the basic assumptions that are made to design a reference model for the self-anchored suspension bridge. This reference design is modelled in a FEM-program to investigate and calculate the force distribution and deformations.
Chapter 2 gives the verification of the reference design on the main design criteria like static strength, stiffness and the buckling stability of the girder.
First results are given of a parameter study in chapter 3. The results of the parameter study are used to determine an optimization of the reference design.
Chapter 4 explores and explains the effects of an increasing span length of a self-anchored suspension bridge all important design aspects.

Table of contents

1 Reference design

To be able to research a bridge behaviour, by change of the main bridge parameters, a reference model is made first. For this reference model the main characteristics of a self-anchored suspension bridge are captured. This part will explain the basic assumption for this model, determination of the main bridge structural components like stiffening girder, main cable, hangers and pylon. Also a description is given of the method of FE-modelling of the bridge structure..

1.1 Basic assumptions

This part gives the basic assumptions that are made for the pre-design process in this research.

1.1.1 City bridge of Nijmegen

In November 2006, the city council of Nijmegen asked for a feasibility study for a suspension bridge to cross the river Waal. This feasibility study should at least include cost estimation, risk analyses, esthetical aspects, technical and economical considerations and is contracted out to the engineering office Iv-Infra. This report intends to cover a part of this total study, namely technical conditions of a self-anchored suspension bridge but with a general approach. Figure 1 gives an overview of the new trace of the new city bridge in Nijmegen city.

Figure 1 Trace city bridge Nijmegen

The total width of the river and river banks is succeeding 1000 metres. The width of the river is an average of 325 metres, see Figure 2.

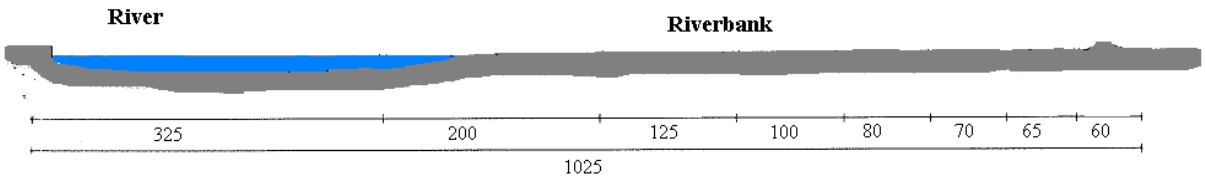

Figure 2 Cross section Waal river near Nijmegen

As explained before this report focuses on the structural behaviour and exploring the span possibilities of a self-anchored suspension bridge. The most important design demands for this city bridge are incorporated for the research under consideration. In that way the results

of this MSc study can be used and interpreted for the city bridge of Nijmegen and also for self-anchored suspension bridges in general.
Most important design criteria are:

- Vertical navigation clearance underneath the bridge deck is 9.10 metres
- Horizontal navigation clearance is 265 metres
- Traffic on the bridge consists of:
  - Local highway traffic with a design speed of 70 km/h
  - public transport like busses
  - bicycles
  - pedestrians
- Highway traffic lanes 2*2. And future expansion to 2*3 lanes
- Bicycles and pedestrian lanes in both ways and physically separated from the highway traffic.
- Design life of the bridge is 100 years.

The number of lanes and type of traffic is determining the loading scheme and the severity of the loads. It also determines the required deck width. This will be explained later on.
The horizontally required clearance determines the smallest free span length. This design aspect will be used in the exploration of the span possibilities, and will be dealt with further on in this report.
Figure 3 shows a simplification of the situation[1] at the Waal in Nijmegen. From that given situation a level of the bridge deck is chosen of 15 meters above ground level.

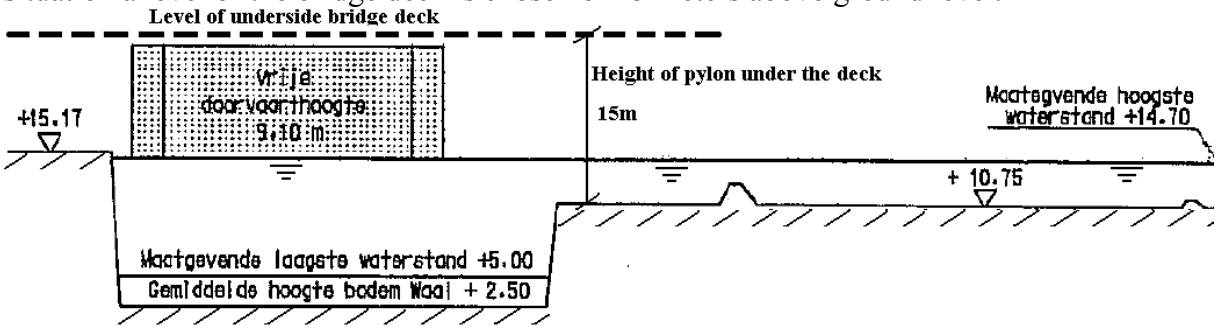

Figure 3 Situation at Waal River

1.1.2 Stiffening girder

Type of girder
For the deck, a steel box girder is used. The box will have a certain width w, height h and thicknesses of web t_w and flanges t_f, see Figure 4

Figure 4 Box girder with equivalent flange thicknesses to account for longitudinal stiffeners

[1] Design criteria of City bridge Nijmegen, June 2006.

In reality a box girder contains more structural details like:

- Longitudinal stiffeners:
  Are needed on the flanges and on the webs. They are required to improve the stability of the relatively thin steel plates to prevent local buckling of the plate elements. Besides that the longitudinal stiffeners are required to transfer and resist the concentrated wheel loading on the deck.
- Transverse stiffeners:
  Are located at intermediate cross frames to improve the cross section against torsion and distortion and to support the longitudinal stiffeners of the deck.
- Cross beams:
  The cross beams support the longitudinal stiffeners and reduce the span length of these stiffeners. The combination of the deck and longitudinal stiffeners act as a beam under bending between two cross beams.
- Cross bracings/frames/diaphragms:
  Prevent the cross section to distort and are designed to resist wind loads, to brace the compression flanges and distribute vertical self weight and live loads.

Only the first detail, longitudinal stiffeners, will be taken into account in the modelling of the box girder because only these elements contribute to the bending stiffness of the cross section.

System for stiffening girder
As for the largest built self-anchored suspension bridges like the Konohana and Yeong Grand bridge, see literature survey §2.6, a continuous stiffening girder is chosen for the reference model in this research. No hinges at the pylon or at mid span are therefore applied. A system without hinges is in general more stiff than a system with one or more hinges. To achieve the largest span possible, a system should be chosen with the best stiffness behaviour: a continuous stiffening girder.

Material
For the structural elements like the deck and pylon, a steel grade S355 is used in this research which has the following properties:

Yield strength $f_y = 355$ N/mm^2
Modulus of elasticity $E = 210000$ N/mm^2

Plate thicknesses
The longitudinal stiffeners on the deck plate and bottom flange of the box girder contribute to the bending stiffness of the cross section, but not seriously to the torsional stiffness and shear resistance of the cross section. The longitudinal stiffeners of the top flange, bottom flange and the web are taken into consideration by assuming them as part of the area of the flange and web. So an equivalent plate thickness will be used including the area of those stiffeners. The following designation is used is this research:

t_{plate} : for plate thickness which does not include required plate area for longitudinal stiffeners.
$t_{eq\ plate}$: for equivalent plate thicknesses including the area for longitudinal stiffeners.

For instance for the calculation of shear stresses and effective width of the cross section, the net plate thickness t_{plate} is used.

For the minimum required plate thicknesses the NEN-EN 1993-2:2003 part c1.2.2 states:

Deck plate thickness in the carriageway $t \geq 16$ for an asphalt layer > 40 mm.
Thickness of stiffeners: $t_{stiff} \geq 6$ mm.

Furthermore it is stated in the NEN-EN 1993-2:2003 that the minimal required plate thicknesses for deck plates and stiffeners are:

Table C.1: Dimensions of bridge deck with longitudinal stiffeners

	open section stiffeners	hollow section stiffeners
thickness of deck plate t_D	$t_D \geq 14$ mm	$t_D \geq 14$ mm
spacing e_{LS} between stiffeners	$e_{LS} \sim 400$ mm	$600 \text{ mm} \leq e_{LS} \leq 900$ mm
edge distance e_E of first stiffener	$e_E \geq e_{LS}$	$e_E \geq e_{LS}$
spacing of cross beams e_{crossb}	$e_{crossb} \leq 2700$ mm	$2500 \text{ mm} \leq e_{crossb} \leq 3500$ mm
ratio of depth of stiffener to depth of crossbeam h_{stiff}/h_{crossb}	$h_{stiff}/h_{crossb} \leq 0,5$	$h_{stiff}/h_{crossb} \leq 0,4$
plate thickness t_{stiff}	$t_{stiff} \geq 10$ mm	$6 \text{ mm} \leq t_{stiff} \leq 10$ mm
plate thickness of web of cross beam $t_{w,crossb}$	$t_{w,crossb} \geq 10$ mm	$10 \text{ mm} \leq t_{w,crossb} \leq 20$ mm
plate thickness of flange of cross beam $t_{f,crossb}$	$t_{f,crossb} \geq 10$ mm	$t_{f,crossb} \geq 10$ mm

So with an assumed asphalt layer of 50 mm the following minimum required plate thicknesses are used:

$t_{\text{flange top}} \geq 16$ mm
$t_{\text{flange bottom}} \geq 10$ mm
$t_{\text{web, crossbeam}} \geq 10$ mm
$t_{\text{stiffeners}} \geq 6$ mm

To account for the required longitudinal stiffeners, the area of the stiffeners A_{stiff} is estimated[2] by a percentage of the area A_{flange} of the flanges and web A_{web}:

$A_{\text{stiff. top flange}} = 65\% * A_{\text{top flange}}$
$A_{\text{stiff . bottom flange}} = 35\% * A_{\text{bottom flange}}$
$A_{\text{stiff. web}} = 15\ \% * A_{\text{web}}$

These ratio are determined from an existing box girder applied in a recent suspension bridge, see Appendix 6 Design orthotropic steel box of the New Carquinez Bridge.
It clearly shows that the top compression flange needs much more stiffeners for it has to account for local buckling effects and to be able to resist the local wheel loading of the traffic. For the bottom flange less it is visible that less stiffeners are applied because no local wheel loading can occur on this flange. These findings are correspond to the expectation that the deck plate requires more stiffeners than the bottom flange and the estimated percentages will be used from now on to determine the area for longitudinal stiffeners.
The area of the longitudinal stiffeners of web and flanges are taken into account as an additional thickness to the web and flanges, called $t_{equivalent}$. So:

$t_{\text{eq. flange top}} = 1.65 * t_{\text{flange top}} = 1.65 * 16 = 26.4$ mm
$t_{\text{eq. flange bottom}} = 1.35 * t_{\text{flange bottom}} = 1.35 * 10 = 13.5$ mm
$t_{\text{eq. web}} = 1.15 * t_{\text{web}} = 1.15 * 10 = 11.5$ mm

For ease of calculation a simple ratio between thickness of top- and bottom flange is chosen:

$t_{\text{flange top}} = 2 * t_{\text{flange bottom}}$

[2] This estimation is retreived from a similar box girder of the same dimensions: Thimmardy.E. et.al., *New Carquinez bridge. North America's Newest suspension bridge*. Steel bridge 2004 Millau.

For a conservative approach, the following equivalent plate thicknesses are chosen:
Chosen equivalent thicknesses are :

$t_{\text{eq. flange top}}$ =40 mm
$t_{\text{eq. flange bottom}}$ =20 mm
$t_{\text{eq. web}}$ =15 mm

Cross section classification

The Eurocode NEN-EN-1993-1-1 distincts several classifications for steel cross sections. A box girder, with dimensions given in this research, is likely to be classified as class 3 or 4 on which the Eurocode states a definition:

> -Class 3 cross-sections are those in which the stress in the extreme compression fibre of the steel member assuming an elastic distribution of stresses can reach the yield strength, but local buckling is liable to prevent development of the plastic moment resistance.
> -Class 4 cross-sections are those in which local buckling will occur before the attainment of yield stress in one or more parts of the cross-section.

Classification 4 is not applicable because the flanges and webs of box girder are locally stabilized by longitudinal stiffeners. The box girder is assumed to have a cross section classification 3.
So assumed is that the normal force in box girder is resisted by the total area of the cross section, no effective cross section is taken into account for the normal force.

Bearing system of girder

The bearing system of the stiffening girder should ensure vertical, horizontal (transverse and longitudinal) fixation. For simplification of the bearing system no temperature influence is considered because it is assumed that the extra provisions needed for temperature influence does not influence the considered aspects of the global structural behaviour of the bridge in this research scope. Therefore a simple symmetrical bearing system is chosen. The total bearing system consists of several slide- and fixed bearings.
In transverse direction all bearings are horizontally fixed. In longitudinal direction only one pair is horizontally fixed, the rest allows for horizontal movement. The deck is horizontally fixed at one of the pylons, as is generally[3] done for suspension bridges.
In vertical direction all bearings are fixed. Next figure shows a scheme of the bearing system.

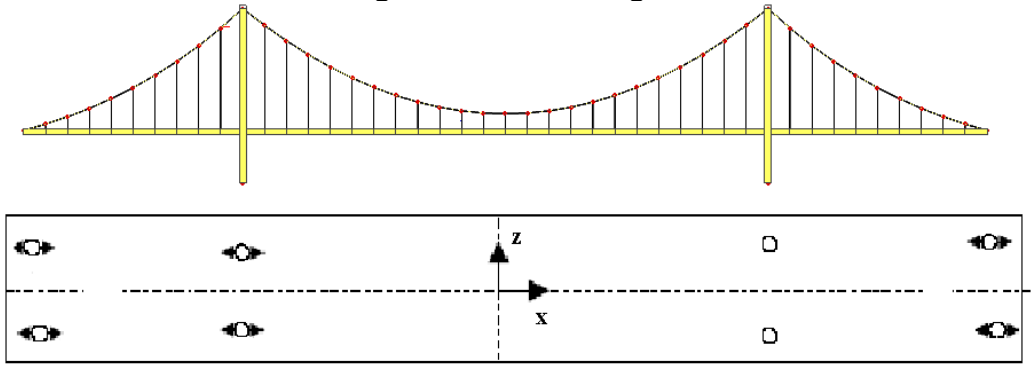

Figure 5 Bearing system

[3] Gimsing, N.J., *Cable supported Bridges*, Wiley&Sons, 1998

Deck width
The deck width is depending on the required number of traffic lanes for the city bridge of Nijmegen. This bridge has to accommodate:

- 2*2 traffic lanes. And a future expansion for 2*3 traffic lanes
- Pedestrian and bicycle lanes

The Dutch ROA (guidelines design highways) states the following requirements for clearances and width of lanes:

	Vo = 120 km/h	Vo 90 km/h
a. Lane	3,5	3,25
b. dividing line	0,15	0,15
c. side line	0,2	0,2
d. safety strip	0,6	0,3
e. hard shoulder	3,25	3,25
l. side strip	0,5	0,5
m. object distance	1,5	1

Figure 6 Width of lanes [m]

Applying this, results in a total deck width of 35.6 metres.

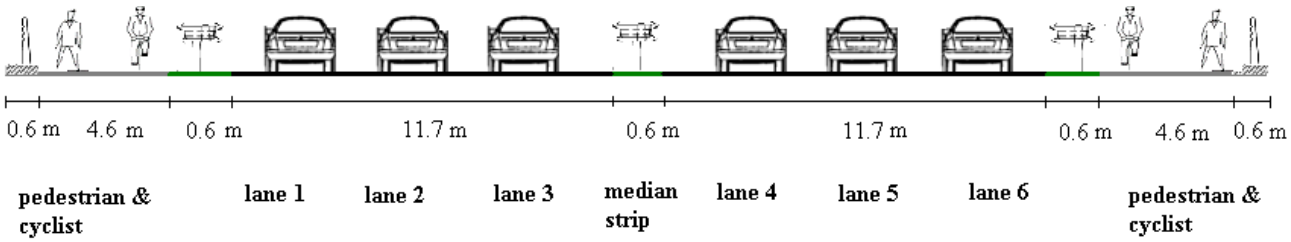

Figure 7 Total deck width

For the deck system, a square box girder is chosen and the width is chosen according the required deck width as shown in Figure 7. In this case a width of 35.6 metres is required.

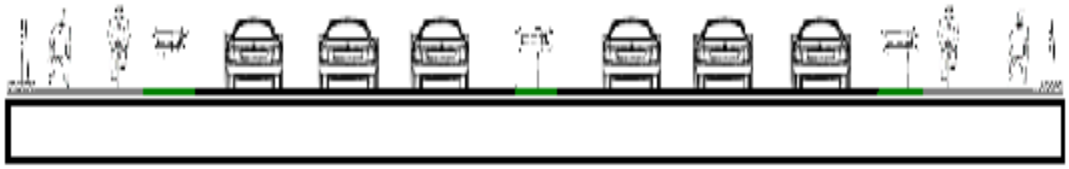

Figure 8 Box girder

In reality a box girder would have a shape similar to that of in Figure 9. In here the webs are placed inclined for aero dynamical reasons. Assuming a square box girder, like in Figure 8, is a valid procedure regarding the mechanical properties like axial, bending and torsional stiffness.

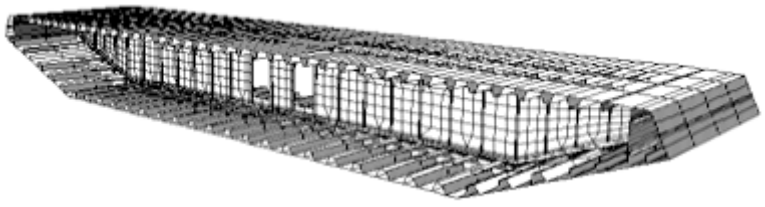

Figure 9 Box girder shape

1.1.3 Loading scheme

For analysing the structural behaviour and exploring the span possibilities only the main loadings are taken into account. These are vertical loadings such as:

- Permanent loading
  - Self weight (according to EN-1991-1-1:2002)
    $\gamma_{steel} = 78.5\ kN/m^3$
  - Asphalt layer of 40 mm
    $\gamma_{hot\ rolled\ asphalt} = 23\ kN/m^3$
    Assumed application of hot rolled asphalt, the permanent load caused by asphalt load is: $0.040 * 23 = 0.92\ kN/m^2$.
- Variable loading
  - Traffic loading uniform distributed (highway traffic, pedestrian, bicycles)
  - Traffic loading concentrated axle loads

According to NEN-EN 1991-3 load model 1 is used to define the vertical loads of traffic. The next table defines the concentrated loads and the uniform distributed loads.

Location	Tandem system	UDL system
	Axle loads Q_{ik} (kN)	q_{ik} (or q_{rk}) (kN/m^2)
Lane Number 1	300	9
Lane Number 2	200	2,5
Lane Number 3	100	2,5
Other lanes	0	2,5
Remaining area (q_{rk})	0	2,5

Table 1 Concentrated and uniform distributed loads

The given values for Q_{ik} and q_{rk} include a dynamic amplification. For pedestrian and cycle actions the density of the uniformly distributed load is: $q_{fk} = 5\ kN/m^2$
This value for pedestrian load is conservative because NEN-EN-1991-3 part 5.3.2 states that a reduced value can be applied for bridges with individuals exceeding 10 metres.

Furthermore NEN-EN 1991-3 part 4.3.2 states that:

> No more than one tandem system should be used considered per lane; only complete tandem system shall be considered.

In Figure 10 the total loading scheme is illustrated for the complete width of the girder. The load model shown in Figure 10 represents the situation to be used for the design of the bridge components like main cable, hangers, girder and pylon. This because the largest reaction forces exist for the cable plane.

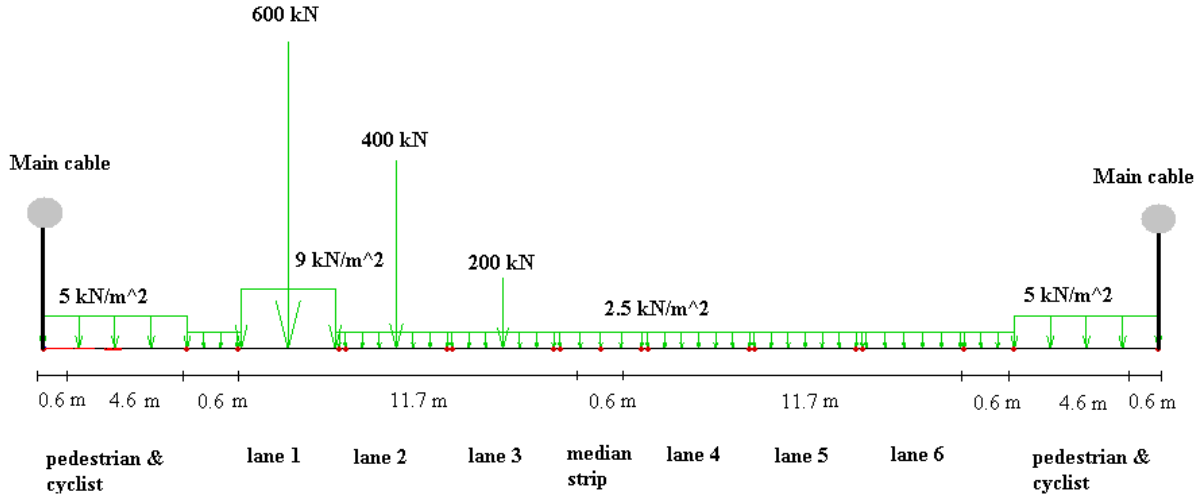

Figure 10 Traffic loading scheme in transverse direction of the deck

1.1.4 Dimensions

A span length of 150 metres is chosen as a starting point for the so called reference model. With this chosen main span of 150 metres it is possible to investigate later on the influence of an increasing span length to about 500 metres on the mechanical properties of the stiffening girder. Based on the literature survey, see the appendix of the literature survey, on self-anchored suspension bridges, a few dimensional ratio's are kept fixed:

- Main span to side span = 2.4
- Main span to hanger distance = 24

Other ratio's like girder slenderness, and sag to span ratio are part of the research and which will be varied.
The required vertical clearance of 9.10 metres remains fixed. So the pylon height under the deck remains fixed on 15 metres.

1.1.5 Cable configuration

For the configuration of the main cable, a parabolic shape is chosen. In reality a cable has a catenary shape when it is loaded by its self weight. The catenary shape is well approximated with a parabolic line. Therefore a parabolic shape is assumed for the main cable in main- and side span.

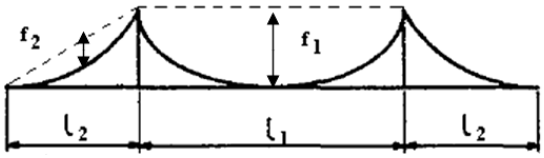

Figure 11 Parabolic shape cable

The sag of the cable in the mid of the side span f_2 is determined by[4]: $f_2 = f_1 * \frac{l_2^{\,2}}{l_1^{\,2}}$

The literature study has shown that that sag of the main span varies between 1/5 to 1/8 of the main span.
Furthermore a vertical hanger configuration is chosen. Until now, only one self-anchored suspension bridge has been built with inclined hangers in the longitudinal direction of the bridge. So a vertical configuration is considered more as standard design.
Longitudinal inclined hangers have some advantages and disadvantages. The global stiffness of the bridge is increased but more problem are expected with respect to erection of the bridge and fatigue in the hangers.

1.1.6 Pylon frame

The pylon frame can have different appearances. Similar to the cable stayed- and conventional suspension bridges, H- and A- frames can be used in self-anchored suspension bridges. In this research not much attention goes out to the design of a pylon frame, so a standard H-frame is chosen with a steel box cross section. In that way the relevant mechanical properties as bending- and axial stiffness can be assigned easily.

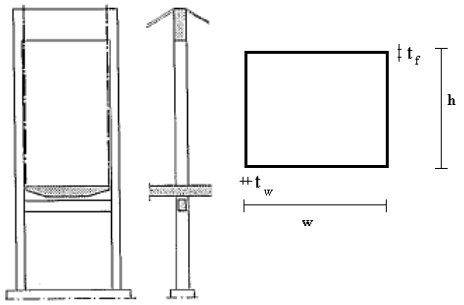

Figure 12 H- frame pylon Figure 13 Cross section pylon

[4] Ulstrup, C., *Rating and preliminary analysis of suspension bridges*. Journal of structural engineering, Vol. 119, No.9. September 1993.

1.1.7 Self weight

A suspension bridge is modelled according to its final desired geometry under self weight. In many cases the main cable is given a pretension so that under dead load the bridge adopt it final desired shape.
So the ideal FE model[5] of a suspension bridge should represent this situation that on application of the self weight load, the geometry of the bridge does not deviate from the desired final shape of the bridge.
Furthermore, a general assumption in suspension bridge design is to have a reduced global bending moment to about zero under self weight loading. This means that one wants to achieve that the self weight load is completely supported by the main cable. This can be approximately achieved by manipulating the initial tensile force in de the main cable. The initial tensile force in the main cable can be found by trial and error until a situation is created with minimum deck deflection and minimum bending stresses caused by the global bending moment in the stiffening girder.
In the FEM program this initial tensile force on the main cable is done by applying a temperature load that causes the cable to become shorter which is just a modelling tool to apply a pretension on a structural member. Figure 14 shows the deflection due to self weight only (deflection in mm). When the main cable is given a certain amount of pretensioning (determined iteratively), the deflection of the girder is reduced to nearly zero, see Figure 15.

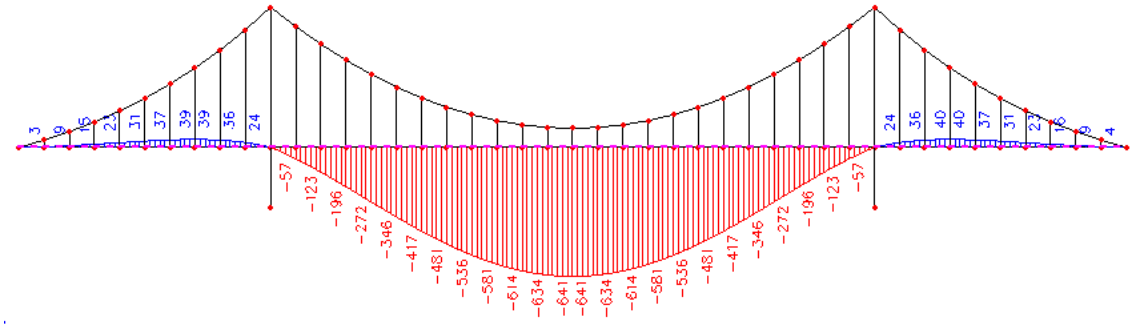

δ_{max} = 641 mm

Figure 14 Deflection of girder [mm] due to self weight only

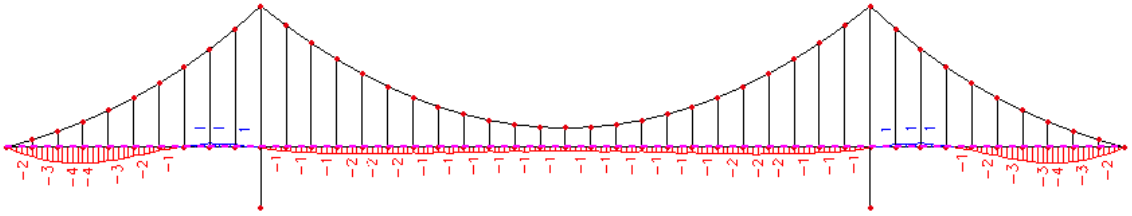

δ_{max} = 1 mm

Figure 15 Deflection of girder [mm] due to self weight after pretensioning the main cable

Also the bending moments reduce to nearly zero. Figure 16 shows the bending moment distribution due to self weight only and Figure 17 shows the bending moments after pretensioning of the main cable. Figure 17 clearly shows the reduced global bending moment to zero and the resulting small local bending moment between the hangers.

[5] Ren, *W. Roebling suspension bridge. 1:Finite element model and free vibration response*, Journal of bridge engineering, March/April 2004, pp 110-118.

Because the global bending moment is reduced to nearly zero, the assumption that the bending stresses in the girder are almost reduced to zero under self weight loading, is hereby verified.

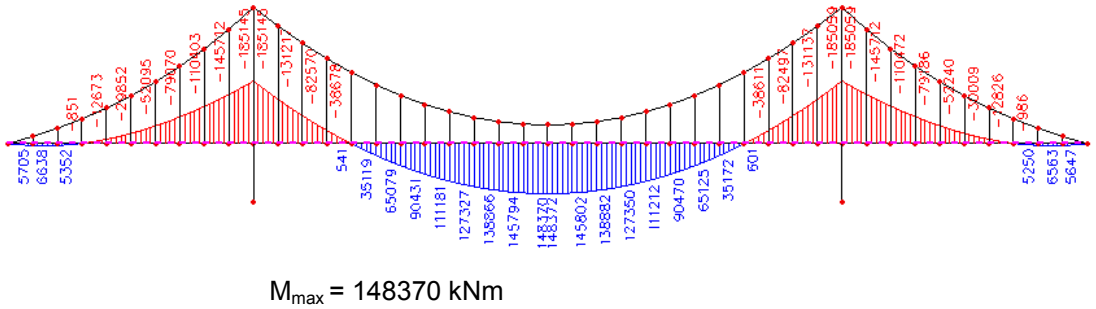

M_{max} = 148370 kNm

Figure 16 Global bending moments [kNm] in girder due to self weight

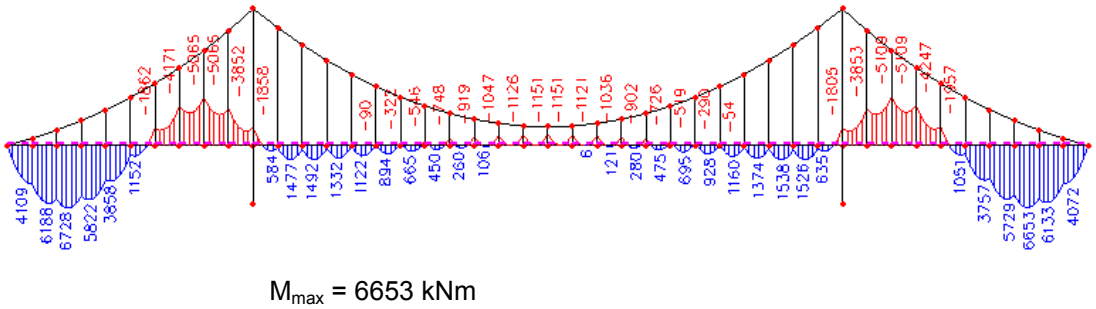

M_{max} = 6653 kNm

Figure 17 Bending moments [kNm] in girder due to self weight after pretensioning main cable

1.2 Three dimensional modelling

For modelling the bridge, the FEM program SCIA ESA-PT 6.0.185 version is used. Such a program enables the designer to model a structure and to apply certain loads and loading combinations from which the effects like member forces and deflections can be calculated. There are several ways to model a structure, depending on the type of structure and design phase. Structures and parts of structures can be modelled with beam-, plate-, solid and cable elements, etcetera. With beam elements the model is built up with one dimensional line elements. Plate elements are two dimensional and solid elements are three dimensional elements.

With respect to the scope of this research, the bridge will be modelled with beam elements. This enables to model the total bridge structure and calculate member forces due to certain load cases and combinations.

The scope of the model is to be able to analyse the model statically and dynamically in a three dimensional way and to be able to analyze the effects of symmetric and asymmetric loading statically. Also an assessment will be made with respect to the geometric non linear effects of a cable supported bridge, the so-called second order effects.

Figure 18 shows the FE-model of the bridge which will be used for this study.

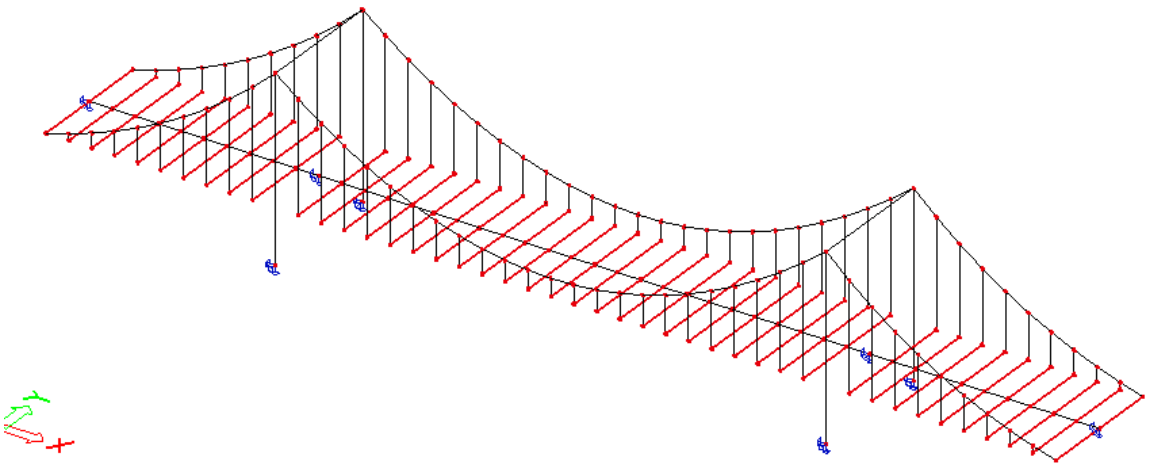

Figure 18 Model with beam elements

Pylon

The pylon is modelled as a simple portal frame. The cross section consists of a steel box. At the basement the pylon is rotational fixed to provide for longitudinal stiffness to structure. The pylon is loaded by an axial compression force and a bending moment due to horizontal force on the pylon caused by the tensile force in the main cables.

The pylon is fixed supported in transverse and longitudinal direction of the bridge. For ease of modelling, the deck, represented by the stiffening girder, is vertically supported on the 'outside world' at the pylon. One rotation fixed support creates the effect of two supports on the stiffening girder. More detailed information is given further on in this paragraph which explains the modelling of the stiffening girder.

Modelling the pylon and bridge deck this way, cancels out any influence of the girder support on the pylon. This is assumed to be negligible.

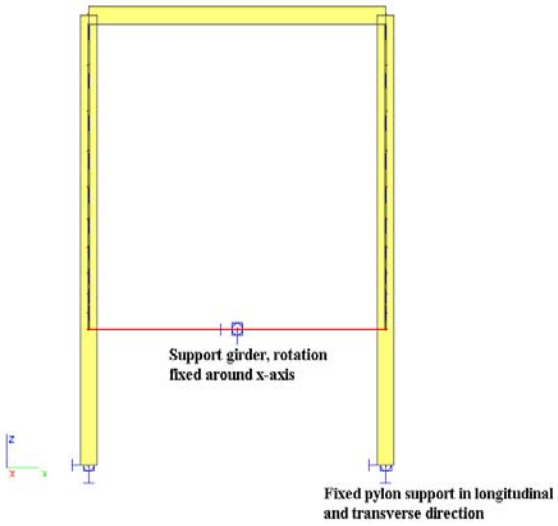

Figure 19 Pylon frame

Main cable

Two different ways of modelling the main cable and hangers have been explored: cable elements, and hinged truss elements (like a chain where every link is hinged connected). See appendix 1 for the differences between these types of models for the main cable structure. Based on the findings that no significant differences on mechanical behaviour for the two alternatives where visible, one method to model the main cable is used from now on; modelling with cable elements.

The main cable is modelled with cable elements. These are beam elements with a very low bending stiffness. Also no shear forces exist for the cable. The cable element is subjected to its own weight and accounts for the slackening effects in cables under self weight load.

An example is given to illustrate the effect of a cable element. Figure 20 shows on the top a beam element with a certain span, on the bottom a cable element with the same span and mechanical properties and self weight loading. The cable element displays a larger deformation.

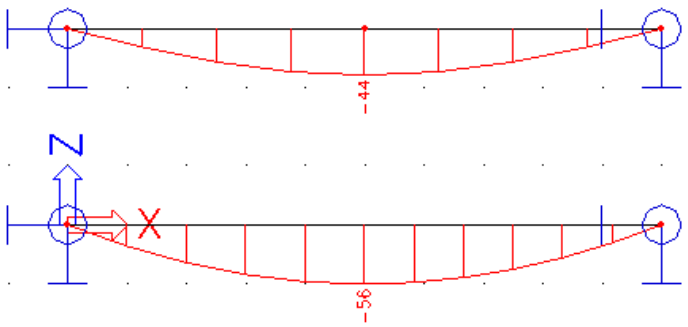

Beam element

Cable element

Figure 20 Deformation beam- and cable element

Another effect of a cable element which can be distinguished, is that the slack causes a tension in the cable and therefore a horizontal reaction on the supports.

For modelling the cable, an equivalent modulus of elasticity has to be used to account for elastic stretch and lengthening of the cable due to geometry change. These two effects reduce the modulus of elasticity. The equivalent modulus of elasticity can be determined using the formulae developed by H.J. Ernst. Euro code EN-19931-11 states for the effective modulus of elasticity:

$$E_t = \frac{E}{1 + \frac{w^2 l^2 E}{12\sigma^3}}$$

in which

E	is the modulus of elasticity of the cable
w	is the unit weight
l	is the horizontal span of the cable
σ	is the stress in the cable due to self weight and permanent loading

Due to the relative small center to center distance of the hangers, the effect of elastic stretch and lengthening due to change of geometry can be neglected. The cable spans a very short distance between each hanger. So in this research the modulus of elasticity for the different cable types is equal to the given modulus of elasticity for the several available cable systems, see Figure 21.

	High strength tension component	E_Q [kN/mm²]	
		steel wires	stainless steel wires
1	Spiral strand ropes	150 ± 10	130 ± 10
2	Full locked coil ropes	160 ± 10	–
3	Strand wire ropes with CWR	100 ± 10	90 ± 10
4	Strand wire ropes with CF	80 ± 10	–
5	Bundle of parallel wires	205 ± 5	–
6	Bundle of parallel strands	195 ± 5	–

Figure 21 Modulus of elasticity of cable types

For the reference model a bundle of parallel wires is chosen on the first hand.

Cable type

For the reference design the same cable type is chosen for the main cable as well as for the hangers. A cable fabricated with a bundle of parallel strands has the largest modulus of elasticity compared to other cable types and is therefore chosen. And also for increasing span lengths it becomes impossible to apply prefabricated locked coil.

Stiffening girder
A single beam element is used to model the stiffening girder. In that way the mechanical properties can easily be adopted. The girder is located in the middle of the two cable planes and is connected to hangers by means of 'rigid arms'.
A rigid arm is a connection between nodes with infinite stiffness which transfers all deformations from one node to the other node.
An example is given in Figure 22 to illustrate the behaviour of a rigid arm. A simple model is given of two horizontal beams that are connected with a vertical rigid arm. The top beam is simply supported and the bottom beam in unsupported and connected with a rigid arm to the top beam. The top beam is loaded with two load cases; a concentrated load and a torque at mid span. For both situations it is shown that the rigid arm transfers the deformation to the lower beam.

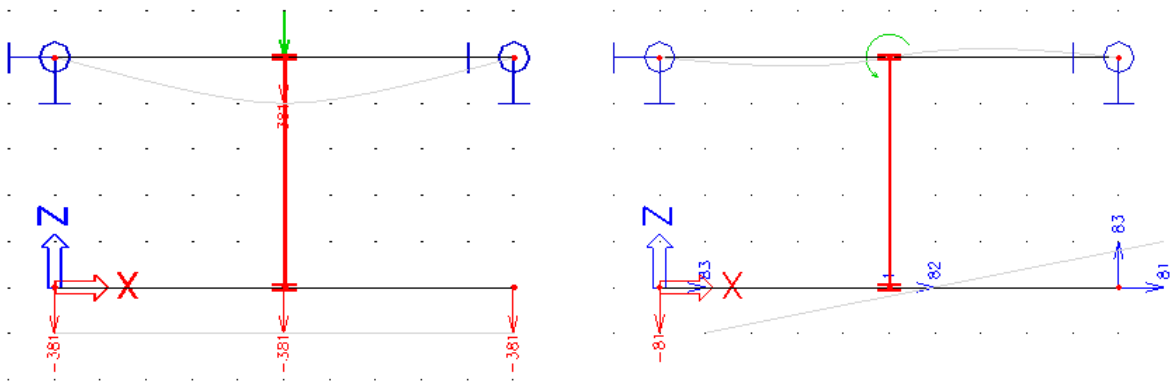

Figure 22 Rigid arm

On the left side is illustrated that the concentrated nodal force deflects the top beam and the bottom beam follows the same vertical translation. On the right side the beam is loaded with a bending moment causing the top beam to bend as illustrated. The unsupported bottom beam follows this deflection by means of a rotation and translation.

So the rigid connection between the cable plane and the stiffening girder transfers the deformation of the cable and hangers to the stiffening girder. For the analyses of the required mechanical properties of the stiffening girder, reference is made to Figure 18 in which application of rigid arms is visible.

Supports
Along the length of the bridge, the girder is vertically supported on four locations: end supports and at the pylons. All the supports are vertically fixed and also rotation fixed around the longitudinal direction of the bridge deck to create a support reaction similar to a system of two supports.
The stiffening girder is vertically supported on bearings at the pylon. The cross section of the pylon will be a simple square box section. In that the mechanical properties can be easily assigned in the model.

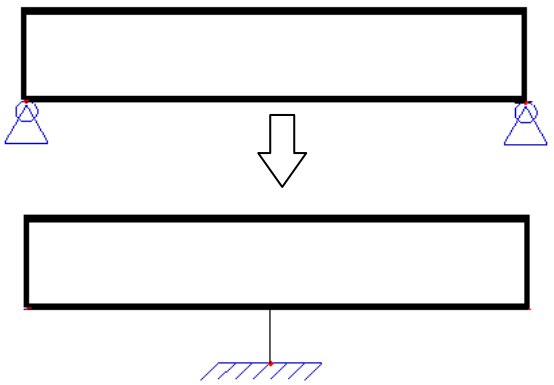

Figure 23 Modelling support of stiffening girder at pylon

Loads
To apply the before mentioned traffic loads in the model, it is translated to a resulting line load which acts as a distributed line load along the longitudinal direction of the stiffening girder. Because of the asymmetry of the traffic loads, the resulting line load has a certain eccentricity to the gravity centre of the box girder and a value of $q_{res,traffic}$ = 131.5 kN/m based on the information given in Figure 10, see also . Figure 24

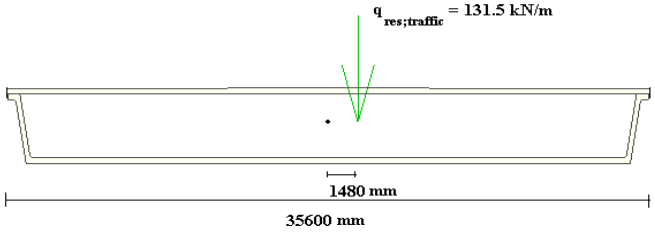

Load	Area
q_{fk} = 5 kN/m^2	Pedestrian and cyclist area
q_{rk1} = 9 kN/m^2	Lane 1
q_{rk} = 2,5 kN/m^2	Other lanes and remaining area
131,5 kN/m^1	Resulting Line load

Figure 24 Resulting line load on box girder from distributed traffic load

Also the axle three loads are reduced to a resulting concentrated load F_{res} = 600 + 400 + 200 = 1200 kN with an eccentricity of 7.7metres. For pre-design reasons the concentrated loads are left out of consideration because there global influence is not significant. For local design of the orthotropic deck it becomes important to consider these local loading conditions for design of longitudinal and transverse stiffeners.

1.3 Dimensioning

This part makes a first estimation of the required dimensions for the main bridge parts; girder, pylon, main cable and hangers.

1.3.1 Design stress

Transverse stresses
For the stress verification a distinction should be made between the upper and lower flange. The lower flange is loaded only in length longitudinal direction of the bridge and consists of normal stresses caused by bending moments and axial forces. The upper flange is extra loaded due to local traffic loading. This means there exists a number of stresses longitudinal as well as in transverse direction. According to annex E of the Eurocode NEN-EN-1993-2 the following combination needs to be taken into account.

E.1 Combination rule for global and local load effects

(1) When considering the local strength of stiffeners of orthotropic decks effects from local wheel and tyre loads acting on the stiffener and from global traffic loads acting on the bridge should be taken into account, see Figure E.1.

(2) To take account the different sources of these loads the following combination rule may be applied to determine the design values:

$$\sigma_{Ed} = \sigma_{loc,d} + \psi\sigma_{glob,d} \quad (E.1)$$

$$\sigma_{Ed} = \psi\sigma_{loc,d} + \sigma_{glob,d} \quad (E.2)$$

where σ_d design value of stress in the stringer due to combined effects of local load σ_{loc} and global load σ_{glob}

$\sigma_{loc,d}$ design value of stress in the stringer due to local wheel or tyre load from a single heavy vehicle

$\sigma_{glob,d}$ design value of stress in the stringer due to bridge loads comprising one or more heavy verhicles

ψ combination factor

In which the combination factor $\psi = 0.7$ for main span over 40 metres or determined on the basis of the weight distributions of several lorries.

In this study the calculation of stress is limited to an assessment of the global stresses. Because the local stresses caused by wheel loading on the deck have to be taken into account, a certain design stress level is chosen for the global stresses.

To account for longitudinal-, transverse stresses and fatigue, which is most of times the governing design aspect on detail level, a design stress level of 200 N/mm^2 is assumed for the structural steel used for the girder. This design stress level is used for determining the required cross section of the structural members in the bridge. This design value for the stress is used for determination of cross sections under static actions. Although a fatigue assessment is still necessary, it is left out of consideration in this research.

Stress distribution

The stress distribution is assumed to develop linearly over web of the cross section with a maximum stress in the outer fibres of the cross section.

The normal stresses are caused by two components; the normal stresses caused by a normal force and the normal stresses caused by a bending moment. These two components can be superposed to determine the total normal stress that acts in the outer fibres. This maximum normal stress (caused by the design value of the normal force and bending moment) may not exceed the design value of the yield strength f_y.

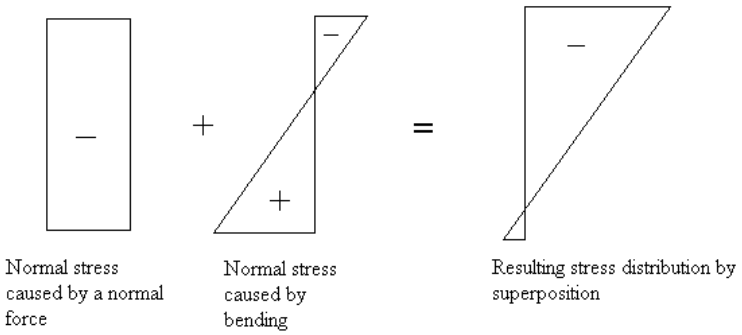

Figure 25 Superposition of linear stress distribution over the web of the cross section

The bending stress distribution over the top and bottom flanges will be calculated according to the effective width method in which a reduced cross section is determined, A_{eff}. The normal stresses can be linearly distributed over this reduced area of the cross section of the top and bottom flanges, see Figure 26. The effective width be is determined according the Euro code.

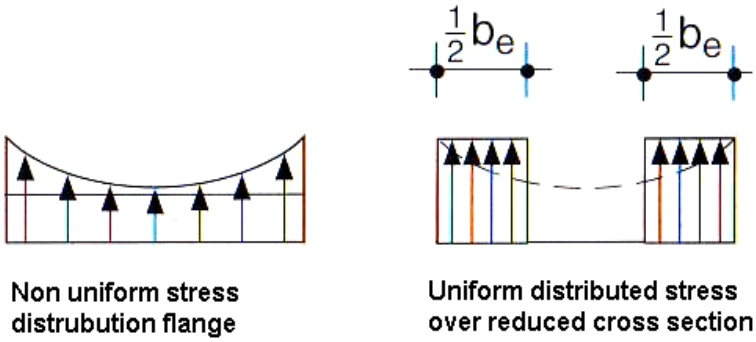

Figure 26 Distribution stresses in flanges

So the stress distribution over the cross section of the box girder is:

-Normal force in the deck N_{Ed} A total

-Bending moments in the deck $M_{y,Ed}$ A effective

1.3.2 Estimation by hand calculation

Stiffening girder

The bending stiffness EI of the girder is one of the most important design factor. For the first estimation of the dimension of the cross section of the box girder an average height slenderness is chosen 1/70 * main span (based on data given in the literature survey of this research). So the box girder height is: 1/70 * 150 = 2.1 metres

The girder is chosen to be of a continuous type which means that there are no hinges in the girder.

Used plate thickness in for instance the girder of the Konohana bridge varied between 12-20 mm.

Chosen equivalent thicknesses for the reference model in this research (so including an additional needed area for the application of longitudinal stiffeners on deck plate and bottom flange) are as mentioned earlier, see §1.1.2:

$t_{eq.\ flange\ top}$ =40 mm

$t_{eq.\ flange\ bottom}$ =20 mm

$t_{eq.\ web}$ =15 mm

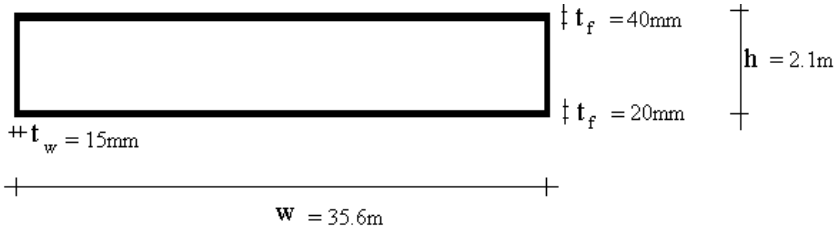

Figure 27 Cross section box girder

The mechanical properties of the box girder with these characteristics are given in Table 2.

Table 2 Mechanical properties stiffening girder

A totaal	2.2 m^2
I_y	2.12 m^4
I_z	245 m^4
I_t *	5.33 m^4
Self weight	173 kN/m

* = The St. Venant torsional constant I_t is based on a cross section with the area of longitudinal stiffeners excluded. Because the longitudinal stiffeners have a negligible contribution to the torsional stiffness of a cross section.

Compared to the applied box girder in for instance the Jiang Yin suspension bridge[6] the presented mechanical properties in Table 2 have realistic values, see Figure 28 for the mechanical properties of this stiffening girder.

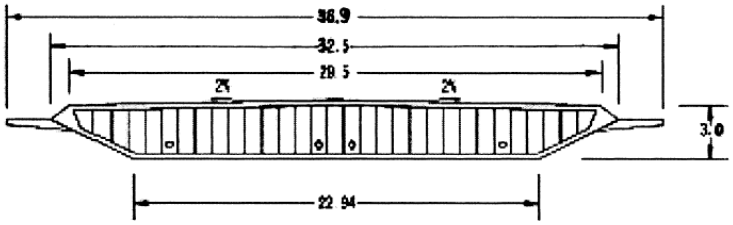

Section geometrical and material feature of the main member[a]

Substructures	J_d (m⁴)	I_2(m⁴)	I_3(m⁴)	m (t/m)	E (MPa)	γ
Steel box girder	4.82	93.32	1.844	18.0	210,000.0	0.3

Figure 28 Mechanical properties box girder Jiang Yin bridge

In the Appendix 4 Comparable box girders some more results on comparable bridge decks are presented.

Cable

The main properties are expressed in the modulus of elasticity for different existing cable types. Together with the cross sectional area A of the cable, these two properties determine the axial stiffness EA of the cable.

An approximation of the cross section is determined by the largest normal force in the cable. The horizontal component of the tension H in the cable, is constant along the main cable. In the mid of the main span, only the H is acting in the cable because the cable is horizontal on this location. The largest tensile force in cable acts directly on the side span side of the pylon: the cable on this location has the largest angle with the horizontal. See Figure 29.

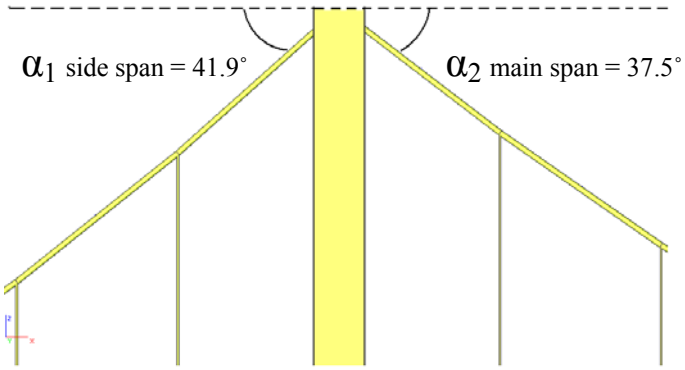

Figure 29 Angle of main cable in side and main span

The horizontal component H on location is the same and also a vertical component V acts in the cable. The largest normal force N_{cable} in cable is therefore determined by :

$N_{cable} = \sqrt{H^2 + V^2}$ and

$H = \frac{q_{G+Q} * l^2}{8 * f_1}$ in which

q_{G+Q} = uniformly distributed load

G = permanent load

[6] Cheng, J. et. al., Nonlinear aerostatic stability analysis of Jiang Yin suspension bridge. Engineering structures 24, 2002, pp 773-78.

Q = variable load
l = length of the main span
f_l = sag of the cable in main span

For the first approximation of the dimension of the cable the fatigue strength criterion is used.

- Fatigue strength criterium

$$\Delta\sigma_{per} = \frac{N_q}{A} = \frac{N_q N_g}{A N_g} = \frac{N_q}{N_g}\sigma_g$$

And so,

$$\sigma_g = \left(\frac{q}{g}\right)^{-1} \Delta\sigma_{per}, \text{ because } \left[\frac{N_q}{N_g} = \frac{q}{g}\right]$$

The following steps are taken to determine the cable dimensions:

1. analyzing $\eta = q/g$
2. assuming a maximum level of Δs
3. finding the maximum stress caused by self-weight + permanent loading
4. analyzing a cable diameter based on results step (3).

η = ratio between variable load and self weight.
q = variable load
g = self weight of the structure + permanent loading

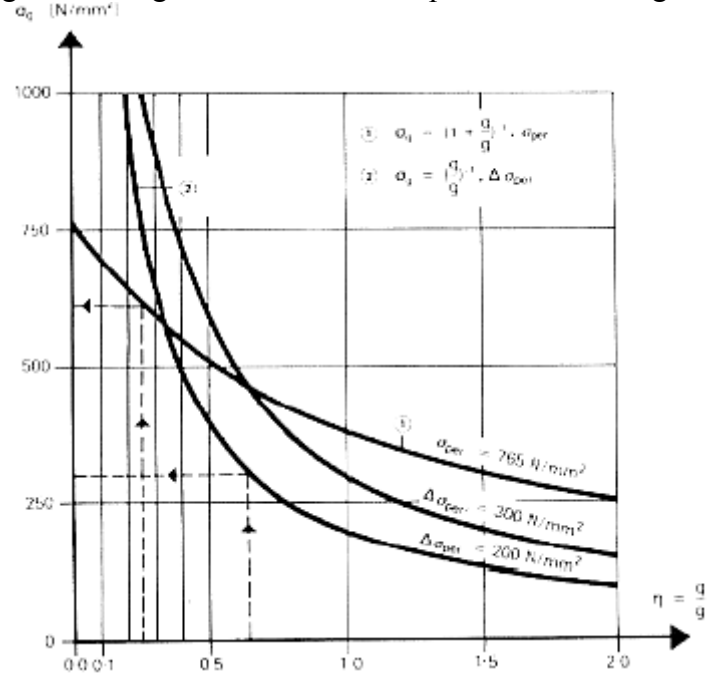

Figure 30 Allowable cable stress

1:
According to NEN-EN 1991-3 part 4.6.2, in fatigue load model 1 the following values for the axle loads Q_{ik} and uniformly distributed loads q_{ik} have to be used:

$0.7 * Q_{ik}$
$0.3 * q_{ik}$

But the contribution of the concentrated axle force of 1200 kN is due to the length of the bridge relatively small and therefore not included in this pre-design. Also the influence of the

variable load Q_{ik} is very small for the main cable, the hangers are more sensitive for these loadings.

Variable load q =	0.3 *131.5 kN/m	traffic load
Self weight g =	173 kN/m	box girder
	6 kN/m	estimation cable weight, diameter d = 300mm
	32.8 kN/m	asphalt layer of 40mm

Ratio $\eta = \frac{0.3*131.5}{173+6+32.8} = 0.19$

2:
Maximum level of $\Delta\sigma = 200$ N/mm^2 is assumed, see Figure 30.

3:
Maximum allowable stress caused by self weight and permanent loading σ_g is approximately $\sigma_g = 600$ N/mm^2. (determined by use of the design graph in Figure 30)

4:
Total permanent load design value $G_d = \gamma_G * (173 + 6 + 32.8) = 1.35 * 211.8 = 285.9$ kN/m
Design value of the horizontal component of tension in the cable

$$H_{d,G} = \frac{q_G * l^2}{8 * f_1} = \frac{285.9 * 150^2}{8 * 30} = 26803\,\text{kN}$$, so per cable acts 13402 kN

Maximum design value of the axial tension force in the main cable

$$N_{d,G,cable} = \sqrt{H_{d,G}{}^2 + V_{d,G}{}^2} = \sqrt{H_{d,G}{}^2 + (\tan\alpha_1 * H_{d,G})^2} = 18006\,\text{kN}$$

The required effective area is therefore $A_{effective;required} = \frac{N_{d,G}}{\sigma_g} = 30000\,\text{mm}^2$

The effective required diameter of the cable is therefore: $d_{\text{cable required}} = 200$ mm (leaving the fill factor of the cable out of consideration). To be a bit conservative an effective diameter $d_{\text{cable}} = 240$ mm is chosen.

Hangers
The hanger distance is 6.25 metres. To determine the required cross section, it is assumed that the self weight and permanent load of the girder is uniformly distributed over the hangers. So each hanger carries 6.25 metres of the girder. As the hangers are more sensitive for the variable axle loading Q_{ik}, a distribution of 50 percent in each hangers is assumed for pre-design estimation.
The following steps are taken to determine the hanger dimensions:
1:
In fatigue load model 1 the values for the axle loads 0.7 * Q_{ik} and uniformly distributed loads 0.7 * q_{ik} are used:

Variable load q =	0.3*131.5	kN/m	traffic load
Q=	0.7*1200	kN	axle loads
Self weight g =	173	kN/m	box girder
	6	kN/m	estimation cable weight, with d = 200mm
	32.8	kN/m	asphalt

Ratio $\eta = \frac{0.3*131.5 + (0.7*0.5*1200)/6.25}{173+6+32.8} = 0.51$

2:
Maximum level of $\Delta\sigma = 200$ N/mm^2 is assumed

3:
Maximum allowable stress caused by self weight and permanent loading σ_g is approximately $\sigma_g = 350$ N/mm^2. (determined by use of the design graph in Figure 30)

4:
Total permanent load design value $G_d = \gamma_G * (173 + 6 + 32.8) = 1.35 * 211.8 = 285.9$ kN/m
Design value of the vertical force in the hanger
$N_{d,G,hanger} = 6.25 * 285.9 = 1787$ kN per two hangers, so that is 894 kN per hanger

$$A_{effective;required} = \frac{N_{d,G}}{\sigma_g} = 2556 \text{ mm}^2$$

The required diameter of the hanger is therefore: $d_{\text{hanger required}} = 51$mm (leaving the fill factor of the cable out of consideration). To be a bit conservative a diameter of the hanger of $d_{hanger} = 55$ mm is chosen.

pylon:
The pylon should have an axial stiffness and a bending stiffness because it is loaded with a large axial compression force caused by the vertical tension component of the main cable And also a bending moment, caused by a horizontal deflection of the pylon, can act in the pylon with a maximum at the base.

$$H_{d,G+Q} = \frac{q_{G+Q} * l^2}{8 * f_1} = \frac{(1.35 * 211.8 + 1.5 * 131.5) * 150^2}{8 * 30} = 45298 \text{ kN}$$, so that is 22649 kN per cable.
The normal force in the pylon is therefore:

$$N_{d,G+Q,pylon} = \tan\alpha_1 * H_{d,G+Q} + \tan\alpha_2 * H_{d,G+Q} = 37700 \text{ kN}$$
With an assumed design yield strength of $\sigma_d = 200$ N/mm^2, the minimum required cross section of the pylon is:

$$A_{required,pylon} = \frac{N_{d,G+Q,pylon}}{\sigma_d} = 188505 \text{ mm}^2$$. To account for a possible additional bending moment, a cross section of 300000 mm^2 is chosen.

A minimum plate thickness is assumed of $t_{pylon} = 25$ mm.
The pylon is represented by a square cross section and mechanical properties are:

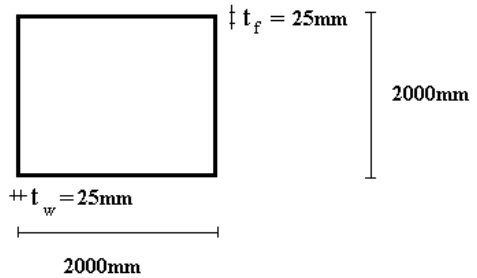

A_{total}	0,3 m^2
I_y	0,45 m^4
I_z	0,45 m^4

Figure 31 Schematization of cross section of the pylon

This approach makes it easy to assign certain mechanical properties to the pylon and keeping in mind that the same mechanical requirements can be achieved by a totally different cross section, for instance with much more higher plate thickness and other dimensions. So the emphasis lies on the mechanical requirements of the pylon and not the geometric properties.

1.3.3 Final dimensions reference model

Loading cases

- To determine the final dimensions of the structural components, the governing loading conditions for strength and stiffness need to be determined. Several cross sections are considered and the governing loading conditions for each cross will be determined. For pre-design, only symmetric loading cases are considered where the traffic loading is centrally positioned on the deck.

The three symmetrical load cases are considered:

- Load case 1: traffic load over full length

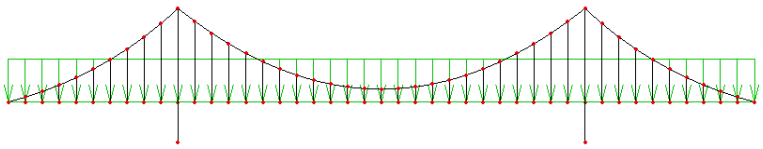

Figure 32 Load case 1

- Load case 2: traffic load over mid span

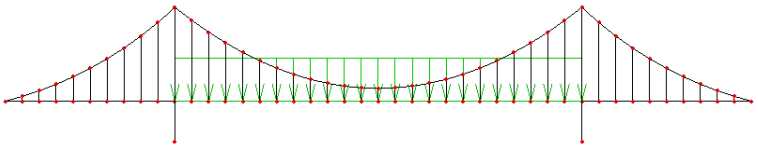

Figure 33 Load case 2

- Load case 3: traffic load over side span

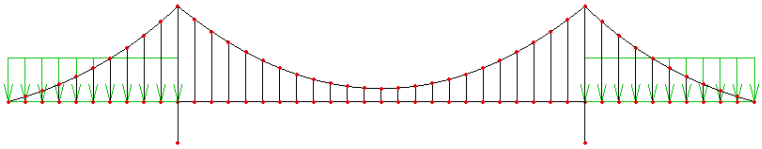

Figure 34 Load case 3

- Several asymmetric traffic load cases will be discussed in §3.5, here an evaluation is given of the consequences of asymmetric loading of the bridge. In case of asymmetric loading, traffic load is eccentrically positioned on the deck, see Figure 24.

These load cases represent the different traffic conditions and will be combined with the self weight of the bridge, permanent loading like asphalt layer, and the pretensioning of the main cable.
Because of the little influence of the axle load on the global behaviour, these are left out of consideration. The load is symmetrically applied, without eccentricity as a line load along the length of the stiffening girder.

Governing cross section for static strength and stiffness
The three considered load cases have three different effects for the moment distribution and deflections along the length of the bridge. Later on four cross section of the girder are verified on the stresses if they meet the static strength criteria. Those four cross sections are:

1. End support
2. Mid of side span
3. Support at pylon
4. Mid of main span

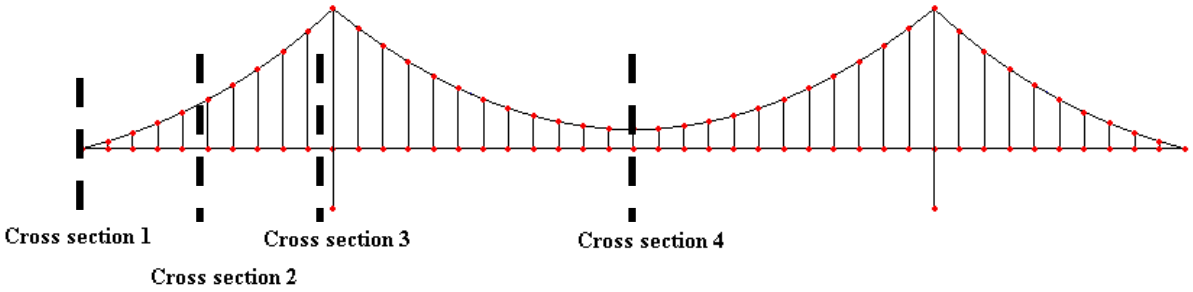

Figure 35 Considered cross section 1-4

In the next figure an illustration is given of the moment distribution caused by the three different traffic load cases and due to self weight of the bridge including pretension of the main cable as explained in §1.1.7.

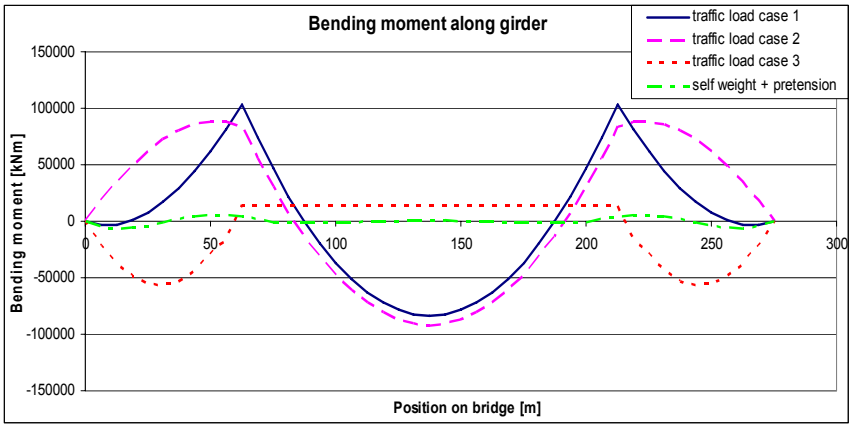

Figure 36 Bending moment along the deck

The following can be said about the bending moment distribution:
- Cross section 1 End support: The bending moment in the end support is zero, only the normal force determines the level of stress in this cross section.

- Cross section 2 Mid of main span: Load case 2 traffic over the mid span is governing for stress distribution in this cross section.

- Cross section 3 Support at pylon: Load case 1 traffic over the entire length of the bridge is governing for this cross section and causes the largest bending moment along the length of the bridge at the support location. Figure 36 shows that the hogging moment at the support location of the girder near the pylon is quite large. In practice this kind of local problems at supports can be solved by:

- Local application of additional plate thicknesses to reduce the stresses under the design stress level.
- Adjustment of the internal forces by movement of the supports. For statically undetermined systems, the load distribution due to traffic loading and therefore the

stress distribution can be greatly affected by a displacement of the intermediate or end supports.

- Cross section 4 Mid of main span: Load case 2 traffic over the mid span is governing for the stress distribution in this cross section.

For the deflection of the girder clearly shows that load case 2 causes the largest deflection at the mid of the main span. Load case 3, traffic load on side spans, gives an upward deflection of the girder. So when the stiffness criteria are checked, the deflection of the main span has to be within a specified limit.

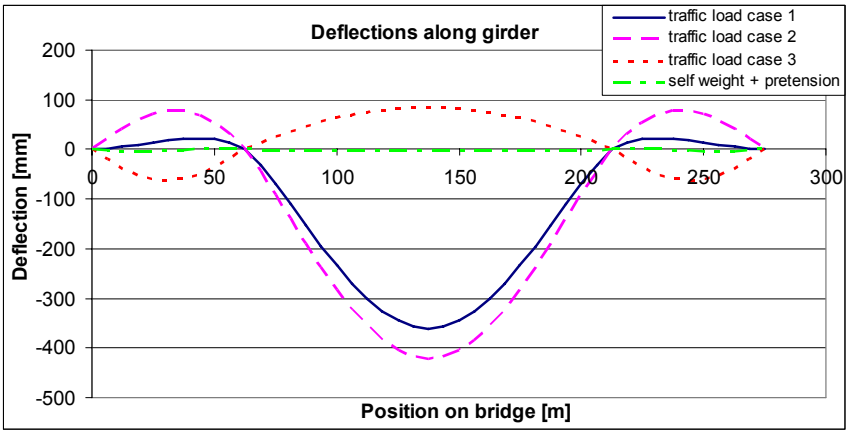

Figure 37 Deflections along the deck

Stress distribution
From the previous figures it can easily be seen that the longitudinal stresses caused by bending and axial force in girder at pylon support location, are decisive. For ease of designing only one cross section is considered, namely the mid of the main span. Designing for the stress conditions at this location, determines the cross section to be used along the whole length of the girder.

Reference design
For the mid of the main span, a maximum allowable design stress of 200 N/mm^2 is chosen for pre design purposes. After a hand calculation of several bridge components, the bridge dimensions and mechanical properties for the reference design are presented in Tabel 3.

Tabel 3 Dimensions reference design

Girder	t_flange_top_eq	40	mm
	t_flange_bottom_eq	20	mm
	t_web_eq	15	mm
	heigth	2100	mm
	width	35600	mm
Main cable	diameter	160	mm
Hangers	diameter	55	mm
Pylon	width	2000	mm
	depth	2000	mm
	total height	50000	mm

This reference model will be checked on the design criteria like; static strength, stiffness, stability, and frequency behaviour. See Figure 38 for the final dimensions of the reference model for the research that is described in this report.

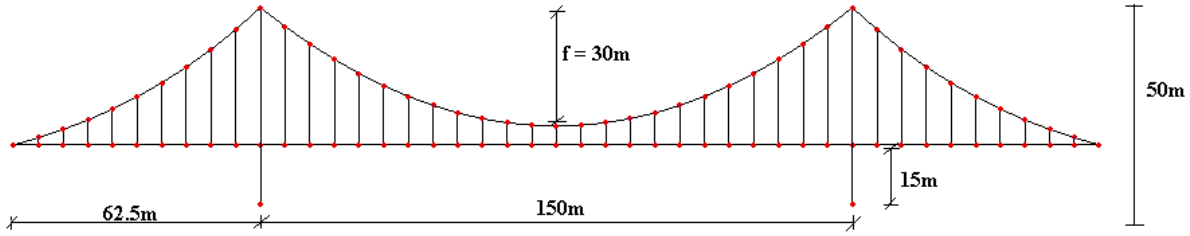

Figure 38 Final dimensions reference design

2 Verification of reference design

The reference design has to meet certain design criteria according to the Eurocode. This chapter explains the method for the verification of the reference design on static strength, stiffness and stability. Secondly the reference is verified according to the described method. Verification on stresses, deformation and stability of the reference is given in this chapter.

2.1 Method for verification on static strength, stiffness and stability

The design should be verified on certain criteria to satisfy on static strength as well as fatigue strength, stiffness and stability. A verification of the design according to the Eurocode will be made. This part explains the method for checking the design for the mentioned criteria like strength, stiffness and stability. Also an assessment has to be done for the frequency behaviour of the bridge. Fatigue strength is not considered in this M.Sc. study because it is assumed that this will not govern the global design of bridge.

2.1.1 Static strength (ULS)

When checking the design on static strength, the level of stresses may not exceed certain material related design values. Stresses are caused by normal forces, bending moments and a combination of these two. Shear forces will be left out of scope because these will not govern the global design. According to the Euro code, strength criteria have to be checked in the ultimate limit state (ULS).
The level of stresses will be checked in the decisive cross section of the:

- Pylon combination of bending moment and normal force
- Girder combination of bending moment and normal force
- Cable only a normal force
- Hanger only a normal force

Design values
According to the Eurocode the following design values for the yield strength of the steel themselves can be used.

Table 3.1: Nominal values of yield strength f_y and ultimate tensile strength f_u for hot rolled structural steel

Standard and steel grade	Nominal thickness of the element t [mm]			
	$t \leq 40$ mm		40 mm $< t \leq 80$ mm	
	f_y [N/mm^2]	f_u [N/mm^2]	f_y [N/mm^2]	f_u [N/mm^2]
EN 10025-2				
S 235	235	360	215	360
S 275	275	430	255	410
S 355	355	510	335	470
S 450	440	550	410	550

Figure 39 Design values steel

For this research the rather standard steel grade S355 is used.
For the main cable and hangers different steel grades can be used, so called high strength steel. The nominal tensile strength for steel round wires is 1770 N/mm^2.

–	steel wires	round wires:	nominal tensile grade:	1770 N/mm²
		Z-wires:	nominal tensile grade:	1570 N/mm²
–	stainless steel wires:	round wires:	nominal tensile grade:	1450 N/mm²

In the ULS, design values have to be applied for the permanent and variable actions that act on the structure. According to the Eurocode EN-1990 the following partial load factors for determining the design values are used:

For self weight and permanent loading: $\gamma_{Gj,sup} = 1.35$
For variable loading: $\gamma_{Qi} = 1.5$

Effective width and shear lag
In the elementary beam theory the longitudinal normal stresses induced in the flanges are assumed to be uniformly distributed across the flange width. In case of wide flanges this assumption is not correct. The stresses in wide flanges are non-uniformly distributed due to shear deformation of the flange plates. This phenomenon is called shear lag.

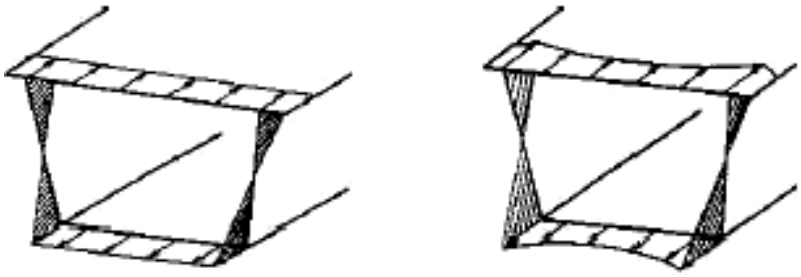

Figure 40 Left: stress distribution without shear deformation. Right: Stress distribution with shear deformation

When checking the stress level of the girder, the effect of shear lag should be taken into account (shear lag in the pylon will not be considered).
Eurocode NEN-EN 1993-1-5 part 3.1 states that shear lag effects in the flanges may be neglected when it satisfies:

$b_0 < L_e/20$ for ultimate limit state
in which b_0 is the deck width and L_e is the length between points of zero bending moments

In this case the deck width of the box girder is 35.6 metres and the main span of the reference model is 150 metres, so this criterion will never be satisfied. So shear lag effects in the flanges of the box girder can not be neglected.
For the pylon the effective width effect with respect to shear lag is neglected and left out of consideration.
The governing cross section depends on the effective width along the girder, the loading conditions and the combination of normal force and bending.

Three cross sections (table 3.1 NEN-EN 1993-1-5) will be checked:

-sagging moment of main span	β1
-sagging moment of side span	β1
-hogging moment at support pylon	β2
-end support	β0

The effective width for each cross section is:

$$b_{eff} = \beta * b_0$$

β is β_1, β_2 or β_0 depending on the considered cross section. β is called the effective width factor and is determined according to table 3.1:

So for the top and bottom flange, an effective width is determined for several cross sections (mid of the side span, at support location at pylon, mid of the main span). In combination with the acting normal stresses this will result in a governing cross section of the stiffening girder which has to satisfy certain unity check on strength.

Table 3.1: Effective[s] width factor β

κ	location for verification	β – value
$\kappa \le 0{,}02$		$\beta = 1{,}0$
$0{,}02 < \kappa \le 0{,}70$	sagging bending	$\beta = \beta_1 = \frac{1}{1 + 6{,}4\ \kappa^2}$
	hogging bending	$\beta = \beta_2 = \frac{1}{1 + 6{,}0\left(\kappa - \frac{1}{2500\ \kappa}\right) + 1{,}6\ \kappa^2}$
$> 0{,}70$	sagging bending	$\beta = \beta_1 = \frac{1}{5{,}9\ \kappa}$
	hogging bending	$\beta = \beta_2 = \frac{1}{8{,}6\ \kappa}$
all κ	end support	$\beta_0 = (0{,}55 + 0{,}025 / \kappa)\ \beta_1$, but $\beta_0 < \beta_1$
all κ	cantilever	$\beta = \beta_2$ at support and at the end
$\kappa = \alpha_0\ b_0 / L_e$ with $\alpha_0 = \sqrt{1 + \frac{A_{sl}}{b_0 t}}$		
in which A_{sl} is the area of all longitudinal stiffeners within the width b_0 and other symbols are as defined in Figure 3.1 and Figure 3.2.		

Regarding the resistance of the normal force in the deck N_{Ed}, the total area of the box girder will contribute to this. So no effective width assessment is needed for the resistance of the normal force in the deck

Verification

According tot NEN-EN-1993-1-1 in the ULS the strength verification in the box girder should satisfy the following criteria:

For class 3 cross sections:

In absence of shear force, for class 3 cross –sections the maximum longitudinal stress shall satisfy the criterion:

$$\sigma_{Ed} \le \frac{f_y}{\gamma_{M0}}$$

According to EN-1993-1-11 part 6 for cables, in the ULS, it shall be verified that:

$$\frac{F_{Ed}}{F_{Rd}} \le 1$$

2.1.2 Stiffness (SLS)

The serviceability limit state concerns the functioning of the structure, comfort of people and the appearance of the construction works. Stiffness criteria are expressed in certain deformation tolerances.

- Vertical allowable deflection of girder.
- Horizontal allowable deformation of pylon.

Besides the criteria on displacements, also criteria exist on passenger comfort which are expressed in limitations for vertical acceleration. This criteria is assumed to satisfy for medium span bridges considered in this M.Sc. study.

Further on the following maximum deflection are assumed:

- maximum vertical deflection of $1/350 * L_{main\ span}$ for the stiffening girder

- maximum horizontal deflection of $1/300*L_{pylon}$ for the pylon

No particular deflections limits could be found in the Eurocode, therefore the following maximum deflections are assumed[7] according to the bridge design of the Kanne self-anchored suspension bridge.
So the vertical deflection of the mid of the main span may not exceed
1/350 * 150 = 0.43 m
The horizontal displacement of the pylon may not exceed
1/300 * 49.75 = 0.17 m

Design values SLS
Stiffness criteria are checked in the serviceability limit state (SLS) The partial factors for determining the design value of the actions in SLS are equal to 1.

2.1.3 Stability (ULS)

Second order analyses (stability)
A second order analyses is performed because in cable supported structures geometrical non linearity can be of importance. In general long span bridges such as cable stayed- and suspension bridges exhibits geometric non linearity due to:

- The combination of axial compression forces and bending moments that act in the stiffening girder and the pylon.
- The non linear behaviour caused by the cable. The relation between forces and the resulting deformations are not linear. (e.g. an increased self weight load in the cable results in a reduction of live load deflection [8,9]. The tensile force in the cable produces a geometrically non-linear stiffness of the cable.)
- Geometry changes in the bridge structure caused by large displacements.

To make an assessment of the geometrical non linearity's in a cable supported bridge, the so called 'n-value' gives an indication. The n-value gives information about the consequences of geometrical non-linearity. In bridge design a general guidance can be used with respect to this n-value:

1 < n < 2	wrong design
2 < n < 3	design problems to be expected
n > 3	proper design, however, geometrical non-linearity should be taken into account
n > 50	consequences of geometrical non linearity can be neglected

Also the Eurocode gives an guidance with respect to the n-value. Eurocode NEN-EN 1993-1-1 part 6.3.1.2 states:

When $\frac{N_{Ed}}{N_{cr}} \leq 0.04$, the buckling effects may be ignored and only cross sectional checks apply.

N_{cr} = is the elastic critical force for the relevant buckling mode based on the gross cross sectional properties.

N_{Ed} = design value of the axial force

[7] These stiffness criteria were also used for the Self-anchored suspension bridge in Kanne in Belgium.
[8] Gimsing, N.J., *Cable supported Bridges*, Wiley&Sons, 1998
[9] Gasparini,D. V. Gautam. Geometrically Nonlinear Static behaviour of Cable Structures. Journal of Structural Engineering, October 2002, pp 1317-1329.

Because $N_{cr} = n * N_{Ed}$, according to the Eurocode buckling can be ignored when the n-value is: n ≥ 25

Determination of n-value and Euler buckling force N_{cr}

The amplification of the deflections can be determined by the difference between the deflection calculated by a linear and a geometrical non-linear calculation.

The amplification factor is: $\frac{n}{n-1} = \frac{\delta_2}{\delta_1}$ in which

δ_2 = the deflection determined by a second order analyses (geometric non-linear)

δ_1 = the deflection determined by a first order analyses (linear).

Rewriting the formula for the amplification factor leads to formula to determine the n-value: $n = \frac{\delta_2}{\delta_2 - \delta_1}$

With this n-value the Euler buckling force N_{cr} is determined by: $N_{cr} = n * N_{Ed}$

This means that the n-value represents the ratio between the design value of the axial force and the Euler buckling force. An evaluation of the calculation of the Euler buckling force is made further in this report when a stability check is done.

The next example explains and compares the calculation of the Euler buckling force with the n-value and the theoretical buckling formula. As shown in Figure 41 both results correspond. The second order deflections are calculated with the FE program ESA PT 6.0.185.

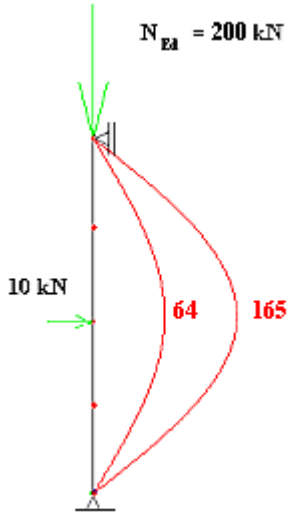

Figure 41 Example buckling force

Column properties:

I_y = $1.56*10^{-5}$ m^4

E = 210000 N/mm^2

A = $2.7*10^{-3}$ m^2

L = 10 m

The theoretical Euler buckling force: $N_{cr} = \frac{\pi^2 EI}{l_{buc}^{\ 2}} = 324kN$

Buckling force according to the n-value:

$\delta_1 = 64mm$

$\delta_2 = 165mm$

$n = \frac{\delta_2}{\delta_2 - \delta_1} = \frac{165}{165 - 64} = 1.63$

$N_{cr} = n * N_{Ed} = 1.63 * 200 = 327kN$

According to the guidelines regarding the interpretation of the n-values, the presented example on this page would mean an improper design because the n-value is < 3.

The same method is used to make an assessment of the second order effects in self-anchored bridge in this M.Sc. study. Further on in this report a stability check is done for the stiffening girder.

Stability check according to the Eurocode
Because the stiffening girder is subjected to a normal force and a bending moment, the buckling resistance should be assessed for a member in bending and compression. The Euro code 1993-2:2003 states that members under combined bending and axial bending should satisfy:

$$\frac{N_{Ed}}{\frac{\chi N_{cr}}{\gamma_{M1}}} + \frac{\beta_m (M_{y,Ed} + \Delta M_{y,Ed})}{\frac{M_{y,Rk}}{\gamma_{M1}}} \leq 0.9 \text{ in which}$$

N_{Ed} is the design value of the compression force
$M_{y,Ed}$ is the design value of the maximum moment about the y-y axis of the member calculated with first order analyses and without using imperfections
ΔM_y is the moment due to shift of the centroidal axis according to 6.2.10.3
β_m is the equivalent moment factor, see table A.2 of EN-1993-1-1
χ_y is the reduction factors due to flexural buckling from 6.3.1

So for the stiffening girder (buckling of the pylon is not considered), only the global buckling will be considered. Local buckling of the compression flanges is a matter of detailed design of the box girder for the stiffeners longitudinal and transverse, cross beam, and cross frames. The required cross sectional area for stiffeners is included in the equivalent plate thickness that is chosen for the top- and bottom flanges of the box girder.

Buckling reduction factor χ
For the verification of the unity check the buckling reduction factor χ needs to be determined by the following procedure:

Relative slenderness

$$\lambda = \sqrt{\frac{Af_y}{N_{cr}}}$$

In which

$$N_{cr} = n * N_{Ed}$$

N_{cr} = is the elastic critical force for the relevant buckling mode based on the gross cross sectional properties.
N_{Ed} = design value of the axial force
n = the amplification determined from deflection in the first order (linear) and second order (geometric non-linear) analysis of the bridge model.

$n = \frac{\delta_2}{\delta_2 - \delta_1}$ in which δ_2 is the deflection determined by a second order analyses (geometric non linear)and δ_1 is the deflection determined by a first order analyses (linear).

And now the buckling resistance factor according to the Eurocode is determined by:

$$\chi = \frac{1}{\Phi + \sqrt{\Phi^2 - \bar{\lambda}^2}} \quad \text{but } \chi \le 1{,}0 \qquad (6.49)$$

where $\Phi = 0{,}5\left[1 + \alpha(\bar{\lambda} - 0{,}2) + \bar{\lambda}^2\right]$

$\bar{\lambda} = \sqrt{\frac{Af_y}{N_{cr}}}$ for Class 1, 2 and 3 cross-sections

$\bar{\lambda} = \sqrt{\frac{A_{eff} f_y}{N_{cr}}}$ for Class 4 cross-sections

α is an imperfection factor

N_{cr} is the elastic critical force for the relevant buckling mode based on the gross cross sectional properties.

(2) The imperfection factor α corresponding to the appropriate buckling curve should be obtained from Table 6.1 and Table 6.2.

Table 6.1: Imperfection factors for buckling curves

Buckling curve	a_0	a	b	c	d
Imperfection factor α	0,13	0,21	0,34	0,49	0,76

As mentioned earlier, the box girder is assumed to be a class 3 cross section. And according to the Euro code 1993-1-1, the buckling resistance factor χ for welded box section in general has to be determined by buckling curve b.

So the verification for buckling stability will be done according to the Euro code 1993-1-1:2003 part 5.2 Global analysis and 6.3 buckling resistance of members and EN-1993-2:2003 section 6.3.

2.1.4 Frequency analyses

In order to determine the response of the bridge to dynamical loadings like wind- and traffic loading, it is necessary to evaluate the frequency behaviour. The frequency behaviour of the a bridge can be characterised by their natural frequencies.
Dynamic wind actions can cause several response phenomena of the bridge deck like galloping, vortex shedding and flutter. Dynamic loading depends on many factors[10] such as , weight of the bridge, dimensions, cross sectional shape, displacements, speed and acceleration of bridge components etcetera. It is therefore a complex phenomena and in many cases of possible bridge response to wind a wind tunnel research is required.
Because of the complexity of this topic, this M.Sc. study considers only the natural frequencies of the bridge.

[10] Romeijn, A. *Examples of examination questions for Cable stayed bridges*. December 2005

For the evaluation for risk for vortex shedding as well as for flutter response of the bridge, the natural frequencies of bending and torsion frequencies are required data. The next formulas[11] are used for determining the critical wind speed when vortex and flutter can be expected:

- Critical wind speed vortex shedding V_{cr}:

  $V_{cr;vortex} = 12 * f * d_4$ [m/s] for $b / d_4 \geq 10$

  f = smallest value of the bending frequency f_b or torsional frequency f_t
  d_4 = height of the girder
  The bridge is stable when the next criteria is met:
  $V_{cr} > V_r$
  In which V_r is a reference wind speed according to BS 5400.

- Critical wind speed flutter V_f:

$$V_{cr;flutter} = 4 * f_t * b * \left(1 - \frac{f_b}{f_t}\right) * \sqrt{\frac{m * r}{\rho * b^3}} \text{ [m/s]}$$

In which $r = \sqrt{\frac{I_p}{A_{girder}}}$,

m = mass of bridge deck per unit of length [kg/m]
I_p = polar moment of inertia

The bridge is stable against flutter when:
$V_f > 1.3 * V_r$

- Other instabilities mentioned by BS5400 like wake galloping and Stall flutter have to be checked when:
  $b < 4 * d_4$ in which b = deck width and d_4 = structural height of box girder.

The before mentioned formulas show that response analyses of the bridge requires the natural bending- and torsional frequencies. These will be determined by the FEM using ESA PT 6.0.185

When an evaluation for flutter is made, a general rule of thumb is used that the ratio bending-torsional frequency of 2.0 or more is recommended[12]. This is accepted as a sufficient difference between the bending frequency and the torsional frequency which results in better resistance against flutter, see Figure 42.

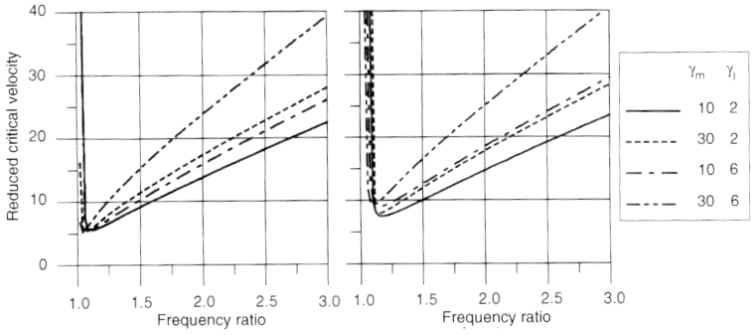

Figure 42 Critical wind speed flutter

[11] Romeijn, A. *Examples of examination questions for Cable stayed bridges*. December 2005
[12] Chen, W. L.Duan. *Bridge Engineering Handbook*. CRC Press 2000.

Determination of frequencies
For beams under bending a general formula[13] is known to determine bending frequencies for several modes. The natural frequency f_n for bending modes can be calculated with:

$$f_n = \frac{C_n}{2\pi}\sqrt{\frac{EI}{ml^3}}$$

The factor C_n depends on the support conditions and the considered frequency mode. For the first bending frequency holds:

$C_n = 9.87$

Figure 43 First bending mode

Next a worked out example is given to compared the bending frequency of a simply supported beam calculated by the before mentioned formula and the frequency calculated when the beam is modelled in FE program ESA PT 6.0.185.

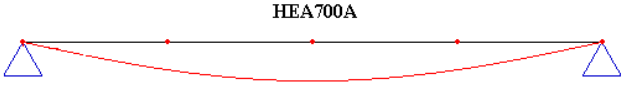

Figure 44 Frequency simply supported beam

Beam properties HEA700A:
I_y = $1.43*10^{-3}$ m^4
E = 210000 N/mm^2
A = $1.91*10^{-2}$ m^2
L = 15 m

- The theoretical bending frequency:

$$f_n = \frac{C_n}{2\pi}\sqrt{\frac{EI}{ml^3}} = 9.786Hz$$

m = mass of the beam [kg]

- Bending frequency according to ESA PT: 9.78 Hz

This example shows that the frequency calculation by ESA is a well approximation compared to the theory. So for further frequency calculation of the bridge deck, the results calculated by ESA PT 6.0.185 are used.

For verification of these results for the bridge deck, a simple approximation method is developed by Raleigh- to determine the first bending frequency of a bridge deck.
An estimation of the first bending frequency can be done with a method developed by Raleigh[14]:

$$f_b = \frac{1.1}{2\pi}\sqrt{\frac{g}{\delta_{max}}} = \frac{0.55}{\sqrt{\delta_{max}}} \text{ hertz}$$

So results of a frequency calculation by ESA PT for the bridge deck will be quickly verified by this formula to confirm if the given values are realistic. Damping effects of the structure are left out of consideration.

[13] Overspannend staal, Rotterdam: Stichting Kennisoverdracht SG, *Deel 3: Construeren* B, 1996.
[14] Romeijn, A. Examples examination question: topic cable stayed bridges.

2.2 Verification of reference design

This part gives the design verification according to the Eurocode as described in the previous paragraph 2. This verification comprises static strength, stiffness and stability of the girder, pylon, main cable and hangers.

2.2.1 Verification reference design on strength

Verification on strength is done for the ultimate limit state (ULS), meaning that the partial factor for permanent loading is 1.35 and the partial factor for variable loading equals 1.5. The total stress calculation is given in Appendix 7 Stress calculation in reference model. Presented stresses are based on an effective cross section, see Appendix 2a Effective width at main and side span and Appendix 2b Effective width at support for calculation of the effective widths.

Girder
Four locations are checked for the girder.

- Mid of the main span:
  Load case 2 (traffic over mid span) is governing for this cross section
  The acting forces are in load case 2:

M_y,Ed,girder	164378	kNm
N_Ed	32827	kN

  This combination of bending and axial force results in the following longitudinal stresses:
  Top flange 139 N/mm^2 in compression.

$$\text{Unity check } \frac{\sigma_{Ed}}{\sigma_{c,Rd}} = \frac{139}{200} = \frac{139}{200} = 0.7 \le 1 \quad \text{Satisfies}$$

  Bottom flange 197 N/mm^2 in tension.

$$\text{Unity check } \frac{\sigma_{Ed}}{\sigma_{t,Rd}} = \frac{197}{200} = \frac{197}{200} = 0.99 \le 1 \quad \text{Satisfies}$$

- Mid of the side span:
  Load case 2 (traffic over mid span) is governing for this cross section
  The acting forces are in load case 2:

M_y,Ed,girder	111377	kNm
N_Ed	32827	kN

  Resulting stresses:
  Top flange 207 N/mm^2 in tension.

$$\text{Unity check } \frac{\sigma_{Ed}}{\sigma_{c,Rd}} = \frac{207}{200} = \frac{207}{200} = 1.04 \le 1 \quad \text{Does not satisfy}$$

  Bottom flange 330 N/mm^2 in compression.

$$\text{Unity check } \frac{\sigma_{Ed}}{\sigma_{t,Rd}} = \frac{330}{200} = \frac{330}{200} = 1.65 \le 1 \quad \text{Does not satisfy}$$

  The stress in the box girder at this location exceeds the assumed design stress of 200 N/mm^2 but are still smaller than the yield strength of steel f_y = 355 N/mm^2. This location require more attention in the final design, for example some additional plate thicknesses at this location can reduce the stresses to an acceptable design level.

- Support at pylon
  Load case 1 (traffic over full length) is governing for this cross section
  The acting forces are in load case 1:

M_y,Ed,girder	193096	kNm
N_Ed	32491	kN

  Resulting stresses:
  Top flange 466 N/mm^2 in tension.

$$\text{Unity check } \frac{\sigma_{Ed}}{\sigma_{t,Rd}} = \frac{466}{200} = \frac{466}{200} = 2.33 \le 1 \quad \text{Does not satisfy}$$

  Bottom flange 783 N/mm^2 in compression.

$$\text{Unity check } \frac{\sigma_{Ed}}{\sigma_{c,Rd}} = \frac{783}{200} = \frac{783}{200} = 3.92 \le 1 \quad \text{Does not satisfy}$$

  This cross section does not meet the strength criteria. But this can be locally solved by application of extra plate thicknesses and adjustment of the supports.

- End support
  Load case 2 (traffic over mid span) is governing for this cross section
  The acting forces are in load case 2:

M_y,Ed,girder	0	kNm
N_Ed	32827	kN

  Resulting stresses:
  Top flange 15 N/mm^2 in compression.

$$\text{Unity check } \frac{\sigma_{Ed}}{\sigma_{c,Rd}} = \frac{15}{200} = \frac{15}{200} = 0.08 \le 1 \quad \text{Satisfies}$$

  Bottom flange 15 N/mm^2 in compression.

$$\text{Unity check } \frac{\sigma_{Ed}}{\sigma_{c,Rd}} = \frac{15}{200} = \frac{15}{200} = 0.08 \le 1 \quad \text{Satisfies}$$

One thing is notable about the stress distribution in the girder in the reference model, compared to the stresses caused by bending the normal stresses caused by the compression force are very low. From this it can be expected that buckling of the girder in this reference design should not be an issue, see §2.2.3 for the stability check of the girder.

Cable
The governing acting normal force in the ULS is caused by loading case 2 (traffic over mid span):
N_{Ed} = 21547 kN
$A_{\text{main cable}}$ = 20106 mm^2

Unity check

$$\frac{F_{Ed}}{F_{Rd}} = \frac{21547*10^3}{\frac{F_{uk}}{1.5\gamma_R}} = \frac{2154710^3}{\frac{f_u * A_{main\_cable}}{1.5}} = \frac{21547*10^3}{\frac{1770*20106}{1.5}} = 0.91 \le 1 \text{ Satisfies}$$

Hangers
The governing acting normal force in the ULS is caused by loading case 1(traffic over full length):
$N_{Ed,hanger}$ = 1254 kN
A_{hanger} = 2376 mm^2

Unity check

$$\frac{F_{Ed}}{F_{Rd}} = \frac{1254*10^3}{\frac{F_{uk}}{1.5\gamma_R}} = \frac{1254*10^3}{\frac{f_u * A_{main\_cable}}{1.5}} = \frac{1254*10^3}{\frac{1770*2376}{1.5}} = 0.45 \le 1 \quad \text{Satisfies}$$

Pylon
The acting normal force in the pylon is
$N_{Ed,\ pylon}$ = 28208 kN
$M_{y,\ Ed,pylon}$ = 25040 kNm (caused by the deflection of pylon towards the midspan)
Resulting stresses:
Top flange 239 N/mm^2 in compression

$$\text{Unity check } \frac{\sigma_{Ed}}{\sigma_{c,Rd}} = \frac{239}{f_y} = \frac{239}{355} = 0.67 \le 1 \quad \text{Satisfies}$$

Bottom flange 40 N/mm^2 in compression

$$\text{Unity check } \frac{\sigma_{Ed}}{\sigma_{c,Rd}} = \frac{40}{f_y} = \frac{40}{355} = 0.11 \le 1 \quad \text{Satisfies}$$

Buckling of pylon
Buckling of the pylon should be considered because a compressive force is acting in the pylon. The pylon is assumed to be fixed at the basement and spring supported at the top of the pylon because it is resisted in longitudinal direction by the main cable which is supported on top of the pylon.

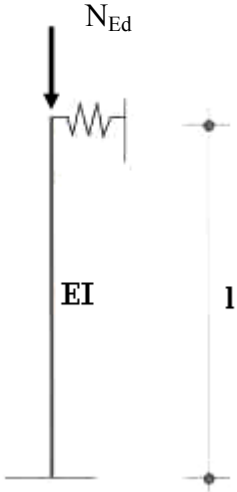

Figure 45 Mechanical scheme pylon

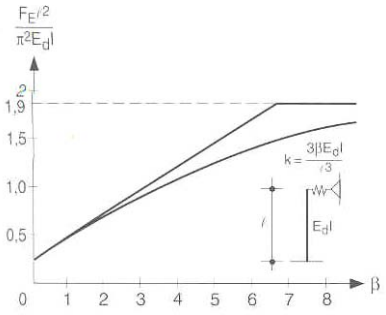

Figure 46 Buckling force of fixed column and translation spring

$N_{Ed\ pylon}$ [kN]	28208
H cable main span [kN]	16748
H cable side span [kN]	16203
δ_{pylon} [mm]	121
Length [m]	50
I_y [m^4]	0.46

Table 4 Properties of pylon

The spring stiffness[15] is determined by $k_{spring} = \frac{\Delta H}{\delta_{pylon}}$ In which ΔH is the difference between the horizontal component of tensile force in main cable in the main and the side span.

[15] Overspannend staal, Rotterdam: Stichting Kennisoverdracht SG, *Deel 3: Construeren* B, 1996.

With the beta factor $\beta = \frac{k_{spring} l_{pylon}}{3EI}$ the ratio between the Euler buckling length and the system length can be found by using the graph presented in Figure 46.
With the forces on the pylon given by Table 4 the buckling force of the pylon can be determined:

$$k_{spring} = \frac{\Delta H}{\delta_{pylon}} = \frac{725000}{0.121} = 5.99 * 10^6 \text{ N/m}$$

$$\beta = \frac{k_{spring} l_{pylon}}{3EI} = \frac{5.99 * 10^6 * 50}{3 * 210000 * 10^6 * 0.47} = 2.45$$

From Figure 46 the ratio between the Euler buckling length and the system length can be found:

$$\frac{N_{cr} l_{sys}^{\ 2}}{\pi^2 EI} = \frac{l_{sys}^{\ 2}}{l_{buck}^{\ 2}} = 0.7 \text{ so } l_{buck} = 59.8 \text{ metres}$$

The Euler buckling force:

$$N_{cr} = \frac{\pi^2 EI}{l_{buc}^{\ 2}} = 270MN >> N_{Ed} = 28\text{MN}$$

So the pylon is stable against global buckling.

2.2.2 Verification reference design on stiffness

Stiffness criteria are checked in the serviceability limit state, meaning that that the partial factor for the loading are equal to 1.
Two deflections are verified, the vertical deflection of the girder at the mid of the main span and the horizontal; displacement of the tower.
Load case 2 is governing for the vertical deflection of girder and displacement of the pylon:

$\delta_{\text{main span}}$ = 422 mm < 1/350 * $L_{\text{main span}}$ < 430 mm

Horizontal displacement of the pylon:

δ_{pylon} = 121 mm < 1/300 * H_{pylon} < 170 mm

On stiffness criteria the reference design meets the requirements.

2.2.3 Verification reference design on stability girder

A stability check has to be done for the stiffening girder because it is loaded with a large axial compression force. A stiffening girder under compression is prone to global buckling effects. To make an assessment of the buckling risk of the girder, the Euler buckling force has to be determined.

$$N_{cr} = n * N_{Ed}$$

in which $n = \frac{\delta_2}{\delta_2 - \delta_1}$

The n-value represents a value that indicates the risk for global buckling of the bridge deck.

As mentioned earlier, an indication for the stability of the bridge deck is the occurrence of second order effects regarding the deflections of the bridge deck.
At first sight, the reference model revealed hardly any second order effects (which means that the deflection calculated by a linear and geometric non-linear analyses does not deviate significantly). There is no amplification of the deflection of the stiffening girder visible in the second order analyses under the given loading conditions. Figure 47 shows that for the three considered load combinations the second order effects are hardly visible. This indicates that the reference bridge model behaves very stiff and that the deflections are relatively low to cause major second order effects.

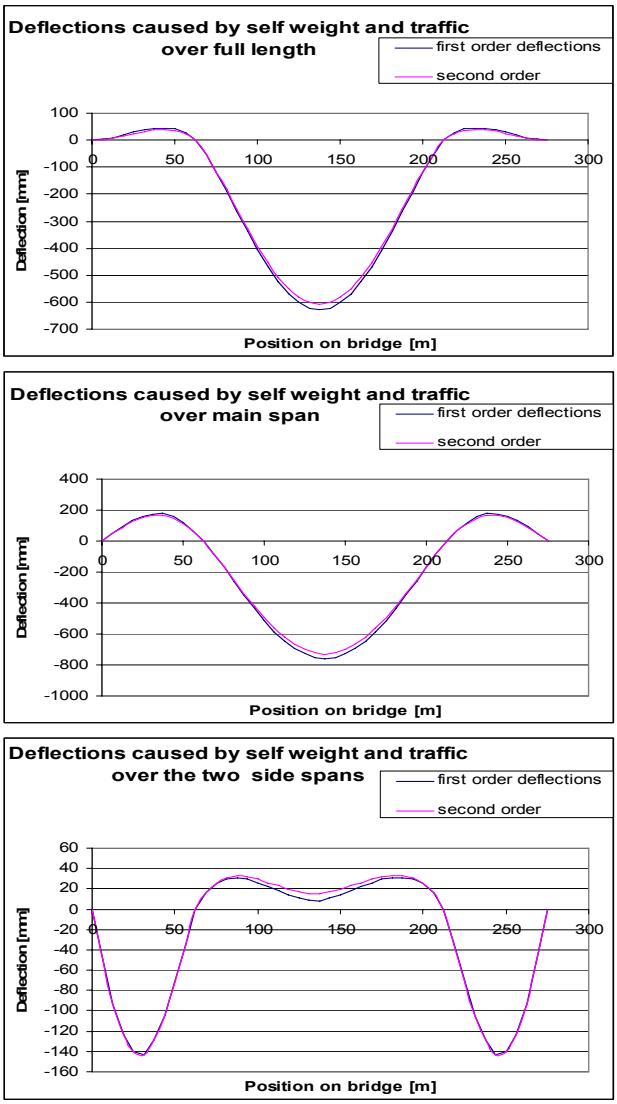

Figure 47 1st and 2nd order deflection due to the three considered loading combinations including pretension of main cable

These results are similar to the design calculations of the self-anchored suspension bridges Kanne[16] bridge and the Nescio[17] bridge. Both calculation documents display the finding that second order effects are hardly visible, both bridges have a similar main span of about 100 metres so is therefore comparable to the reference model in this research.

[16] Alsemgeest,D. *Rebuilding bridge Kanne, Suspension bridge-Static analyses- Check on strength, stiffness and stability*. Iv-Infra, October 2003
[17] Ichimaru, Y., *Design and engineering of 'Nescio' bridge-Amsterdam Rhine canal*. Arup

Causes for the hardly visible second order effects could be that:

- The combination of axial forces and bending moments that act in the stiffening girder and the pylon are not significant enough to cause visible second order effects in the deflection of the stiffening girder. This reference model showed normal stresses in the deck, caused by the deck compression force, of about 15 N/mm^2. This is relatively low.
- The stiffening effect of the girder. The illustration that is presented in Figure 48 indicates that regarding the reference model with a main span of 150 metres, the stiffening effect[18] of the bridge's main girder is significantly large. Figure 48 shows the relation between the non-dimensional maximum deflection v/l against l (v = deflection and l = main span length). For different values of the girder bending stiffness EI, a decreasing influence on displacement is visible when the main span(>2000 metres) is increased. For main span smaller than 2000 metres, this figure indicates that the stiffness of the girder has a significant effect on the reduction of the deflection in the bridge.
  For a main span of 150 metres this would indicate that the stiffness of the deck has large influence on the reduction of the deflections of the total bridge structure. And therefore large geometry changes (which is in many cases a cause for geometric non linear behaviour) in the bridge structure caused by large displacements are not expected to exhibit in relatively small spans like 150 metres of the reference model.

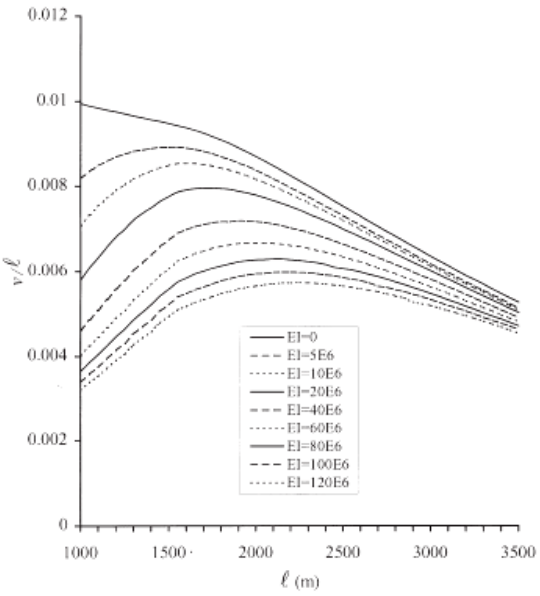

Figure 48 Decreasing stiffening effect

So the combination of the relatively small deflections and stiff behaviour of the girder are causes for the hardly visible second order effect for the reference model in this study.

Alternative approach to determine buckling force N_{cr}

With the present normal stresses in the girder of the reference model of about 15 N/mm^2, no second order effects are visible. When an additional normal force is imposed on the stiffening girder of the reference model of the bridge, second order effects do become visible. Figure 49 illustrates the additional normal force that is applied on the girder, in this case an additional force is applied of about ten times the actual normal force in the girder.

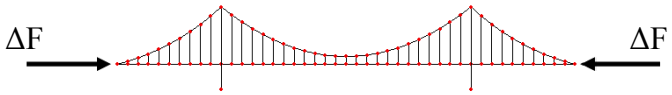

Figure 49 Additional normal force

[18] Clemente,P. G. Nicolosi, A. Raithel. *Preliminary design of very long-span suspension bridges*. Engineering structures 22 (2000), 1699-1706.

In this case an additional force of ΔF=400000 kN is applied, about ten times the design value of the normal force in the deck N_{Ed}. Now an assessment of the Euler buckling force can be made with respect to the three considered load cases. A distinction is made between the main and the side spans because the amplification of the deflections deviates from each other. From this distinction the decisive Euler buckling force can be retrieved, the smallest buckling force to cause buckling in the either the main span or the side span is the governing one.
For the reference model the design value of the normal force is N_{Ed} depends on loading combination as presented below:

- Euler buckling force N_{cr} with traffic over full length

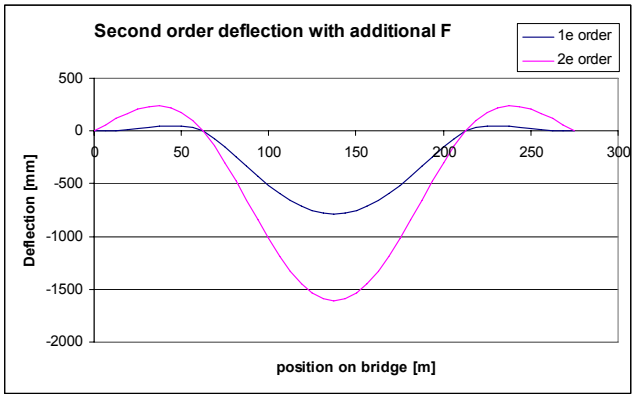

$N_{deck} = N_{Ed} + \Delta F = 432420$ kN
Main span:

δ_1 [mm]	δ_2 [mm]	n-value
790	1608	1,97

Ncr = 1.97 * 432420 = 851867 kN

Side span

δ_1 [mm]	δ_2 [mm]	n-value
48	236	1.26

Ncr = 1.26 * 432420 = 544849 kN

Figure 50 1st and 2nd order deflection with traffic full length

- Euler buckling force N_{cr} with traffic over mid span

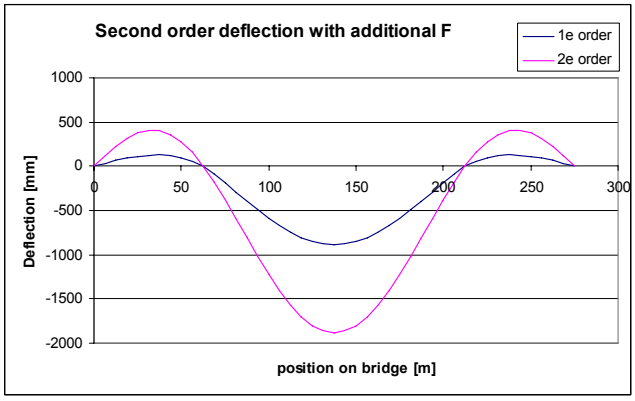

$N_{deck} = N_{Ed} + \Delta F = 432524$ kN
Main span:

δ_1 [mm]	δ_2 [mm]	n-value
883	1882	1.88

Ncr = 1.88 * 432524 = 813145 kN

Side span:

δ_1 [mm]	δ_2 [mm]	n-value
129	407	1,46

Ncr = 1.46 * 432524 = 631485 kN

Figure 51 1st and 2nd order deflections with traffic mid span

- Euler buckling force N_{cr} with traffic over the two side spans

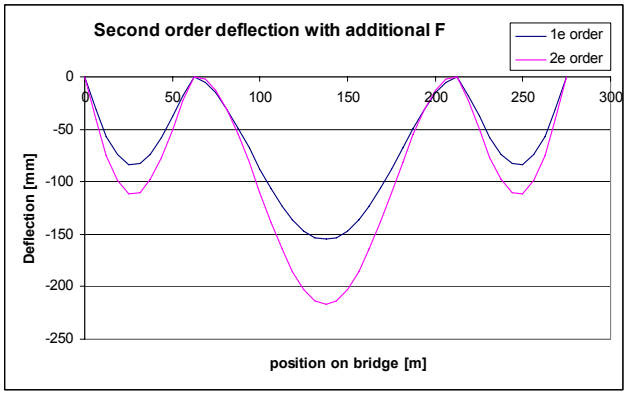

$N_{deck} = N_{Ed} + \Delta F = 423315$ kN
n span:

δ_1 [mm]	δ_2 [mm]	n-value
155	217	3.5

Ncr = 3.5 * 423315 = 1481603 kN

Side span:

δ_1 [mm]	δ_2 [mm]	n-value
84	112	4

Ncr = 4 * 423315 = 1693260 kN

Figure 52 1st and 2nd order deflections with traffic over side spans

Difference in buckling of the main and side span
Buckling of the side span occurs at a lower buckling force than buckling of the main span. For full length- as well as mid span traffic loading the side span is most sensitive to second order effect. The ratio of the Euler bucking force of the main span and side span is about:

$$\frac{Ncr\_side.span}{Ncr\_main.span} = \frac{544849}{851849} = 0.64$$

The difference can be explained by the fact that Figure 50 shows that the buckling of the main span is a downward buckling mode and would therefore encounter upward resistance by the main cables and hangers. Buckling of the side span is an upward buckling mode and would therefore encounter no resistance by the main cable and hangers.
The upward buckling of the side span occurs therefore apparently at a lower buckling force N_{cr} and is decisive over buckling of the main span.

Conclusion regarding buckling
Decisive is buckling of the side span caused by load case 1 (traffic over full length) occurring at a Euler buckling force of :
N_{cr} = 544849 kN which is about 17 times larger than the actual normal force in the girder N_{Ed} (representing an n-value of n = 17 which represents a proper design according to the given guidelines in §2.1.3). So no buckling instability is expected in the reference model, the buckling resistance of the stiffening girder is sufficient.

The stability check according to the Eurocode:

$$\frac{N_{Ed}}{\frac{\chi N_{cr}}{\gamma_{M1}}} + \frac{\beta_m (M_{y,Ed} + \Delta M_{y,Ed})}{\frac{M_{y,Rk}}{\gamma_{M1}}} \le 0.9$$

$$\frac{N_{Ed}}{\chi N_{cr}} + \frac{\beta_m M_{y,Ed}}{M_{y,Rk}} = 0.477 \le 0.9 \text{ Satisfies this criteria}$$

In which
N_{Ed} = 32420 kN
N_{Rk} = N_{cr} = 544849 kN
χ = 0.484 (see Appendix 5a Stability check reference model for calculation stability check)
β_m = 1.27
$\Delta M_{y,Ed}$ = not applicable because the entire cross section is assumed to resist the acting normal force in the cross section of the box girder.
γ_{M1} = 1
$M_{y,Rk}$ = $_{fy}$ * $W_{\_eff\ box\ girder\ side\ span;\ top}$

Overall conclusion is that the bridge girder is satisfies the stability check according to an alternative approach and the Eurocode check. Therefore the conclusion can be made that the stiffening girder in the reference model is stable against buckling.

Further research on the stability phenomena of the stiffening girder will be presented in the parameter study. The stability will be researched as function of the bending stiffness of the box girder.
Also an exploration is done to the buckling behaviour for an increasing main span, see §4.2.2.

2.2.4 Frequency behaviour

An estimation of the first bending frequency can be done with a method developed by Raleigh[19]:

$$f_b = \frac{1.1}{2\pi}\sqrt{\frac{g}{\delta_{\max}}} = \frac{0.55}{\sqrt{\delta_{\max}}} = \frac{0.55}{\sqrt{0.641}} = 0.69 \text{ hertz}$$

In which
δ_{max} = maximum deflection under self weight = 0.641 m, see Figure 14.
g = gravitational acceleration

The results of the calculation of the first bending frequency for the reference model are determined with ESA PT and the Raleigh method and are given in Table 5.

Table 5 First bending frequency comparison

	Raleigh	ESA PT
1st Bending frequency [Hz]	0,69	0,74

So the Raleigh method gives a good approximation of the results for the first bending frequency given by ESA PT. The small difference between the two results are caused by the fact that the Raleigh method is an quick approximation method and that the formula is based on a simply supported beam. Because the bridge deck, in the bridge design under consideration, is a continuous girder and is therefore more stiff than a simply supported girder, the first bending frequency is in that case higher.
Further frequency calculations by ESA PT are assumed to be of realistic value.

Natural frequencies reference design
Table 6 gives the natural frequencies of the reference design.

Table 6 Natural frequencies reference design

1st $f_{bending}$ [Hz]	1st $f_{torsion}$ [Hz]
0,74	5,2

Because the first bending and torsional frequency are clearly well separated, no problems are expected regarding flutter instability for instance. The ratio between the first bending and torsional frequency is well above two.

[19] Romeijn, A. Examples examination question: topic cable stayed bridges.

3 Parameter study into the structural behaviour

Introduction
This chapter presents the results of a parameter study and the influences on the structural behaviour of a self anchored bridge. Objective of this part of the study is to gain insight in the behaviour of a cable supported bridge and to study the effect and sensitivity of the mechanical properties of girder, pylon and cable on the bridge's behaviour:

- EI girder
- EI pylon
- EA cable
- Sag to span ratio

This part of the final thesis will investigate the influence of before mentioned key bridge parameters on the structural behaviour:

- Global stiffness (deflections)
- Reaction forces (normal force deck and vertical support reaction)
- Bending moments at support and in the main span of the stiffening girder.
- Stability of the girder (n-value deck): the n value of the deck gives information about the consequences of geometrical non linearity. The following guidance can be used to interpret the n-values:
- Frequency behaviour (lowest torsional and bending frequency)

The structural behaviour will be investigated under influence of the girder-, cable, pylon and sag properties. Results are analysed and presented in tables and graphs to visualize the effects.

Load condition
Only load case 1(traffic over the entire length of the bridge) in combination with self weight, permanent loading and pretensioning of the main cable is considered in this parametric study.

Results of the parameter study
Results of the parameter study are presented in graphs which illustrate the developments of:

- Bending moments in girder at support and main span
- Deflection of pylon and girder at mid of the main span.
- Frequencies, 1st bending and 1st torsional frequency
- The ratio of the bending moment carried by the deck and cable

These topics show the most significant effects under influence of the different design parameters.

3.1 Girder influence

In this part the structural height of the box girder is varied which changes the bending stiffness (and also the torsional stiffness). Based on realistic values of the slenderness of the girder, that has been retrieved from literature survey, the structural height is varied from 1/50 up to 1/100 of the length of the main span. A slenderness of 1/50 means a structural height of 3 metres and 1/100 a height of 1.5 metres. The next table shows the girder height with corresponding flexural stiffnesses and torsional stiffnesses.

Increasing the bending stiffness has a significant effect on the moment distribution, see Figure 53. A larger stiffness of the girder means the bending moments increase significantly, with approximately 95 %, see Figure 53. Figure 54 clearly shows that with an increasing stiffness, the girder tends to carry a larger part of the total bending moment and smaller part is carried by the main cable, reducing the normal force.

height [mm]	I_y [m^4]	I_t [m^4]
1500	1,1085	2,78139
1600	1,26	3,15281
1700	1,4213	3,54602
1800	1,5925	3,96076
1900	1,7735	4,39681
2000	1,9643	4,85393
2100*	2,1651	5,33188
2200	2,3758	5,83044
2300	2,5964	6,34938
2400	2,8269	6,88849
2500	3,0674	7,44755
2600	3,3179	8,02633
2700	3,5785	8,62463
2800	3,849	9,24224
2900	4,1296	9,87896
3000	4,4203	10,5346

*=Reference model

Table 7 Girder mechanical properties

The total bending moment in the main span presented in Figure 54 is determined by:

$M_{y;Ed;total} = 2*(H_{main\ cable;Ed}* \text{ cable sag}) + M_{y;Ed;deck}$

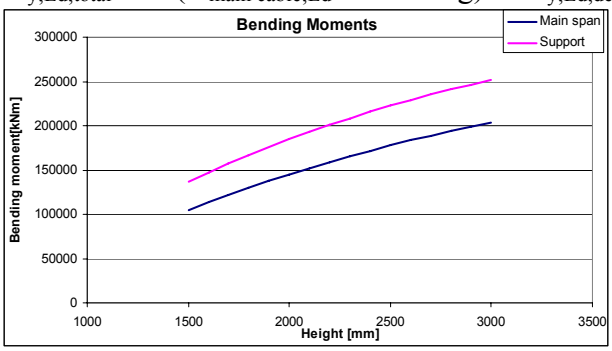

Figure 53 Maximum bending moment in the girder

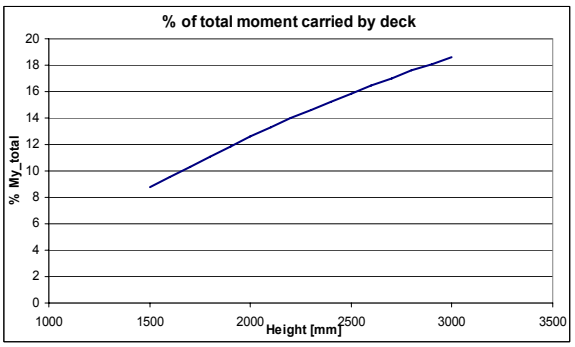

Figure 54 Contribution of the girder to bending moment

Looking at the stiffness, an increasing stiffness of the girder result in larger global stiffness because the deflection reduces significantly. Figure 55 shows this tendency of a decreasing deflection of the girder and displacement of the pylon. Girder and pylon deflection is reduced with approximately 50%. An increasing global stiffness also results in higher bending and torsional frequencies, see figure 40.

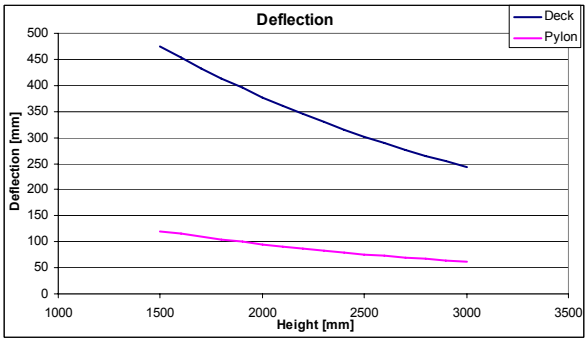

Figure 55 Maximum deflection in the girder

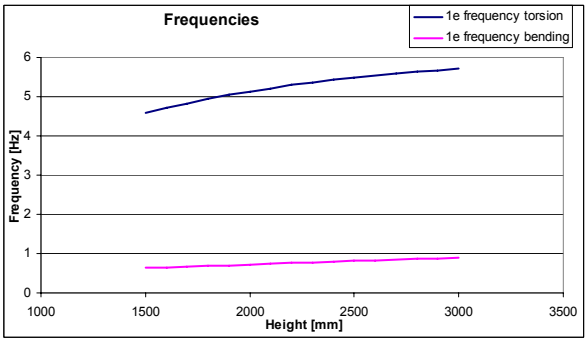

Figure 56 Natural frequencies

The stiffness of the girder has a clear visible influence on the stiffness, strength and frequency behaviour of the bridge.

Regarding the reaction force, the normal force in the deck and resulting vertical reaction at the end support, Figure 57 shows that both maximum reaction forces decrease with a stiffer deck. With a stiffer deck, a larger part of the bending moment is carried by the girder which leads to decreasing normal force in the cable.

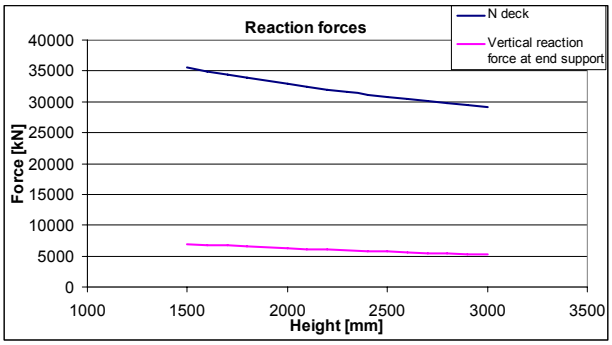

Figure 57 Reaction forces

3.1.1 Stress level in box girder

The stress level in the flanges of box girder is determined by:

$$\sigma_{top} = -\frac{N_{Ed}}{A_{box}} - \frac{M_{y;Ed}}{W_{eff;top}}$$

$$\sigma_{bottom} = -\frac{N_{Ed}}{A_{box}} + \frac{M_{y;Ed}}{W_{eff;bottom}}$$

So the stress level in the flanges depend on the normal force N_{Ed} in the girder, bending moment $M_{y;Ed}$ in the girder, the section modulus W_{eff} and cross sectional area A_{box} of the girder.

Figure 53 and Figure 57 show that choosing for a more slender girder results in significant reduction of the bending moments $M_{y;Ed}$ and an increasing normal force N_{Ed} in the girder. A side effect is that the effective section modulus W_{eff} also decreases with an increasing slenderness of the girder. This development is expressed in the stress level in the flanges of the box girder in the mid of the main span of the bridge, see Figure 58. This figure shows that the development on the stresses as a function of the girder slenderness λ (height/length main span) remain quite constant.

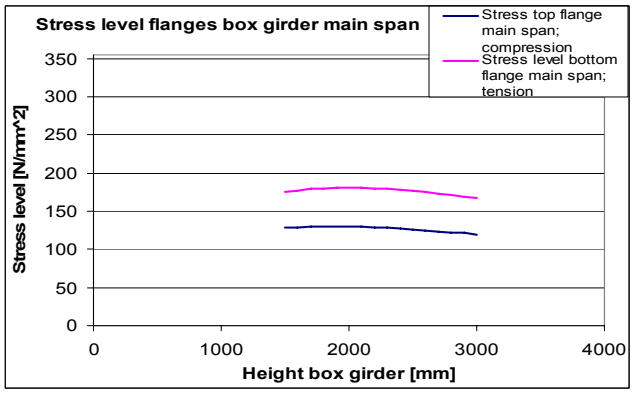

Figure 58 Stresses in flanges of the box girder

3.1.2 Stability of the stiffening girder

The resistance against buckling of the main girder is mainly determined by the bending stiffness EI of the box girder. Two approaches will be set out in this part in order to compare and verify the results of the calculation of the Euler buckling force of the stiffening girder. Also an approach on the maximum girder slenderness will be given.

1. Additional normal force ΔF

First approach, as mentioned earlier, is that on the bridge deck an additional normal force is applied to be able to analyze the second order deflections and determine the buckling force, see Figure 59. The bridge model proved to be very stiff (see 2.2.3) and second order effects only became visible by increasing the normal force on the deck, in this case by applying an external additional force ΔF.

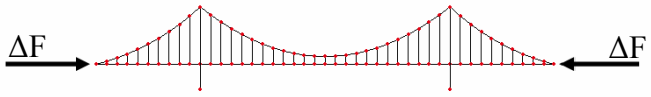

Figure 59 Additional normal force applied on the girder

2. Spring model of bridge deck

The second approach is to model the bridge as supported by discrete springs with a certain spring stiffness k [N/m], see Figure 60. This model is used to analyze the buckling effect of the main span because the spring stiffness in the side is zero for an upward deflection. In this model the girder is also loaded by a normal force N_{Ed}, similar to acting normal force in the reference design; N_{Ed} = 32420 kN.

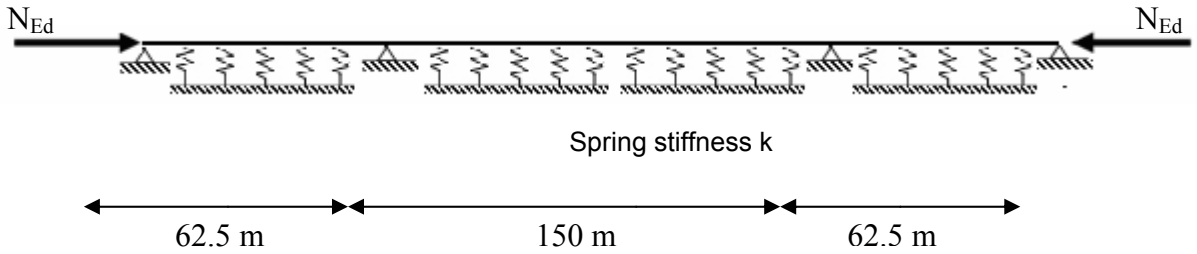

Figure 60 Spring supported bridge deck

According to Engesser's[20] formula, the Euler buckling force for a girder supported by springs depends on the spring stiffness (in this case the springs represent the hangers on which the girder is supported) and the bending stiffness of the girder.

Engesser formula: $N_{cr} = 2\sqrt{cEI}$ in which c is a bedding constant equal to the spring stiffness divided by the individual distance between the springs (in this case the c.t.c. distance between the hangers).

Spring stiffness k

A spring stiffness k is iteratively chosen for the springs that result in similar deflections of the spring supported girder, under full length traffic loading of the main span, as in the reference bridge model under the same loading condition. In case of an upward deflection of the side span, the girder will not be resisted by the hangers, in that case the spring stiffness k = 0 in the side span.

[20] Overspannend staal, Rotterdam: Stichting Kennisoverdracht SG, *Deel 3: Construeren* B, 1996.

As mentioned earlier only a traffic loading over the entire bridge length is considered, as shown in 2.2.3 this is decisive for buckling of the stiffening girder. Figure 61 presents a graph of the relation between the Euler buckling force of the main span of the bridge deck and the stiffness of the deck (moment of inertia of the box girder ranging from a girder height of 1500-3000 mm, representing a range of deck slenderness λ from 1/100 to 1/50) regarding the two models. The deck slenderness is defined as λ = construction depth h of the girder/main span length l.
Also the buckling force of the side span is plotted in the graph, which is governing over the buckling force of the main span (see §2.2.3).

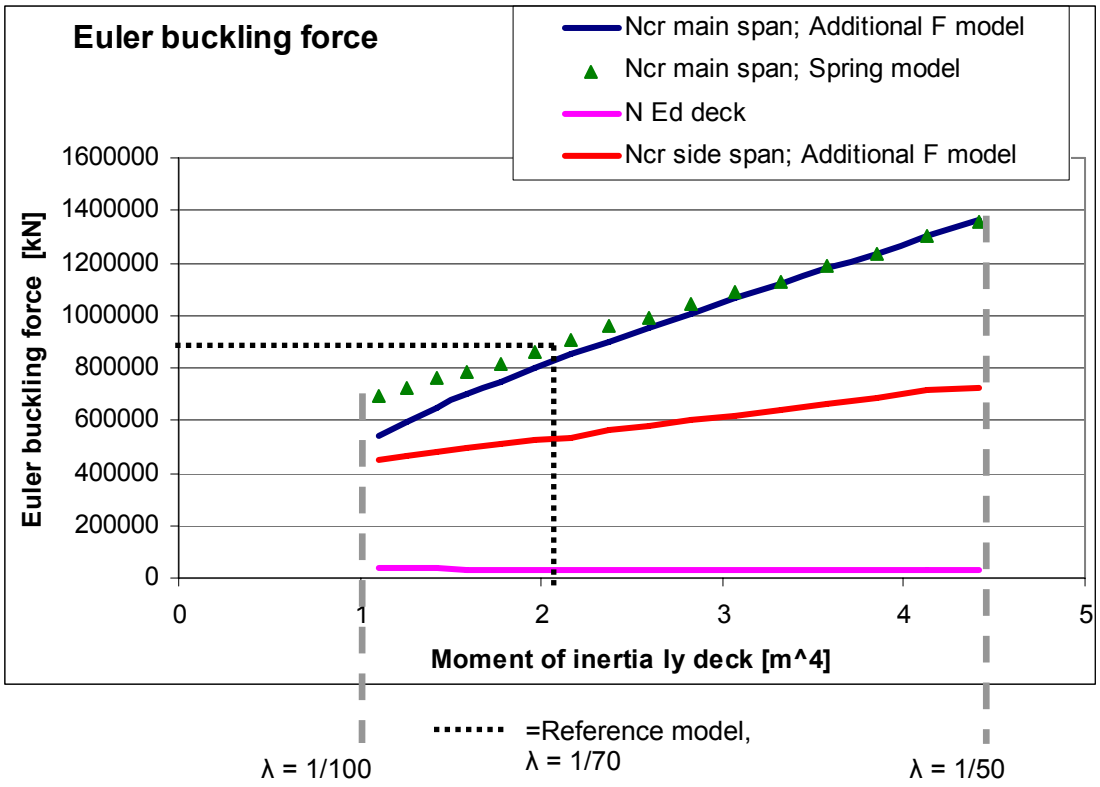

See also Figure 50: N_{Ed} = 32420 kN
$N_{cr;main\ span}$ = 851867 kN

Boundaries of considered deck slenderness λ =1/100 – 1/50

Figure 61 Euler buckling force as a function of the stiffness of the deck

Both approaches display a similar development with respect to the Euler buckling force of the main span of the stiffening girder. The Euler buckling is in all cases well above the acting normal force in the deck N_{Ed}. So also in case of a more slender deck with a slenderness λ = 1/100, the resistance against buckling is still significant.

The buckling behaviour of the main and side span presented in Figure 61 can also be expressed in the so called n-values, see Table 8 n-values for main and side span based on the computed bridge model.

Table 8 n-values for main and side span related to the moment of inertia of the box girder

$I_{y;girder\ [m^4]}$	n-value main span	n-value side span	
1,11	15,2	12,7	
1,26	17,0	13,3	
1,42	18,9	13,9	
1,59	20,6	14,6	
1,77	22,4	15,3	
1,96	24,3	16,0	
2,17	26,2	16,3	= reference design
2,38	28,2	17,5	
2,60	30,2	18,4	
2,83	32,3	19,2	
3,10	34,5	20,1	
3,32	36,8	21,0	
3,58	39,1	21,9	
3,85	41,5	22,9	
4,13	44,1	24,3	
4,42	46,6	24,9	

These n-values also clearly show that the side span exhibits more geometrical non-linear effect, indicating that the side span is decisive for the buckling stability of the stiffening girder and that the geometrical non-linearity's decrease for both the main and the side span when the stiffness of the deck is increasing.

Conclusion regarding the buckling stability
Figure 61 shows that the buckling stability of the girder requires attention in the design process of a self-anchored suspension bridge. But a girder with a slenderness to about λ = 1/100 is expected to have enough resistance against buckling. Extrapolating this graph for even more slender girders, meaning a higher slenderness λ =1/100..1/150 and further, a limitation is expected with respect to the buckling resistance. Buckling than becomes critical and a limiting design factor.
These results confirm the findings presented in the literature survey of this study which showed that the slenderness of stiffening girders in existing self-anchored suspension bridges is limited to about λ = 1/100 (e.g. Konohana bridge, Japan). Compare this to the applied stiffening girders in conventional suspension bridges where no buckling risk of the girder is present, here girder slenderness of λ = 1/200 – 1/300 are common.

3.1.3 Number of hinges

As mentioned earlier in the literature survey, the stiffening girder can either be executed as a continuous girder or as a hinged girder. A continuous girder has no hinges along the length and a hinged girder has two hinges, one at each support at the pylon, see Figure 62.

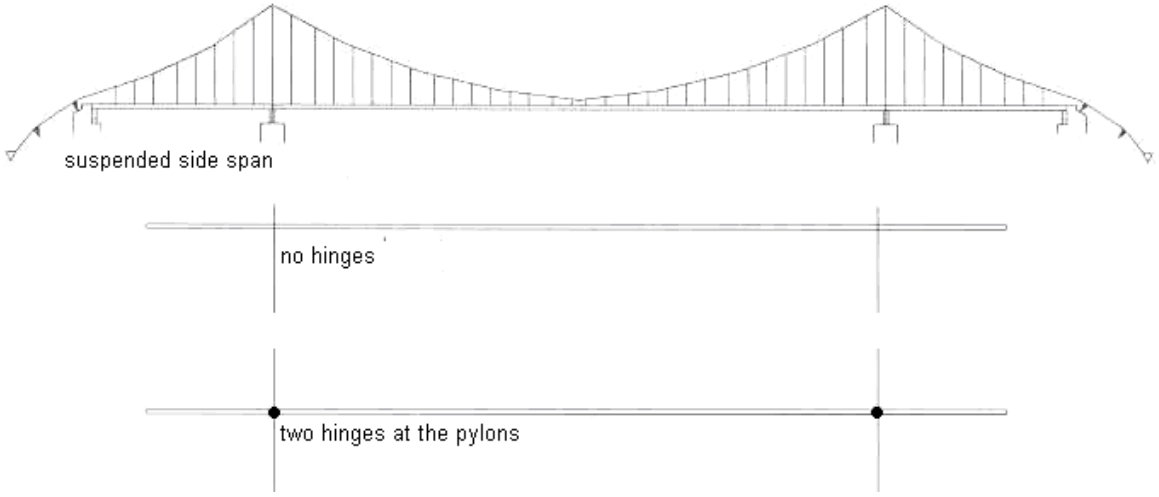

Figure 62 Hinged and unhinged girder

Figure 63 shows clearly that a continuous girder applied in the reference model. with no hinges. is much stiffer. For deflection and frequency behaviour of the first torsional motion, a continuous girder is much stiffer.

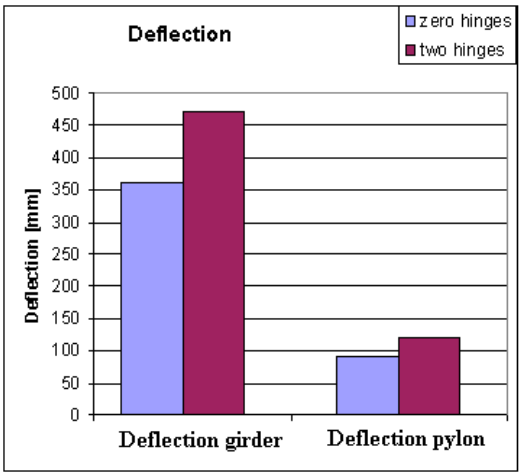

Figure 63 Maximum deflection in the girder

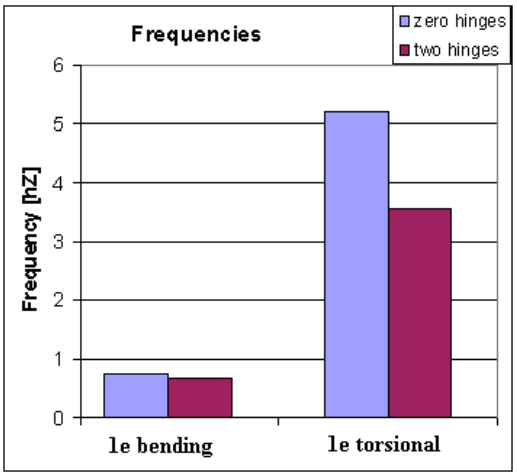

Figure 64 Natural frequencies

From now on only a continuous girder is chosen. Based on the given results and bridges already built like the Konohana and Yeoungjong Grand bridge, a continuous girder is chosen. Results have shown that a continuous girder is displays smaller deflections and offers a better resistance for a torsional frequency motion.

3.2 Main Cable influence

Axial stiffness EA of the main cable is determined by two factors; the modulus of elasticity E that changes with the different cable types, and the cross sectional area A_{cable} of the cable. The influence of the hangers is left out of consideration in this part of the research, it is assumed to have little influence on the global strength and stiffness of the bridge.

3.2.1 Cable type

Four cable types can be applied in cable supported bridges:

- Parallel wires E = 205000 N/mm^2
- Parallel strands E = 190000 N/mm^2
- Full locked coil E = 150000 N/mm^2
- Cable spiral strand E = 140000 N/mm^2

The axial stiffness EA of the main cable is reduced with approximately 25% when choosing for locked or spiral strands compared to parallel wires. A lower axial stiffness of the cable means that larger bending moments will act in the girder, see Figure 65.The girder carries a larger part of the total bending moment when the axial stiffness of the main cable is reduced, see figure 43.

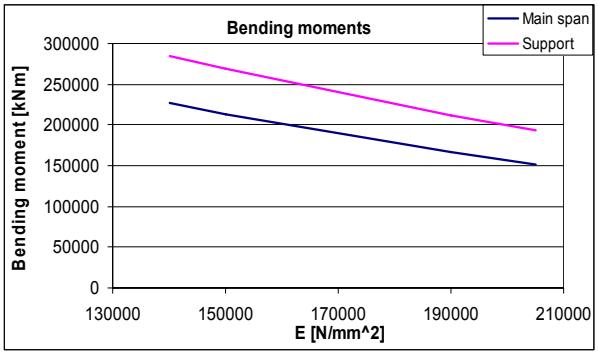

Figure 65 Maximum bending moment in the girder

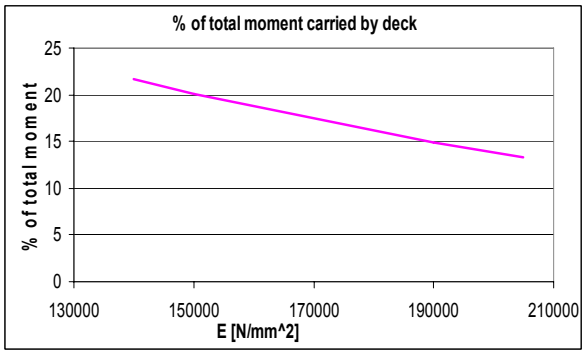

Figure 66 Contribution of the girder to bending moment

Compared to the main cable when it is composed of spiral strands, the parallel wired cable reduces the deflection with approximately 14 %. Little effects are visible on the frequency behaviour.

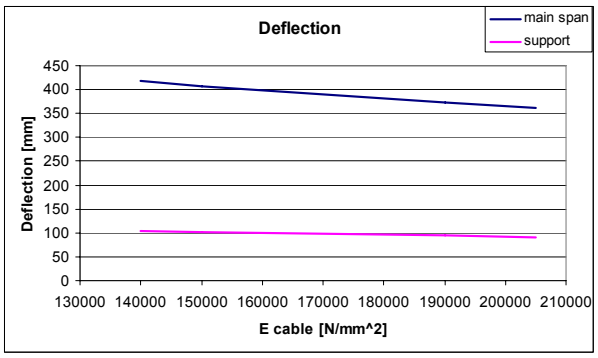

Figure 67 Maximum deflection in the girder

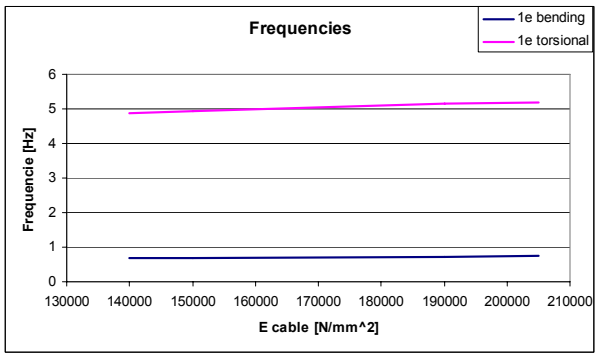

Figure 68 Natural frequencies

3.2.2 Cable cross sectional area

Once a cable type is chosen, the axial stiffness of the main cable can be altered by means of the cross sectional area A_{cable}. The next table shows the cable diameters with the corresponding effective area that are applied.

Table 9 Cable area

diameter [mm]	100	120	140	150	160*	170	180	190	200	210	220	230	240
A eff. main cable [mm^2]	7854	11310	15394	17671	20106	22698	25447	28353	31416	34636	38013	41548	45239

*=Reference model

Increasing the cable's diameter displays significant effects on the maximum bending moment. Increasing the diameter to from 160 mm to 240 mm, the bending moment in the deck reduces to nearly zero, see Figure 69. This means that nearly a 100% of the total moment is carried by the main cable, which is clearly visible in figure 47.

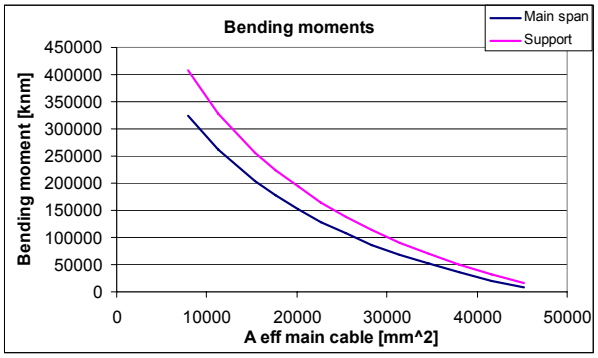

Figure 69 Maximum bending moment in the girder

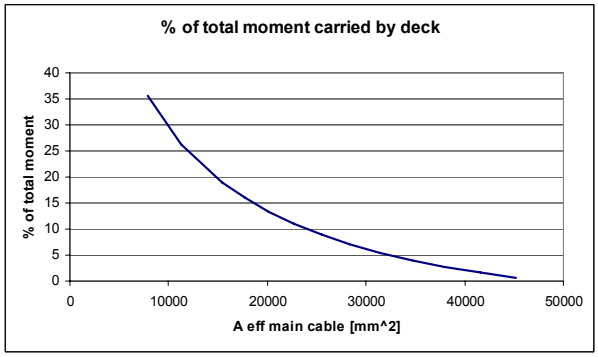

Figure 70 Contribution of the girder to bending moment

Increasing the axial stiffness of the cable has favourable effects for the global stiffness, the girder and pylon deflection both reduce. With respect to the frequency behaviour, the increasing stiffness results in higher frequencies. Although there is a point where an increment of the cable results in a decreasing torsional frequency. The reason for this can be that the self weight of the cable rules out the stiffening effect of the cable.

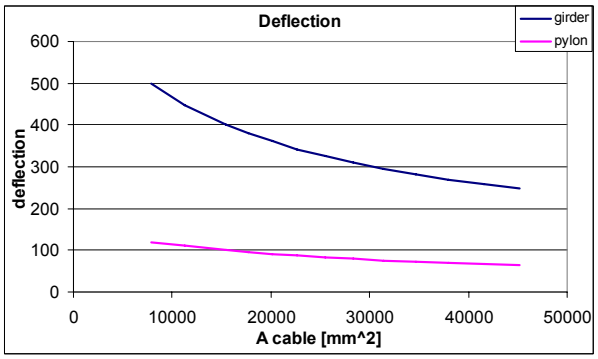

Figure 71 Maximum deflection in the girder

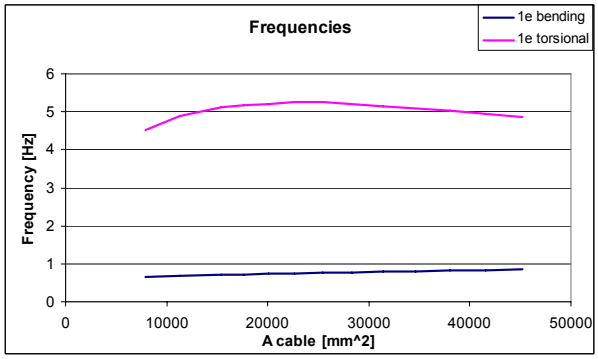

Figure 72 Natural frequencies

A larger contribution of the main cable to the total bending moment leads to much higher reaction forces. The normal force in the deck and the vertical reaction force increase significantly, see Figure 73.

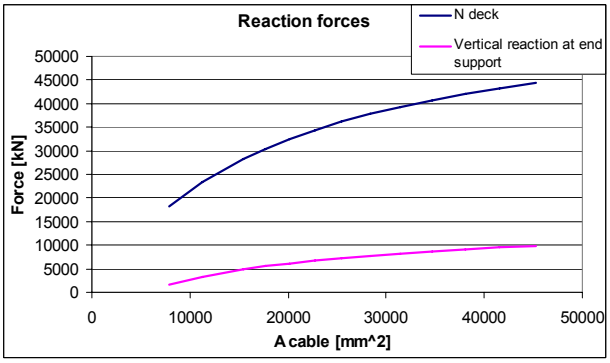

Figure 73 Reaction forces

3.3 Sag influence

As mentioned before the most common sag to span ratio for self-anchored suspension bridges are 1/5 to 1/9. With an increasing sag ratio, the bending moment in girder reduces with approximately 50%, see Figure 74. The cable carries a larger part of the total bending moment when the sag ratio is increased, see figure 52.

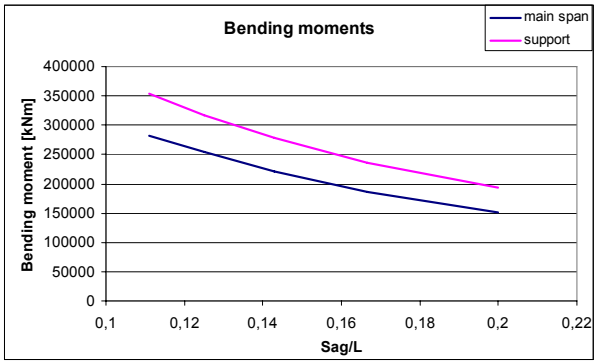

Figure 74 Maximum bending moment in the girder

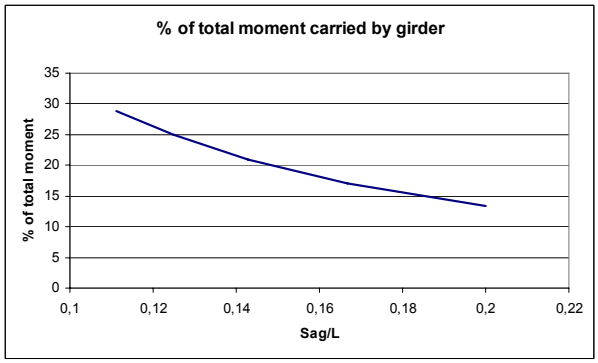

Figure 75 Contribution of the girder to bending moment

A larger sag ratio increases the stiffness of the bridge, the deflection decrease with about 28%. The deflection of the pylon increases because the height of the pylon increases with a larger sag ratio. So with an unchanged bending stiffness of the pylon, its deflection will increase when the height is increased, see Figure 76.
The first torsional frequency motion is coupled with a longitudinal deflection of the pylon, therefore the pylon's stiffness will have effect on the torsional stiffness of the bridge. A larger sag ratio means that the pylon becomes more flexible, so a larger sag ratio decreases the torsional stiffness of the bridge which is visible in figure 54.

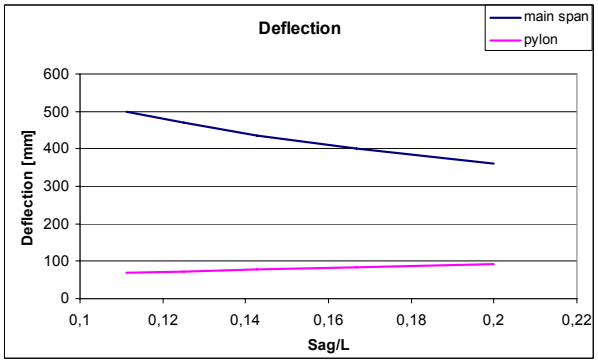

Figure 76 Maximum deflection in the girder

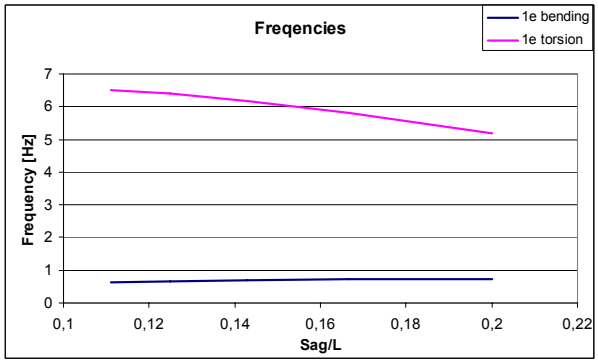

Figure 77 Natural frequencies

Regarding the reaction forces a larger sag ratio decreases the contribution of the cable to the total bending moment. The normal force in the main cable decreases with a larger sag ratio and so does the compression in force in the girder.
Only the vertical reaction force at the end support increases because the vertical component of the main cable's normal force increases with a larger pylon height.

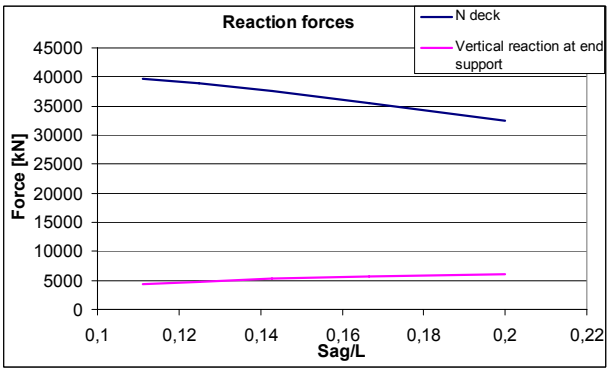

Figure 78 Reaction forces

3.4 Pylon influence

This part presents the influence of the bending stiffness of the pylon in longitudinal direction of the bridge. Looking at the presented results in Figure 79, no significant developments in bending moments as function of the stiffness can be seen.

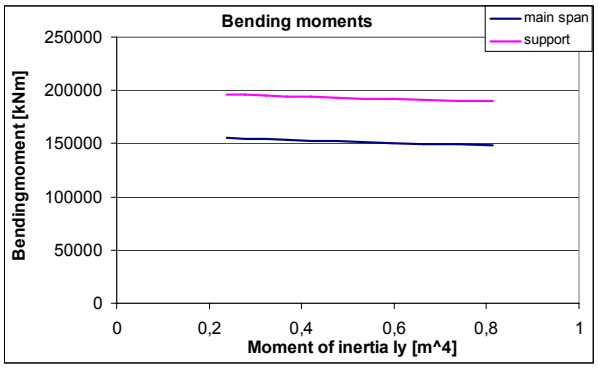

Figure 79 Maximum bending moment in the girder

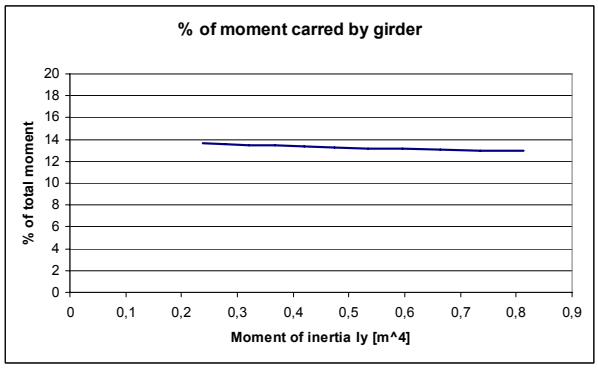

Figure 80 Contribution of the girder to bending moment

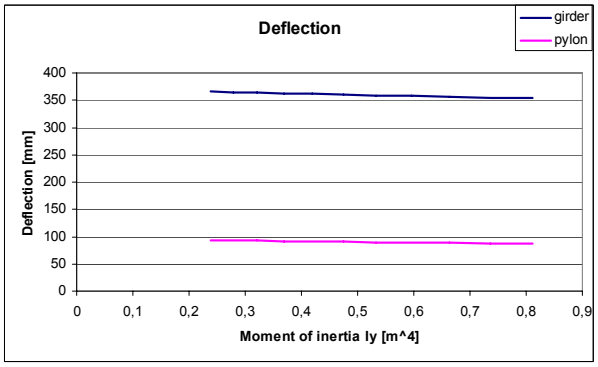

Figure 81 Maximum deflection in the girder

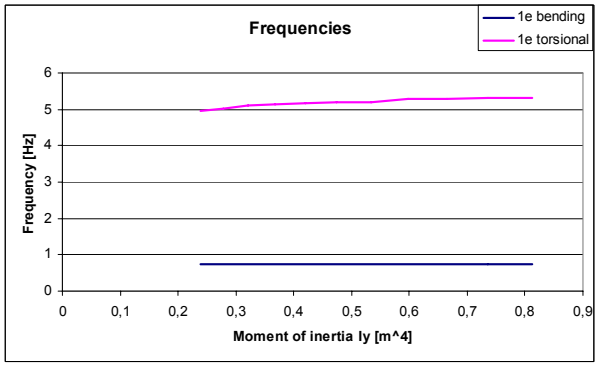

Figure 82 Natural frequencies

Only the frequency of the first torsional motion increases. A torsional motion of the girder exhibits with longitudinal motion of the pylon, therefore a stiffer pylon has a positive effect on the torsional stiffness of the bridge. In that way the pylon offers more resistance against a torsional motion of the girder, see figure 59.

3.5 Asymmetric traffic loading

Until now only symmetric loading has been considered. This part evaluates the effects of an asymmetric position of the traffic loading on the force distribution in the bridge. The traffic loading is combined with the self weight of the bridge and other permanent loads on the bridge including the pretensioning of the main cable.

3.5.1 Full loaded deck

First of a full loaded deck is considered which results in a certain eccentricity, see Figure 24. This full loading conditions is in the model applied as line load of 131,5 kN/m with an eccentricity of 1.48 metres. The effects of such a load condition is given in Table 10.

Table 10 Deck full loaded eccentricity

	Traffic full length	
	Symmetric	Asymmetric
N deck [kN]	32420	32422
H cable 1 [kN]	16452	16743
H cable 2 [kN]	16542	16340
δ cable plane 1 main span[mm]	361	372
δ cable plane 2 main span[mm]	361	349
δ pylon [mm]	91	93
My main [kNm]	152065	152061
My sup [kNm]	193096	193093
My pylon [kNm]	21044	2152
M torsion kNm]	0	16194

Main effects of taking into account the asymmetric effect of a full loaded deck is a torsional moment in the box girder at the support location at the pylon. Also the deck shows a rotation of about 0.04 degrees.

3.5.2 Half loaded deck

The deck is in transverse direction loaded on one half of the bridge deck, see Figure 83

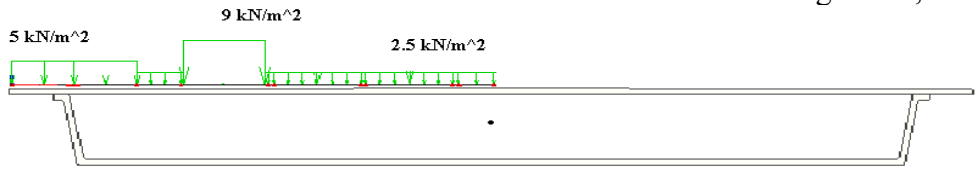

Figure 83 Half loaded bridge deck in transverse direction

This half loaded deck will be applied on the bridge model as a resulting line load of 75.5 kN/m with an eccentricity of 10.1 metres.
Three asymmetric loading positions will be considered (side span loading is not the decisive load case concerning bending moments in-, and deflections of- the stiffening girder, see 1.3.3, so no asymmetric loading of the side span is considered here). The traffic loading is combined with the self weight of the bridge and other permanent loads on the bridge including the pretensioning of the main cable.

- One sided full length traffic loading

Table 11 Asymmetric loading traffic full length

	Traffic full length	
	Symmetric	Asymmetric
N deck [kN]	32420	28754
H cable 1 [kN]	16452	15310
H cable 2 [kN]	16542	13915
δ cable plane 1 main span[mm]	361	247
δ cable plane 2 main span[mm]	361	166
δ pylon [mm]	91	44
My main [kNm]	152065	99166
My sup [kNm]	193096	126525
My pylon [kNm]	21044	12555
M torsion kNm]	0	56067

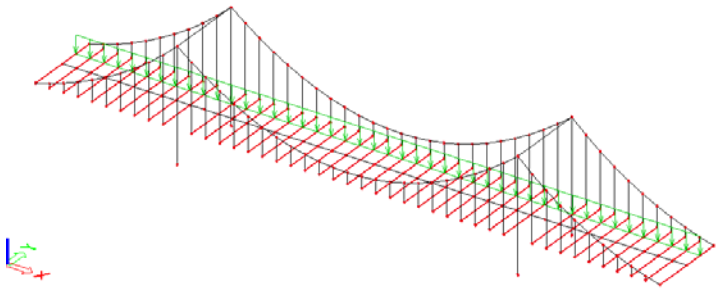

Figure 84 One sided full length loading

Figure 84 presents the considered loading scheme of an asymmetric traffic load over the full length of the bridge. An asymmetric loading has the effect that one cable plane is loaded more than the other cable plane. The normal force in the loaded cable plane is therefore higher than the normal force in the unloaded cable plane but still smaller than in full loading symmetric condition.
The bending moments in the girder as well as in the pylon base, are in case of asymmetric loading much less than in full loading symmetric condition. Also the deflections are smaller than in full loading condition. One of the most adverse effect of asymmetric loading is a torsional moment in the deck.
A second effect of asymmetric loading is the rotation of the deck. Table 11 shows a difference is visible in the deformation of the deck on the loaded side and unloaded side. This results in a very limited rotation of the deck of about 0.13 degrees.

- One sided mid span traffic loading

Table 12 Asymmetric loading traffic mid span

	Traffic mid span	
	Symmetric	Asymmetric
N deck [kN]	32825	28986
H cable 1 [kN]	16820	15400
H cable 2 [kN]	16820	14154
δ cable plane 1[mm]	422	283
δ cable plane 2[mm]	422	202
δ pylon [mm]	121	58
My main [kNm]	164378	106269
My sup [kNm]	163167	109369
My pylon [kNm]	26040	14955
M torsion	0	57799

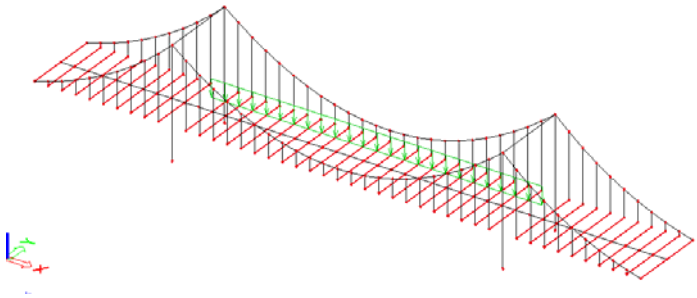

Figure 85 One side mid span loaded

Figure 85 presents the considered loading scheme of an asymmetric traffic load over the mid span of the bridge. Again a redistribution of forces is visible, the loaded cable plane carries a larger part of the vertical traffic loading and displays a higher normal force. The most adverse effects are encountered in the torsional moment in the deck.
The rotation of the deck is due to the difference in deflection of the loaded and unloaded side of the deck is about 0.13 degrees.

- Alternate full length traffic loading

Table 13 Alternate loading traffic full length

	Traffic full length	
	Symmetric	Alternate
N deck [kN]	32420	28754
H cable 1 [kN]	16452	15169
H cable 2 [kN]	16542	14056
δ cable plane 1[mm] [mm]	361	250
δ cable plane 2[mm]	361	165
δ pylon [mm]	91	39
My main [kNm]	152065	99155
My sup [kNm]	193096	126529
My pylon [kNm]	21044	11631
M torsion	0	59695

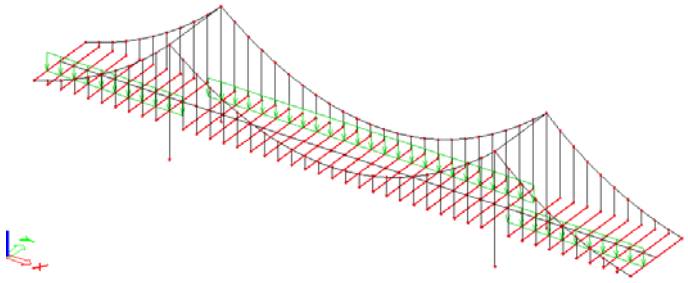

Figure 86 Alternate loading full length

Figure 86 presents the considered loading scheme of an alternating traffic load over the entire length of the bridge. This means that on the mid span the traffic load is situated one the opposite cable plan than the traffic load on the side spans. Table 13 presents the member forces of this loading conditions. A comparable redistribution of cable forces is visible and torsional moment in the deck.
The rotation of the deck is due to the difference in deflection of the loaded and unloaded side of the deck is about 0.14 degrees, also very limited.

Conclusion regarding asymmetrical loading
A consideration of an asymmetrical application of the vertical traffic loading reveals that more attention has to go out for the design of the girder at the support location at pylon. At this location occurs the largest torsional moment in the girder.
The resulting stresses caused by torsion can be distincted in the St. Venant shear flow and restrained warping stresses:

-St. Venant shear stress (maximum occurs in the web because the plate thickness is the smaller than in the flanges):

$$\tau = \frac{M_t}{2A_m t_1} = \frac{59695 * 106}{2 * 35600 * 2100 * 13} = 30.7 \text{ N/mm}^2$$

-Restrained warping stresses:

$$\sigma w = \frac{3 * \Delta M_t}{\sqrt{I_t * A}} = \frac{3 * 59695 * 10^6}{\sqrt{5.33 * 10^{12} * 2.15 * 10^6}} = 52.9 \text{ N/mm}^2$$

These stresses require attention for the detailed design of the support conditions of the box girder at the pylon location.
Asymmetrical loading causes also a rotation of the deck but is limited to about 0.14 degrees which is assumed to be very limited and of acceptable level.

3.6 Conclusion results of the parameter study

This part has shown that many bridge parameters have a large influence on the force distribution and deflections in a self-anchored suspension bridge.
It has been shown that the mechanical properties of the girder, cable and sag ratio govern the design. These bridge parameters have large influence on the deflections and the maximum bending moment in the stiffening girder. The stiffness of the pylon shows little influence on the global behaviour.
Regarding the force distribution and deflection it is favourable to consider:

-A slender stiffening girder, to reduce the maximum bending moment in the girder. It has been shown that even though the slenderness is reduced the stress level in the box remain quite constant, see Figure 58.
-A stiff main cable, to increase the global stiffness of the bridge and to reduce the maximum bending moment in the girder.
-A high sag to span ratio, to reduce the normal force in the deck and the maximum bending moment in the deck.

3.7 Evaluation of the results

This part contains an evaluation and analyses of the results of the parameter study and literature survey. It will give a motivation of the choices that are made to optimize the reference design. The optimization is made with respect to the general performance of the bridge but also with respect to the next topic of this research: increasing the span length.

3.7.1 Criteria

- Distribution of forces:
  - Bending moments in girder
    The sagging moment in the main span and hogging moment at support near pylons, is determining the design of the girder. Designing for bending moments is always more difficult and material consuming than for designing a cross section for normal force only. So reducing bending moments in the girder is favourable.
  - Normal force in cable.
    The level of stresses determines the design of the cable and therefore the axial stiffness.
- Stress conditions in the box girder:

The slenderness of the box girder influences the stiffness and therefore the bending moment in the girder. Also the section modulus is determined by the slenderness which determines the stress level in the cross section. Figure 58 shows the constant development in stress with a decreasing slenderness of the deck. This development justifies the possibility for choosing a more slender deck.

- Deflection of girder and pylon

The deflection of the pylon and girder have to be within limits to meet certain stiffness criteria.

- Frequencies

It is important to consider the level of frequencies. Low torsional frequencies means that the bridge structure becomes more susceptible for flutter risk. Also the ratio between the first bending and the first torsional frequency illustrates the risk for flutter. A ratio close to one is not desirable, in general a ratio of 2 or more is advisable.
The results show that the ratios of the 1st bending to 1st torsional frequencies are in all cases well above 2. So in this stadium this criterion plays a secondary role.

- Girder stability

The compression loaded stiffening girder requires enough resistance against buckling. The bending stiffness is dominating the buckling properties of the girder.

- Erection

For the erection of the main cable two methods are possible. Aerial spinning of cable producing parallel wired cables and erection of a prefabricated locked coil or spiral strand main cable. Especially with large span the last mentioned method becomes impossible.

- Material use/costs

The required mechanical properties of the main cable and girder can be translated to a certain material use for the cross section. Designing cross section for bending moments is always more material consuming that for normal forces. For the cross section of the girder it is profitable to reduce the bending moments that act in the girder.

- Reaction forces

Regarding the reaction forces on the end support and compression force in deck it is desirable to achieve an acceptable level in these forces.

- Examples from practice

Examples like the Konohana Bridge, Yeongjong Grand Bridge and Duisburg Bridge, with a main span of respectively 300 metres, 300 metres and 285 metres, offer experience which can contribute to certain choices in the design phase of a self-anchored suspension bridge.

Optimization of the reference design is achieved by choosing mechanical requirements of the girder, pylon, and cable, and a geometrical sag over main span length ratio which have the most favourable effect on the before mentioned criteria.

3.7.2 Conclusions for optimized reference design

This part presents the chosen dimensions for all the structural elements and chosen ratio for the optimized reference model. This model will be used for the next research topic in this study, namely the exploration of the span length possibilities.

- *Height of stiffening girder*

Its is favourable for reducing the maximum bending, to choose a slender girder. Also for the design of the cross section it results in less material use, larger bending moments require heavier plate thicknesses and a larger amount of stiffeners. §3.1 has shown that also the stress level does not increase and remain on an acceptable level when a more slender girder is chosen. Therefore a slender girder is chosen of 1/95, this is similar to the box girder of the Konohana bridge in Japan. The presented stability analyses in §3.1.2 shows that a more slender girder still possesses enough resistance against buckling.

Although the section modulus is hereby greatly reduced, as shown in §3.1.1 the stress level in the box girder remain on an acceptable level.

- *Sag to span ratio*

§3.3 clearly shows the importance of the sag ratio on the moment distribution. A high sag ratio showed to be favourable for the bending moment distribution, deflections of the deck and the normal force in the deck. Examples like the Konohana bridge and the Yeongjong grand bridge show that such pylon heights are feasible. Therefore a sag ratio of 1/5 is chosen.

- *Cross section pylon*

The results in 3.4 show clearly that the influence of the pylon stiffness, in longitudinal direction of the bridge on the global behaviour, is negligible. So no changes are made in the mechanical properties of the pylon.

- *Cable type*

Although the different cable show a large influence on moment distribution, the erection method is decisive for the cable type choice. For large spans it becomes impossible to use prefabricated locked coil cables and spiral strand cables. With large spans only fabricating a cable by means of aerial spinning is possible. Therefore parallel wires are chosen with a modulus of elasticity E = 205000 N/mm^2.

- *Cross section cable axial (stiffness)*

The cable cross sectional area can be altered to meet static strength criteria of the cable and girder and the deflection criteria of the girder and pylon. The axial stiffness EA of the cable is an important parameter to influence the force distribution and stiffness of the bridge. Increasing EA of the cable increases the stiffness and reduces the bending moments in the girder significantly.

For the optimized reference model a cable diameter of 210 mm is chosen, in that way it meets the static strength and stiffness criteria at the main span:

$\sigma_{bottom\ flange}$	139,6 N/mm^2	< 200 N/mm^2 the design stress at midspan
deflection midspan	422 mm	< 430 mm maximum deflection of midspan
displacement pylon	132mm	< 170 mm maximum deflection of pylon

Unity check stability according to Eurocode:

$$\frac{N_{Ed}}{\chi N_{cr}} + \frac{\beta_m M_{y,Ed}}{M_{y,Rk}} = 0.515 \le 0.9$$ Satisfies. For calculation details see Appendix 5b

Stability check Optimized model.

This optimized model is used to investigate the increasing span length of the bridge on the structural behaviour. Central issue is monitoring the required mechanical properties of the stiffening girder by an increment of the span length.

Conclusion optimized model

The optimized model for further research contains the following properties regarding dimensions of the bridge components, see Table 14.

Table 14 Member dimensions optimized model

Girder	t_flange_top_eq	40 mm
	t_flange_bottom_eq	20 mm
	t_web_eq	15 mm
	heigth	1600 mm
	width	35600 mm
Main cable	diameter	210 mm
Hangers	Diameter	55 mm
Pylon	width	2000 mm
	depth	2000 mm
	Total height	50000 mm

With the above mentioned properties the bridge satisfies the design criteria concerning static strength, stiffness and stability. But now the reduction of the bending moments in the girder is quite significant, see Figure 87. The bending moments in the girder are nearly reduced by 50 percent. Making it much more efficient and cheaper to design and produce.

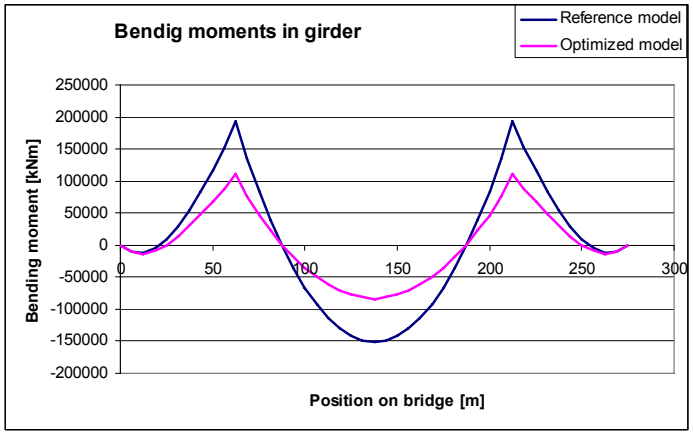

Figure 87 Bending moments along the girder in reference model and optimized model

4 Increasing span length

Now the influence of an increasing span length will be investigated. This chapter tries to find a certain span limit for the self-anchored suspension bridge.
One of the main concerns with an increasing span is the design of the stiffening girder. The increasing axial compressive force, bending moments and second order effects are determining factors in the design of the stiffening girder. Other important aspect is the erection phase of a self-anchored suspension bridge. The distance between the temporary supports can easily govern the girder design regarding the required bending stiffness. Much attention is needed for the design of a stiffening girder to meet the different requirements in finished- and erection phase of the bridge.
In this part of the research the central question :

> What are the effects of an increasing main span length on the required mechanical properties of the stiffening girder?

So the scope is trying to find a limit in span possibilities related to mechanical required properties of the stiffening girder. The considered required properties of the stiffening girder will be the bending stiffness EI_{girder} and the cross sectional area A_{box}.

4.1 Basic assumptions

To be able to increase the span in the reference model and analyzing the effect on the required mechanical properties for the stiffening girder, all other dimensional and mechanical properties should stay fixed. Only then a fair comparison of the results is allowed. Increasing the span in the reference model is done by means of several scaling factors for cable sag, side span, hanger distance, cable diameter, girder slenderness and pylon stiffness, which are fixed in the following ratio:

- sag to span ratio f/l = 1/5

This ratio determines the horizontal component of the cable force and therefore the compression force in the stiffening girder. Keeping this ratio fixed enables to discover the influence of the increment of the compression force on the behaviour of the stiffening girder.

- main span to side span ratio l/l_1 =2.4

This ratio is kept fixed to rule out any influence of main span to side span ratio on the behaviour of the stiffening girder.

- diameter of main cable to main span ratio d/l = 210/150 = 1.4

Theory shows that an increment of the span with l gives an exponential increase of the horizontal cable component H. To maintain the same level of stresses in the cable, the cross sectional area A should therefore be increased. Cross sectional area of a circular cable is proportional to the square of the diameter. So an increment of the span length with l gives a linear increase of cable diameter d (self-weight of the cable per unit of length remains constant under a fixed sag to span ratio, when diameter is unchanged). A fixed diameter to span ratio keeps the level of stresses due to self weight effects constant.

- hanger distance to main span ratio = 1/24

This ratio is kept fixed to rule out any influence of the hanger distance on the behaviour of the stiffening girder. The cross sectional area of the hangers is linearly scaled with an increasing core to cores distance of the hangers.

- deck height to main span ratio (deck slenderness) h/l = 1/95

Based on data in the literature survey, a realistic deck slenderness is chosen. As mentioned earlier a deck slenderness of 1/95*L is chosen.

- The pylon height increases with a larger span because the sag to span ratio is kept fixed. An increasing pylon height requires more stiffness. Therefore the longitudinal stiffness is scaled according to the next schematisation and formula:

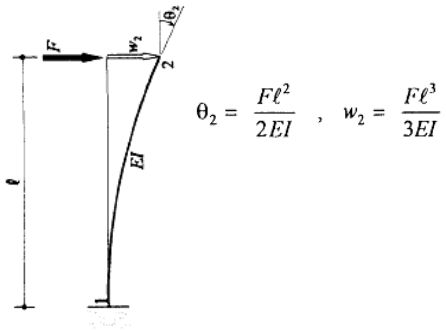

  The ratio $l^3/I_{y\ pylon}$ is kept fixed to have comparable stiffnesses of the pylon in the longitudinal direction of the bridge for increasing span lengths.
- Step size 50 metres. The span length is increased with step sizes of 50 metres. With a step size of 50 metres the span length is increased up to 500 metres. For each step an evaluation is made on static strength, stiffness and stability criteria.
  Based on the literature survey it is expected that a span length of more than 300 metres is challenging for the self-anchored suspension bridge. Earlier presented research to the buckling stability of the girder showed that this can be of importance. Secondly is the erection phase. The distance between the temporary supports can also be a decisive factor for the required mechanical properties of the girder and will we explored in this part.
- Vertical clearance: The vertical clearance under the bridge deck is kept fixed to 15 metres. The pylon height under the bridge deck is therefore also fixed on 15 metres.

Load condition
Only load case 1(traffic over the entire length of the bridge) in combination with self weight, permanent loading and pretensioning of the main cable is considered in this part of the study.

Monitoring developments
Increasing the span length of the bridge will cause several effects on static strength and stiffness. Several effects are monitored to analyse the effects and to verify if the before mentioned scaling assumptions are applicable and valid.

-Stresses in cable, girder and pylon
  Ratio stress caused by bending to stress caused by normal force
-Second order effects
-deformation of girder and pylon
-reaction forces: vertical reaction force on end support and normal force in the deck of the bridge.
-material use of cable, deck, pylon
-effects on erection of the bridge (number of temporary supports etc.)

4.2 Effects of increasing the span by scaling

Introduction

The following effects are visible when the span length of the optimized bridge model is increased to 500 metres and bridge components are scaled according to the before mentioned method, see Table 15 for the main results of member forces and deflections caused by self weight, permanent loads and traffic over the full length of the bridge.

Table 15 Main results of increasing span

L	N_{deck}	H_{cable}	Rz	δ_{main}	pylon	$M_{y;main}$	$M_{y;support}$	1st f_b	1st f_t	1st $f_{transverse}$
150	37682	19136	7679	336	87	83959	111176	0,72	4,43	5,21
200	54028	27361	11306	410	108	100200	139068	0,6	3,4	3,15
250	70944	35857	15048	468	127	115276	168634	0,52	2,81	2,1
300	88679	44773	18966	519	144	128073	198965	0,46	2,35	1,5
350	107413	54178	23091	567	161	139339	232275	0,4	2	1,12
400	127275	64153	27453	613	178	150087	270473	0,36	1,75	0,87
450	148451	74784	32089	660	196	159235	314120	0,32	1,53	0,7
500	171108	86155	37037	706	214	167839	365235	0,29	1,36	0,57

Horizontal equilibrium shows that $2*H_{cable} = N_{deck}$, but Table 15 shows a little deviation caused by the fact a very small part of the horizontal component of the cable force H_{cable} is resist as bending in the pylon's base.

A quick stiffness check ($\delta_{max\ allowable} = 1/350*L_{main\ span}$) reveals that the scaled bridges up to 500 metres performs very constant regarding the maximum allowable deflection of the main span. Figure 88 shows the constant performance regarding deflection of the main span, the unity check varies between 0.9-0.98. In this case the unity check regarding stiffness is determined by:

$UC = \delta_{max\ main\ span} / \delta_{max\ allowable}$

So on stiffness criteria, increasing the main span length up to 500 metres by means of the scaling factors, satisfies and displays a constant performance.

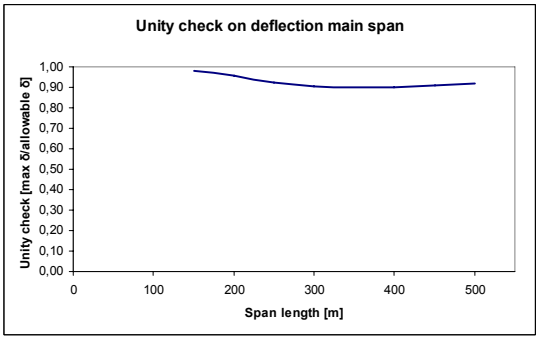

Figure 88 Development on Unity check deflection main span

Because the scaling of the bridge model up to 500m proved to be very constant regarding the global stiffness of the bridge, no adjustments are in made in the previous mentioned scaling assumptions. Now a comparison and analyses is made regarding the developments on all other important design criteria and design aspects with an increasing main span:

- Static strength
- Stability of the stiffening girder
- Frequency behaviour
- Reaction forces
- Material use
- Effects on erection of the bridge

4.2.1 Developments on static strength

To give a total view on strength criteria, the development of the level of the stresses in the box girder, the main cable, the hangers and pylon are presented in this paragraph.

Stresses in box girder

A fixed girder slenderness of $\lambda = 1/95$ is chosen for the several span lengths that are considered. The mechanical properties of the box girder for each span length are given in Table 16.

Table 16 Girder properties for the considered span lengths

Main span [m]	Slenderness λ	height [m]	A_{total} [m]	I_y [m^4]	I_z [m^4]	I_t [m^4]
150	1/95	1,6	2,18	1,26	241	3,15
200	1/95	2,1	2,2	2,17	246	5,33
250	1/95	2,63	2,22	3,4	251	8,2
300	1/95	3,16	2,23	4,9	256	11,62
350	1/95	3,68	2,25	6,68	261	15,52
400	1/95	4,21	2,26	8,78	266	20,07
450	1/95	4,74	2,28	11,1	271	24,77
500	1/95	5,26	2,29	13,77	276	30,09

In order to determine cross sectional requirements (e.g. plate thicknesses) of a box girder in the design process, the compressive and tensile stresses that are present in the top and bottom flanges are calculated. The stresses are caused by two components:

- Bending stresses, caused by the global bending moment in the girder.
- Normal stresses, caused by introduction of the compressive force in the girder by the main cable.

The sum of these two components give the total stress. The actual stresses in the top- and bottom flanges are presented in Figure 89 and Figure 90. For a total overview method of the calculation of these stresses, reference is made to Appendix 7 Stress calculation in reference model.

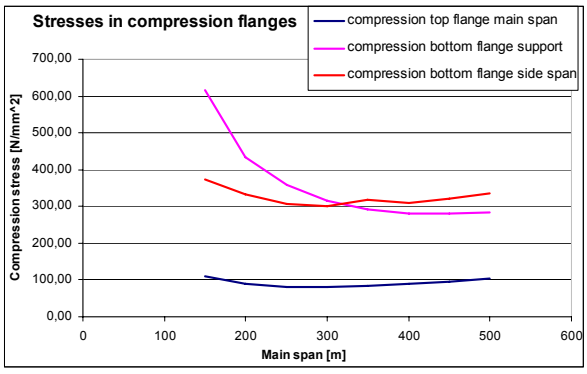

Figure 89 Stresses in compression flanges

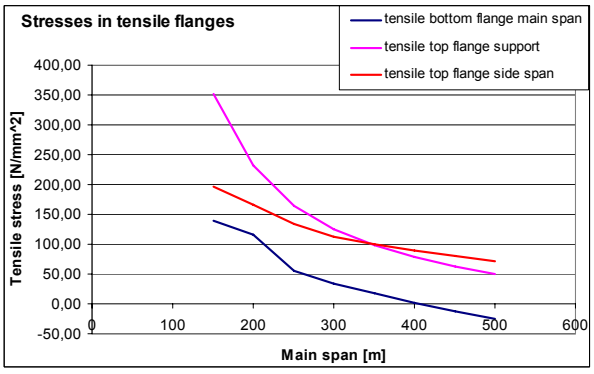

Figure 90 Stresses in tensile flanges

The stresses in the compression flanges of the side and main span of the girder have a nearly constant development according to Figure 89. This indicates that the chosen girder dimensions for each considered span length are properly chosen.
The significant decrease of the compression stresses at the support location is caused by the fact that the hogging moment (but also the sagging moment at main span) does not increase that rapidly with an increase of the main span. In case of an unsupported main span, for instance a simply supported beam, an increase of the main span length l will result in an increase of the maximum sagging moment by l^2. As mentioned earlier the girder of a suspension bridge is continuously stiff supported by the hangers, so increasing the main span of the bridge with a length l does not result in an increase of the global bending moments of l^2 but much less, see Figure 91 where the dotted line represents a development of the bending moment with an increase by l^2 and the actual development of the maximum bending moments in the continuous spring supported deck in main span of the bridge.

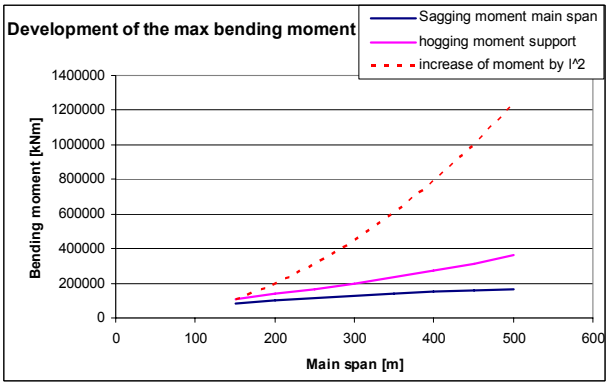

Figure 91 Development of the maximum bending moment in the girder

Figure 90 shows that also the stresses in the tensile flanges of the box girder display an overall decrease on all locations. To explain this development an analyses is made on the stress calculation. The total stress in a flange is calculated by:

$$\sigma_{top} = -\frac{N_{Ed}}{A_{box}} - \frac{M_y}{W_{eff;top}}$$

$$\sigma_{bottom} = -\frac{N_{Ed}}{A_{box}} + \frac{M_y}{W_{eff;bottom}}$$

Besides the confined development of the bending moments other causes for this decrease in tensile stresses in the flanges of the box girder are:

- The chosen girder properties for the considered span length up to 500 metres. For each span the same slenderness λ = 1/95 of the box girder is chosen. So the height of the box girder is with each increment of the main span linearly increased. Section properties like the moment of inertia I_y and the section modulus W_{eff} (for calculation the stresses) increase also. The moment of inertia of a box girder is determined by: $I_{y;total} = I_{y;eigen} + I_{y;steiner}$.
  In which $I_{steiner}$ is the dominating component which is proportionate to the square of height h of the girder (see Table 16). This indicates that the section modulus of elasticity W_{eff} increases approximately linearly according to: $W_{eff} = \frac{I_y}{e_y}$. This combined with the fact that the bending moments do not increase that significant, the bending stresses decrease with an increasing span length, see also Figure 90.

- The contribution of the normal force to the total stresses in box girder.

A graph is presented in Figure 92 which clearly shows that with an increasing span the stress caused by the compressive force in the girder become dominant over the bending stresses. Therefore a decreasing development is visible in tensile stresses presented in Figure 90. Compressive stresses become dominant in the cross section of the box girder for an increasing span.

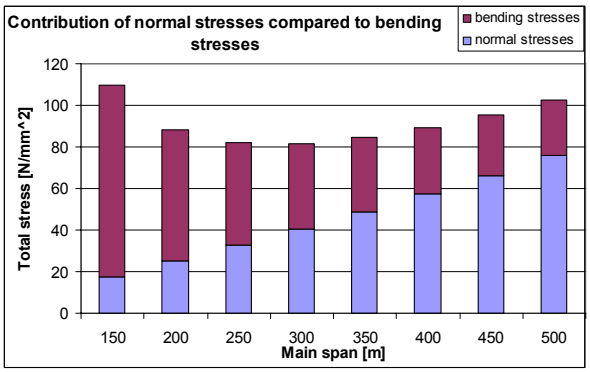

Figure 92 Contribution of the normal compressive stress in the top flange in the main span

Even a point can be reached where compression stresses can occur in the normally tensile bottom flange of the box girder in the main span, see Figure 90, at a main span of 400 metres. This will have effect on the design of the bottom flange in the mid of the main span, if compression stresses occur also here, than local instabilities have to be checked and it is likely that more stiffeners have to be applied (as is the case for the compressive bottom flange at support location at the pylon).

Overall conclusion is that the level of stresses are of acceptable levels, when the span is increased, and that the normal stresses become dominant over the bending stresses.

Stresses in main cable and hangers

The applied main cable and hanger properties for each span length are given in Table 17.

Table 17 Main cable and hanger properties

Main span [m]	d_{cable} [mm]	A_{cable} [mm^2]	d_{hanger} [mm]	A_{hanger} [mm^2]
150	210	34636	55	2376
200	280	61575	64	3217
250	350	96211	71	3959
300	420	138544	78	4778
350	490	188574	84	5542
400	560	246301	90	6362
450	630	311725	95	7088
500	700	384845	100	7854

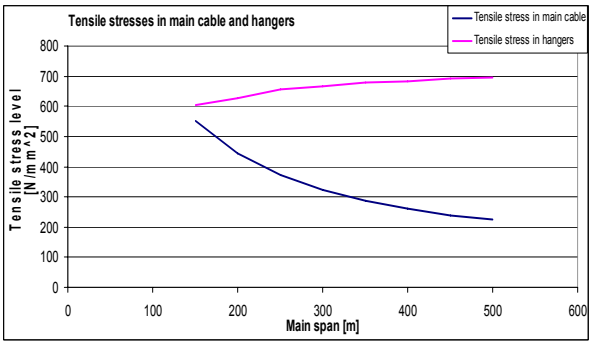

Figure 93 Stress level in main cable and hangers

The level of the tensile stress in the decisive hanger stays approximately on the same level but for the main cable a decreasing stress level is clearly visible in Figure 93. This result indicates that stiffness is the governing design criteria for suspension bridges, even for relative short spans up to 500 metres. The amount of material required for the main cable becomes with an increasing span length less efficient on strength, the additional required main cable area is needed to satisfy stiffness criteria, see also Figure 87.

Stresses in pylon

Without any provisions, an increasing main span would increase the bending moments at the pylon drastically and can therefore become critical, see Figure 94.

In practice the bending moments can artificially be reduced to zero by giving the pylon an outward displacement to counteract the inward displacement caused in finalized stage of the bridge. This method can result in a completely vertical pylon with zero bending[21] in the final self-weight loading condition. Therefore it has no sense to further analyze the stress conditions in the pylon.

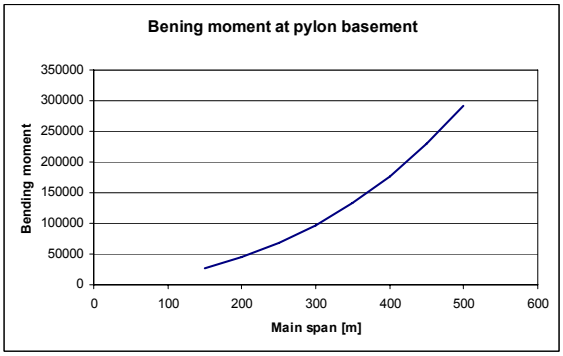

Figure 94 Bending moment at pylon base

4.2.2 Developments on buckling stability of the stiffening girder

With the same approach as described earlier, presented in Figure 95, the buckling force is determined for the stiffening girder of the bridge. For each increment of the main span, with step sizes of 50 metres, the buckling force is determined. An additional force of $\Delta F = 400000$ kN has been applied in order to obtain visible second order effect in the deflection of the stiffening girder.

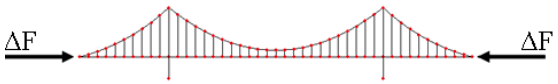

Figure 95 Additional F to determine buckling force

Figure 96 presents the results for buckling force calculation for each considered span length up to 500 metres for a loading combination including self weight, permanent loading, traffic load over the full length of the bridge and pretensioning of the main cable.

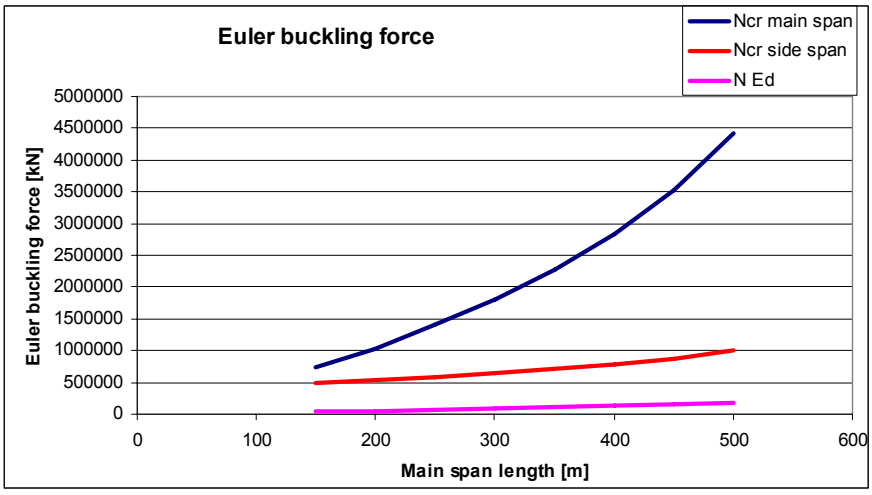

Figure 96 Development of the Euler buckling force deck as a function of an increasing main span

Again buckling of the side span remains governing over bucking of the main span of the girder. The buckling force N_{cr} for the side span is well below the N_{cr} of the main span, even for an increasing main span up to 500 metres.

[21] Gimsing, N.J., *Cable supported Bridges*, Wiley&Sons, 1998

The reason for the increased Euler buckling force for an increasing span is the fact that height of the box girder is linearly increased with the main span. This will increase the moment inertia more than quadratic, see Table 16, and so the bending stiffness is increased with the same proportion.
If the above presented graph is expressed in the so called n-value than it becomes visible that buckling is getting more and more critical with an increasing span. When the n-value defined as:

$$n_{side\_span} = \frac{N_{cr;side\ span}}{N_{Ed}} \text{ and } n_{main\_span} = \frac{N_{cr;main\ span}}{N_{Ed}}$$

The n-value for each considered span lengths are given in Table 18.

Table 18 n-values for main and side span

Main span [m]	n-value main span	Side span [m]	n-value side span
150	19,8	63	12,9
200	19,2	83	9,9
250	19,7	104	8,3
300	20,4	125	7,3
350	21,2	146	6,6
400	22,3	167	6,2
450	23,8	188	5,9
500	25,8	208	5,8

With the earlier given general used guidelines with respect to interpreting the n-values:

1 < n < 2	wrong design
2 < n < 3	design problems to be expected
n > 3	proper design, however, geometrical non-linearity should be taken into account
n > 50	consequences of geometrical non linearity can be neglected

The following conclusions can be made:

- Buckling of the main span is a downward buckling mode and would therefore encounters upward resistance by the main cables and hangers. Buckling of the side span is an upward buckling mode and would therefore encounter no resistance by the main cable and hangers.
  The upward buckling of the side span occurs at a much lower buckling force N_{cr} and is decisive over buckling of the main span.
- The buckling stability of the side span girder becomes more and more a critical design issue with an increasing span up to 500 metres. The so called n-values given in Table 18 indicate that the consequences on geometrical non-linearity have become more evident with an increasing main span. But given the guideline regarding the interpretation of the n-value, the considered span lengths are still considered to be of proper design because the n-value is in all cases well above 3.
- The given approach to research the buckling stability of the girder presented in this part has shown that buckling of the main span is not decisive. In this approach a stiffening girder is chosen with the same slenderness along the complete length of the bridge. With n-values of 20 or more (see Table 18), regarding buckling of the main span, a much more slender girder could be chosen for the main span. This can be of great contribution to the reduction of material use.

So with respect to the buckling stability of the stiffening girder, a self-anchored suspension bridge is possible up to a main span of 500 and maybe even beyond that. Assuming a limitation for the girder slenderness of about $\lambda = 1/100$ regarding the buckling stability of the deck is point of discussion.

4.2.3 Frequency behaviour

A good indication for the resistance against flutter is the development of the ratio between the torsional and bending frequency.
With an increasing main span both bending and torsional frequency decrease significantly but the ratio between these frequencies stay well above the general accepted level of 2, see Table 19. When this ratio is above 2 than the structure should have enough resistance against flutter instability.

Table 19 Frequency ratio for each span length

Main span [m]	1st $f_{bending}$ [Hz]	1st $f_{torsion}$ [Hz]	Ratio f_t/f_b
150	0,72	4,43	6,2
200	0,6	3,4	5,7
250	0,52	2,81	5,4
300*	0,46	2,35	5,1
350	0,4	2	5,0
400	0,36	1,75	4,9
450	0,32	1,53	4,8
500	0,29	1,36	4,7

* This main span length is the same as the Yeoungjong Grand Bridge. The natural frequencies for this bridge are:
1st $f_{bending}$ = 0.454 Hz
1st $f_{torsion}$ = 1.223 Hz
The frequencies calculated in this research are nearly the same, only for the torsional frequency there is a deviation visisble. This is caused by the fact that in in the Yeoungjong bridge a truss girder was applied which has in general a lower torsional stiffness than box girders (used in this research).

A decreasing ratio between the bending and torsional frequency indicates that the bridge structure becomes more sensitive for flutter. This is visualized in Figure 97 where the development of the critical wind speed for flutter and vortex is plotted for the given bending and torsional frequencies in Table 19.

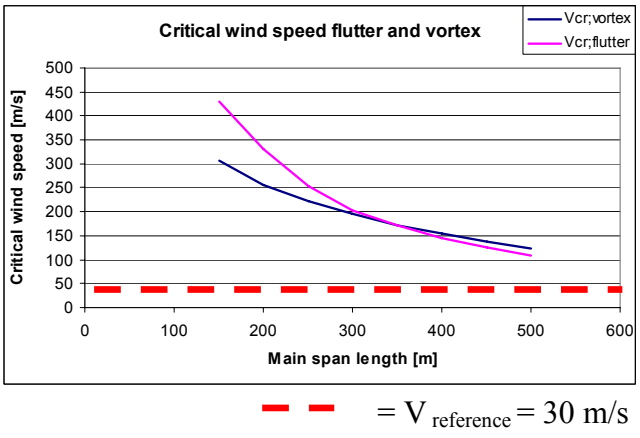

Figure 97 Critical wind speed for flutter and vortex as a function of the main span

The critical wind speeds as presented Figure 97 are determined by:

- Vortex critical wind speed: $V_{cr;vortex} = 12 * f * d_4$

For vortex it should be verified that $V_{cr;vortex} > V_{reference}$

- Flutter critical wind speed: $V_{cr;flutter} = 4 * f_t * b * \left(1 - \frac{f_b}{f_t}\right) * \sqrt{\frac{m * r}{\rho * b^3}}$

For vortex it should be verified that $V_{cr;flutter} > 1.3 * V_{reference}$

$V_{reference}$ is given also by the Eurocode NEN-EN-1991-2-4 Annex A. For the Netherlands counts:

$V_{reference} = 30$ m/s

Figure 97 shows that the flutter phenomena becomes the governing dynamic response phenomena when the main span length is getting larger. But for vortex shedding as well as flutter, a self-anchored suspension bridge up to 500 metres should be stable, the critical wind speed of both vibration motions is well above the reference wind speed $V_{reference}$.

Wake galloping and Stall flutter are not considered because the following criterion is not met:
$b<4*d_4$ in which b = deck width and d_4 = structural height of box girder.
So the bridges up to 500 metres considered in this study are not vulnerable for these vibration motions.

4.2.4 Developments on reaction forces

The reaction forces at the end support have to be anchored into a:

- Vertical anchorage, which resist the vertical component of the cable force.
- Horizontal anchorage, which resists the horizontal component of the cable force.

As the horizontal reaction force is resisted in the deck, only a vertical reaction force has to be resisted externally. As described earlier in the literature survey of this study, there are two ways to anchor this uplifting vertical component of the main cable force:

- tie down cables/structure. The deck is vertically anchored and tied down to a foundation which activates a ground mass to compensate the vertical action. Also a big counter mass like a concrete block could be applied.
- a bracket at the location of the connection of the main bridge and approach bridge. The weight of the approach bridge will balance the vertical force.
- a combination of these two mentioned methods.

Governing loading combination for the vertical reaction force in the end support is when the side spans are unloaded, then no reducing effect of the traffic loading on the side span is present. Figure 98 shows the increase of the vertical reaction force in the end supports for an increasing main span.

The critical issue will be the horizontal anchorage of the main cable, see Figure 98. The combination of the rapidly increasing horizontal cable force and the much more complex nature of the horizontal anchorage makes it a bottleneck in the design process.

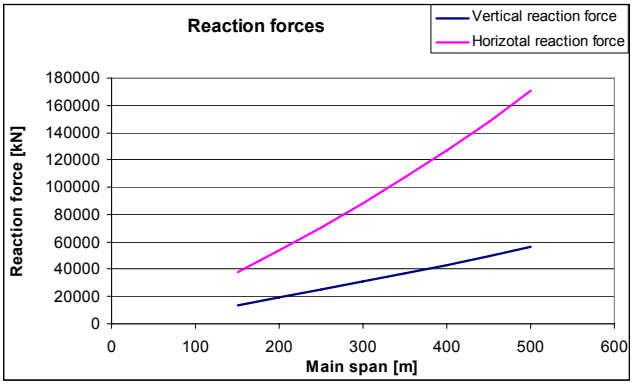

Figure 98 Reaction forces in end supports

The horizontal anchorage is a much more complex structure due to the fact that the main cable has to be splayed in many individual strands which all have to be anchored individually. Many provisions like strands shoes, sockets, steel plates and stiffeners are required to introduce the cable force in the bridge deck, see Figure 99.

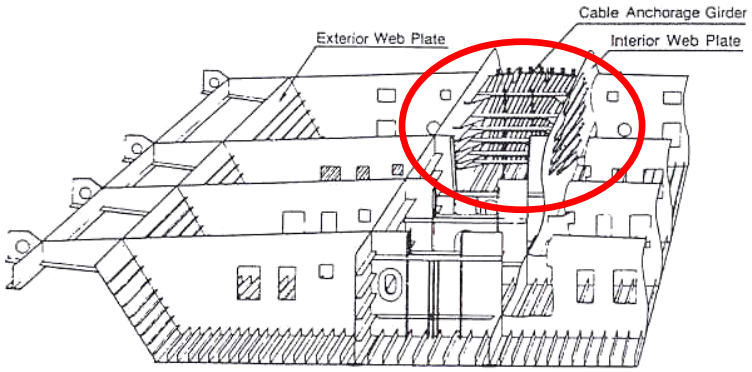

Figure 99 Cable anchorage Konohana Bridge

The vertical anchorage is a relatively less complex structure then the horizontal cable anchorage. A vertical counter force has to be activated which is much more easy to introduce into a heavy concrete block or a bracket connection to the approach span.

4.2.5 Material use

This part gives an estimation of the amount of steel use in the self-anchored suspension bridge. The main bridge components like deck, pylon, main cable and hangers are executed in steel in this study. The total steel use is sum of these components.
For each span up to 500 metres the amount of steel has been calculated and a differentiation is made to the steel use of each of the before mentioned bridge components.
Basic assumptions for the determination of the material use include:

- Girder: material use for the girder includes
  -Top- and bottom flanges
  -Webs
  -Longitudinal stiffeners on top and bottom flanges and web
  -An estimate of diaphragms and bracing with an intermediate distance[22] of 2.5 times the construction depth h of the box girder
- Cables: effective area of the main cable and hangers
- Pylon: estimation of the material use for the box section of the pylon includes longitudinal stiffeners.

Figure 100 shows the total amount of steel used for a main span up to 500 metres. For an increasing main span the required amount of steel grows almost linearly. If a differentiation is made to the several before mentioned bridge component it becomes clear that the dominant part in material use is the stiffening girder. Figure 101 shows that the girder consumes by far the most amount of steel. But it also becomes visible that with an increasing span the required amount of steel in the main cable is getting significant.

[22] Romeijn, A. *CT5125 Steel Bridges Part 1&2*. Faculty of Civil engineering and Geosciences

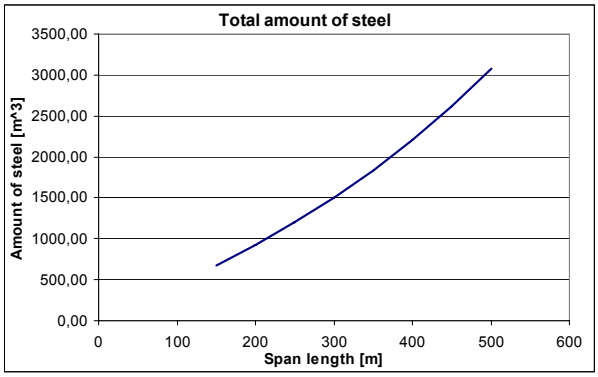

Figure 100 Total amount of steel

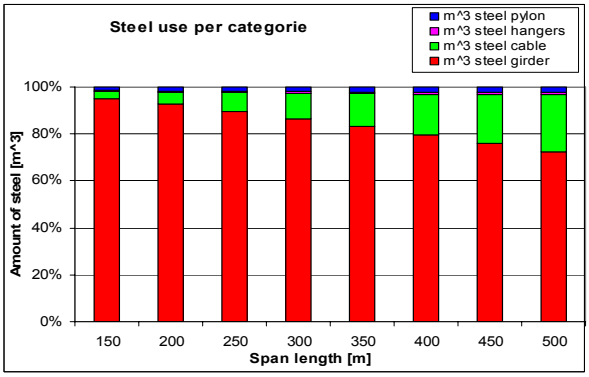

Figure 101 Steel use per category

The total steel use can also be expressed in the steel use per meter of length of the bridge. Table 20 gives an estimation of the steel use per meter of bridge based on the assumption of this research.

Table 20 Steel use per meter

Main span length [m]	150	200	250	300	350	400	450	500
Steel use [ton/m]	19,1	19,7	20,5	21,4	22,4	23,6	24,9	26,3

Regarding these findings the following remarks have to made:

- As Figure 101 clearly shows is that much attention needs to go out for the design of the stiffening girder. Saving material in this bridge component can reduce the total amount of steel use significantly. Weight saving can be achieved by adjusting the girder slenderness, reducing the structural height improves the self weight. But this will have effect on the buckling resistance, frequency behaviour and erection phase of the bridge.
- Figure 101 shows also a development of the relatively growth of the required steel for the main cable. Although this material (high strength steel) is more expensive than the structural steel used for the other bridge components, this bridge element has the most efficient load transfer (because it is only tensile loaded) and it is therefore profitable to put more material in the main cable in order to be able to reduce the material use in the stiffening girder. Because the stiffening girder is loaded with large bending moments, this bridge component is much less efficient in material use because many provisions have to made with respect to local stability within the plated box girder.
  Also the presented parameter study has shown that increasing the axial stiffness of the main cable (putting more material in the cable) reduces the bending moments significantly in the stiffening girder.

So an optimization can be made with respect to the ratio of axial stiffness of the main cable and the required material use for the box girder. Putting more material in the main cable can reduce the required mechanical properties and material use of the stiffening girder. In that way a significant reduction can be achieved in the total material use and therefore the costs.

4.2.6 Effects on the erection

There are two main erection methods to distinct nowadays:

- Cantilever method by means of the cable stayed method
- Erecting by use of temporary supports

For a more detailed description of both methods, reference is made to the literature survey of this study, part 6.2.1.
Both methods have in common that erection of the deck has to take place prior to the erection of the main suspension cable.
Great advantage of the first mentioned method is the elimination of temporary supports in the navigation channel. But the fact is that this method implies building a cable stayed bridge first, then erect the main cable and subsequently take away the cable stays. This will justify technically and economically the choice for a cable stayed bridge, and not a self-anchored suspension bridge. Only esthetical reasons remain as justification to build a self-anchored suspension bridge.
The second mentioned method, erecting on temporary supports, is nowadays the most accepted method to erect a self-anchored suspension bridge. Both Konohana bridge and Yeoungjong Grand bridge (and many others) have been built using this method. The economical and technical feasibility of this erection method depends on several factors like:

- The number of temporary supports
- The distance between the temporary supports

These two factors greatly influence the design of a self anchored suspension bridge in costs, erection and structural properties of the stiffening girder. An optimum should be achieved in the number of- and distance between the temporary supports in order to reduce the cost and the need for excessive bending stiffness of the stiffening girder.

Number of- and distance between temporary supports
For the considered bridges in this study with a main span up to 500 metres, an exploration is given now on the consequences for erection on temporary supports.
A calculation is made to determine the maximum free span length of the box girder based on the assumptions that:

- The box girder is simply supported between two temporary supports. So for the effective width calculation only the β_1 factor is calculated for sagging bending.
- Only self weight of the steel box girder is taken into account, because no traffic loading and permanent loading like asphalt occurs in this stadium of the bridge erection.
- According to NEN-EN 1991-2-6 part 4.1.3, the safety factor for self weight during erection $\gamma_{G;sup} = 1.05$
- The maximum bending moment in the box girder during this stage is determined by the distance between the temporary supports according to:

$$M_{\max;sagging} = \frac{1}{8} * q_{selfweight} * l_{temp.\sup.}^{2}$$

Based on these assumptions the maximum achievable free span length of the box girders (applied in the bridge models up to 500 metres) are given in Table 21.

Table 21 Achievable free span length and number of required temporary supports

Main span length [m]	Side span length [m]	Height box girder [m]	Maximum free span length [m]	Temporary supports in main span	Temporary supports in each side span	Total temporary supports
150	63	1.6	56	2	1	4
200	83	2.1	72	2	1	4
250	104	2.6	95	2	1	4
300	125	3.2	122	2	1	4
350	146	3.7	144	2	1	4
400	167	4.2	164	2	1	4
450	188	4.7	180	2	1	4
500	208	5.3	196	2	1	4

This table shows that for each span length the box girder, with a slenderness of $\lambda = 1/95$, has enough stiffness to span over 1/3 of the main span, meaning that 2 temporary supports are sufficient for each considered span length.
Also a temporary support in the side span is necessary for all span lengths, making the total required temporary supports 4. But Table 21 shows that the temporary supports in the side span can be eliminated if:

-A less slender deck is chosen, in that way the section modulus W_{eff} is increased and therefore the maximum free span length during erection is bigger.

-The side span length is reduced. In that way the free span length of the box girder is sufficient enough to span the complete side span in erection phase.

Elimination of the temporary supports in the side span reduces the total number of required temporary supports to 2. But in general it is not a problem to situate temporary supports in the side span, it is the main span where the temporary support will cause more problems.

Required lifting capacity

With 2 temporary supports in the main span, huge deck sections have to be lifted by a (floating) crane or strand jack systems. An increasing span of the bridge has large consequences on the required lift capacity of the crane. Table 22 gives an indication of the required crane capacity to lift the huge deck section (approximately with a length of 1/3 of the main span) on two temporary supports in the main span.

Regarding erection cost an optimization has to be made with respect to the number of temporary supports and the lift capacity of the (floating) crane.

Main span [m]	Deck section length [m]	Crane capacity [tons]
150	50	945
200	67	1269
250	83	1597
300	100	1931
350	117	2268
400	133	2611
450	150	2958
500	167	3309

Table 22 Required lifting capacity

4.3 Evaluation and conclusion for an increasing span length

Several design issues have been evaluated in this chapter with respect to an increasing main span of a self-anchored suspension bridge. This part will briefly discuss these design criteria and mention the critical issues which require consideration in the design process of a self-anchored suspension bridge in general.

- *Stiffness*

An important aspect to influence the force distribution in a (self-anchored) suspension bridge is the ratio between the deck bending stiffness EI_{girder} and the axial stiffness EA_{cable}. It is more profitable to put more material in the main cable (increasing axial stiffness) in order increase the stiffness of the bridge and to reduce the bending moments in the stiffening girder. Designing and dimensioning structural bridge members under bending is always less effective and more material consuming then that of members under tensile loading, such as the main cable.
The stiffness criteria, expressed in allowable deflections, are easily met by choosing the proper dimension for the main cable. For a bridge span length up to 500 metres, global stiffness is not a critical design issue.

- *Static strength*

The stress levels in main cables have shown that stiffness is the governing design criteria over static strength criteria of the main cable.
For the box girder a distinction can be made between tensile and compressive area for the top and bottom flanges. Critical area is the support of the girder near the pylon. The large hogging moment introduces high compressive stresses in the bottom flange at this location. But in practice these stresses can be adjusted by means of support displacements in construction phase of the bridge.
A second critical issue is that for an increasing span, the compressive stresses (introduced by the main cable) in the girder become dominant. This can have consequences on the local stability for the normally tensile bottom flange in the mid of the main span. More stiffeners are required then on the bottom flange in the main span.
But overall for an increasing span length, stress levels in the box girder are of manageable levels. Local additional plate thicknesses and stiffeners are required for some locations depending on the span length.

- *Buckling stability of the stiffening girder*

An upward buckling of the side span is the decisive buckling mode of the stiffening girder. Downward buckling of the main occurs at a much higher buckling force N_{cr} than for the side span.
Research to the buckling phenomena of the side span has shows that with an increasing span, the resistance against buckling of the side span reduces. Up to a main span length of 500 metres, buckling of the stiffening girder should be analyzed in the design process but it is possible to reach such a span length.
The chosen slenderness $\lambda = h/l_{\text{main span}}$ of about 1/95 (until now the most slender deck ever applied in a self-anchored suspension bridge; Konohana bridge in Japan) of the box girder is sufficient to reach a span length of 500 metres. With respect to buckling of the main span of girder, even a much more slender deck in the main span seems possible. Investigating the possibility of a variation of the deck slenderness in longitudinal direction of the bridge (application of stiffer deck in the side than in the main span) could greatly reduce the material use.

- *Frequency behaviour*

Regarding the natural frequencies, the torsional and bending frequencies are well separated for a span length up to 500 metres when a box girder is applied. The ration between $f_{bending}$ and $f_{torsion}$ is well above 2. So the self-anchored bridge type in this research has enough resistance against flutter.
For an increasing span, flutter becomes more critical than vortex shedding of the deck. But the critical wind speed for both vibration motions is well above the reference wind speed $V_{reference}$ indicating that bridges up to 500 have enough resistance against these two phenomena.
Attention has to go out to the aerodynamical shape of the girder. For cable supported bridges it is generally advised to execute wind tunnel test to check if the bridge model has enough resistance against vortex and flutter girder instabilities.
The natural frequencies obtained in this research give room for the possibility of choosing a more slender deck than $\lambda = 1/95$ that is chosen in this research.

- *Reaction forces*

Due to the complex nature of the horizontal anchorage of the main cable, the horizontal anchorage requires much attention. For an increasing main span, the horizontal cable force increases rapidly and is has enormous consequences for the horizontal anchorage. The introduction of the horizontal cable force requires many provisions like anchor shoes, plate stiffeners. With an increasing main, the main cable diameter increases and contains more strands to be anchored.
For the large span bridges an anchorage in which the cable is looped around the deck is worth consideration (as applied in the East Bay bridge, see 5.5.4 of the literature survey)

- *Material use*

By far the biggest part of material use is required for the stiffening girder. For a bridge model with a main span up to 500 metres, at least 70 percent of the total material use is taken by the stiffening girder. And for an increasing main span also the contribution of the material use in the main cable becomes significant. Up to 25 percent of the material use can be taken by the main cables and hangers.
So the biggest cost reduction can be achieved by saving material in the stiffening girder. This can be achieved by:

-Reducing the slenderness of the girder in the main span. As shown earlier, for buckling resistance a more slender girder can be applied in the main span than in the side span.
-Increasing the axial stiffness EA_{cable} in order to reduce the bending moment in the girder.
-Optimization of plate thicknesses along the length of the girder.

- *Effects on erection of the bridge*

With a slenderness of the girder of $\lambda = 1/95$, a free span length of more than one third of the main span can be reached. This results in 2 required temporary supports in the main span and one in each side span. The temporary supports in the side span can be eliminated by:

-Reducing the side span length
-Increasing the stiffness of the girder, keeping attention on the buckling stability of the side span is necessary.

Erection of the deck on temporary supports results in a relatively high required stiffness of the deck to reach a certain free span length. Not the stability phenomena of the deck but the erection method is governing for the required slenderness of the deck.

Conclusion

This chapter has presented the exploration of the span possibilities of a self-anchored suspension bridge with a main span up to 500 metres. It has been shown that it is technically feasible to achieve a span length up to 500 metres. The expected problems regarding the buckling stability of the main girder has turned out to be feasible for span lengths up to 500 metres. Main topics of attention for designing a self anchored suspension bridge with a large span are:

-Support conditions of the girder at the pylon. Large compressive and tensile stresses in the flanges of the flanges of box girder can occur. The hogging moment at this location introduces high stresses in the flanges. Attention has to go out for support displacement during erection of the bridge which can reduce the stresses in finalized condition of the bridge.

-The possibility of compressive stresses in the bottom flange of the box girder in the main span. This zone is in general an area where tensile stresses occur due to the global bending moment. So in normal tensile stress condition in the bottom flange of box girder in the mid of the main span, no local buckling stability has to be considered. But for a larger getting main span of a self-anchored suspension bridge, compressive stresses can occur in the bottom flange at the mid span, see §4.2.1 for a main span length of about 400 meters and beyond that. This requires more longitudinal stiffeners to resist local buckling instabilities which is more material consuming and therefore more costs are involved.

-Required slenderness of the box girder is mainly dominated by the erection method on temporary supports and not so much the buckling stability. Depending on the circumstances during erection the slenderness of the box girder is can be even more slender than $\lambda = 1/95$.

-Buckling of the stiffening girder. There is a difference in the buckling force N_{cr} of the side- and main span. Based on the assumptions in this research, buckling of the girder in the side span is decisive. A chosen girder slenderness of $\lambda = 1/95$ is sufficient to resist buckling. For the main span even a more slender girder is possible because the n-value is about 20-25 for a span length up to 500 metres. A slender girder can be of great contribution of cost reduction, since at least 70 % of the total steel use in the bridge is taken by the girder.

-Horizontal anchorage. Introducing the cable force in the deck requires attention for splaying the and individually anchoring of the steel strands. With an increasing main the axial compressive force increases quickly.

-Erection method. Stiffness of the deck and the related free span lengths determine the required number of temporary supports during erection. Increasing the stiffness of the deck also increases the maximum distance between the temporary supports but requires more lifting capacity and is more material consuming.

-In this case a sag over span ratio has been chosen of 1/5 in order to reduce the bending moments and normal force in the girder. Regarding the buckling stability of the girder, which is sufficient with a girder slenderness of $\lambda = 1/95$, a smaller sag ratio can be considered which increases the normal force the deck. Decreasing the sag to span ration contributes to the reduction of the main cable length and pylon height.

5 Erection aspects of the New City bridge at Nijmegen

A successfully design of a self-anchored suspension depends also on the feasibility of the erection method. As shown earlier the required mechanical properties of the girder can depend greatly on the chosen construction method. So the way of construction should already be considered early in the design process.
Choosing an erection method mainly depends on local conditions of the surrounding area of the construction site of the bridge and criteria imposed by the client. Therefore it is hard to conclude something in general for a construction method in case of self-anchored suspension bridges. To make an assessment for the construction method, the situation of Nijmegen and the Waal river is used again.
A brief exploration is made to point out the critical issues in erecting a deck prior to the main cable.

5.1 Criteria Nijmegen City

Chosen design by engineering office Iv-Infra
The feasibility and design of a self-anchored anchored suspension bridge for Nijmegen was researched by engineering office Iv-Infra Amsterdam. This design proposes a main span of 335 metres which would mean that the longest existing span is exceeded by more than 10 percent.
To explore and evaluate a construction method for a self-anchored suspension bridge at Nijmegen presented in this chapter, focus is made on a main span of 350 metres. In that way nearly the complete river is spanned.

Design criteria regarding erection
Several design criteria are defined by the city council of Nijmegen regarding the erection of the New City Bridge. The following statements[23] count for the Waal river near Nijmegen where the construction site is located:

Part 3.1.3 Navigation clearance

ID	Description
11,2,4,2	The minimal required vertical navigation clearance of 9.10 metres should be available for at least 80% of the of normal navigation width (265 metres)

Part 3.5.4 Erection

ID	Description
11,6,5,3	Shipping traffic must be able to continue and encounter as little nuisance as possible during erection of the bridge
11,6,5,4	No obstacles are allowed in the navigation channel
11,6,5,5	The minimal required navigational clearance (width and height) may be temporary altered during erection
11,6,5,6	The minimal required vertical navigation clearance may not be smaller than that of the Railway bridge that is in the vicinity of the New City Bridge
11,6,5,7	The normal navigation width (265 metres) should be maintained as much as possible during erection of the bridge. A partial obstruction of the navigation channel is allowed incidentally

[23] PvE Stadsbrug versie 1_0 20juni06.pdf, collected from the website:
http://www2.nijmegen.nl/mmbase/attachments/359936/PvE_Stadsbrug_versie_1_0_20juni06.pdf

So no clear restrictions are defined for the possibility of- and distance between temporary supports in the Waal river. Temporary and partly blocking of the navigation channel is allowed, enabling the erection on temporary supports in the Waal river for constructing a self-anchored suspension bridge.

5.2 Exploration of erection methods

A short exploration is given on the erection methods of the two most significant self-anchored suspension bridges; Konohana and Yeoungjong Grand bridge. And because of the unique character and construction method, the construction method of the Nescio bridge in Amsterdam is given.

5.2.1 Existing methods

An exploration of existing and most recent construction methods comprise the erection on temporary supports and utilizing temporary cable stays.

Construction Konohana bridge
The main aspects in the construction of the Konohana Bridge are presented in Appendix 8a Erection of Konohana Bridge. The main features are summarized here:

- Distance between temporary supports of 120 metres
- Heaviest section lifted by a floating crane of 2670 tons
- 2 temporary supports in the main span
- 1 temporary in one of the side spans. This side span was situated partly over land where the crane could not reach to lift a deck section. There it needed temporary support in one of the side span.
- The deck section in the middle was erected at the end a lifted on two ends of deck which cantilevered out over the temporary supports.

Construction of Yeongjong Grand Bridge
The main aspects in the construction of the Konohana Bridge are presented in Appendix 8b Erection of Yeoungjong Grand Bridge. The main features are summarized here:

- Distance between temporary supports of about 100 metres
- Heaviest section lifted by a floating crane of 3072 tons
- 2 temporary supports in the main span
- 1 temporary in each of the side spans. The deck section in the middle was erected at the end a lifted on two ends of deck which cantilevered out over the temporary supports.

Construction Nescio bridge Amsterdam
The main aspects in the construction of the Konohana Bridge are presented in Appendix 8c Erection of Nescio bridge The main features are summarized here:

- Heaviest section lifted by a floating crane of 570 tons[24]

[24] Habraken, A., Y. Ichimaru, *Nesciobrug Amsterdam, Met een slinger over het kanaal*, Bouwen met Staal 193, December 2006

- The lifted deck had total a length of 200 metres.
- The deck was completely prefabricated and transported on a barge to Amsterdam, travelling over more than a 100 km.
- Deck was lifted in one piece (of 200 metres) and supported on the permanent end supports and by temporary stay cables attached to the pylon.

During the erection of the Nescio bridge temporary stay cables were used. Given the relative light weight of the deck section of 570 compared to sections used for the Konohana and Yeoungjong Grand bridge, it was possible to use only two stays in the main span to support the deck.

Conclusion
This brief exploration shows that these three most recent self-anchored suspension bridges exhibit two main similarities in erection, i.e.:

-lifting large and heavy deck section up to almost 3100 tons with lengths of 100-200 metres.
-temporary support of the deck by means of a temporary piers for heavy deck sections
-temporary support of the deck by means of temporary stay cables for relatively light weigh sections.

5.2.2 Alternative methods

Some possibilities are briefly discussed in order to explore the erection of the main cable prior to the deck.

Possibility of erecting main cable prior to the girder
This method would enable a construction sequence that is similar to a conventional suspension bridge where the main cable is erected first and the deck is lifted in sections and connected to the hangers. In this way the temporary supports are eliminated. But with an absence of an external anchorage the horizontal cable force has to be resisted by means of :

- Compressive struts in the side span

To resist the horizontal cable force, a compressive strut is needed in the side span that reaches from the end support to the basement of the pylon.

Figure 102 Compressive strut in each side span

The compressive struts require an enormous length and therefore very prone to buckling. Also the pylon's basement will have to resist a horizontal component which has consequences for the pile foundation that is mainly designed for vertical loading and bending moments.

- Bending of the pylon

The earlier erected side spans (with or without the use of temporary supports) could be utilized as a compressive strut to stabilize the horizontal cable force.

Figure 103 Utilizing the erected side span

The deck will have to be horizontally fixed at the pylon and introduce the horizontal force in the pylon resulting in a bending moment. Also the foundation of the pylon has to resist a horizontal force which is not a desirable situation.

- Erecting a temporary external anchor block

The self weight condition of the bridge is so large compared to the traffic loading condition, that the required dimensions for a temporary external anchorage are almost that of an anchorage required for a finalized situation of the bridge. This method will justify for a permanent external anchorage resulting in a conventional suspension bridge and is therefore not logical to consider.

Figure 104 Temporary external anchorage

To be able to erect the main cable prior to erection of the deck, requires drastic temporary measures and will not be further considered.

Nijmegen city

Based on these findings a point of departure is defined to explore a construction method for a Bridge in Nijmegen. Based on the heavy required box section for the city bridge at Nijmegen the generally most accepted construction method will be briefly discussed in the next paragraph: constructing with temporary piers in the Waal river.

Points of interest are evaluating the consequences for the:

-distance between temporary piers
-required dimensions of the deck
-required lifting capacity of the (floating) crane
-structural consequences for the deck
-distance of cantilevering over the temporary supports

Point of departure will be a bridge with a main span of 350 metres, similar to the design proposal of engineering Iv-Infra offered to the city council of Nijmegen.

5.3 Constructing with temporary piers in the Waal river

First a brief exploration is given in the achievable maximum distance between the temporary supports. Emphasis is made on the fact that many variances are possible on the distances and number of temporary supports in the main- and side span. The brief exploration given in this part focuses mainly on the recognition of general structural problems for the deck under self weight loading that occur during this stage.

For navigational purposes it is desirable to maximize the distance between the temporary supports. The basic assumption for this exploration are:

- The box girder is simply supported between two temporary supports or between zero bending location in the bending moment line. So for the effective width calculation the β_1 factor for sagging and β_2 factor for hogging moment are determined by the effective length L_{eff} between the temporary and permanent supports.
- Only self weight of the steel box girder is taken into account, because no traffic loading and permanent loading like asphalt occurs in this stadium of the bridge erection.
- According to NEN-EN 1991-2-6 part 4.1.3, the safety factor for self weight during erection $\gamma_{G;sup} = 1.05$
- Temporary supports in the side will not be a critical issue and is assumed to be located at the mid of the side span. Other configuration are possible but will not greatly influence the critical main span conditions during erection.

5.3.1 Simply supported between temporary supports

As shown in §4.2.6, the free span length of a simply supported box girder with a slenderness of $\lambda = 1/95$ is about 144 metres (with girder properties as shown in Table 16). This situation means that the temporary supports would reduce the navigation width (265 metres) of the Waal river significantly, see Figure 105 . To lift a deck section of 144 metres long requires a lift capacity of about 2800 tons.

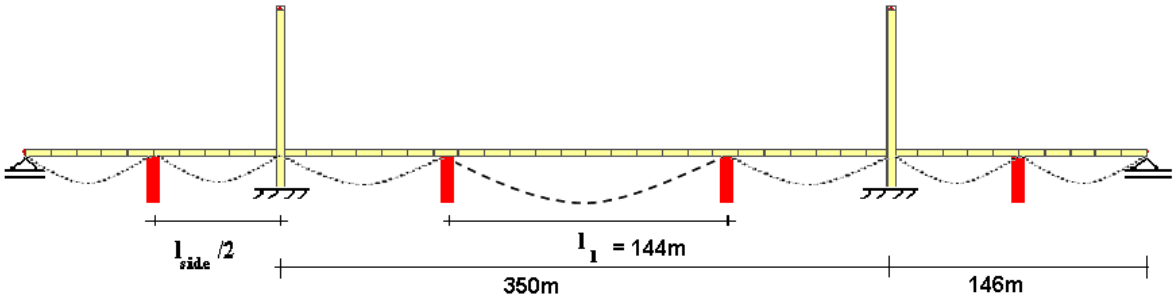

Figure 105 Temporary supports Waal river

Some measures to increase the distance between the temporary supports are for instance:

- Increasing the strength of the deck, for instance by means of choosing for a less slender deck.
- Temporary pretensioning of the lifted deck section by an internal pretensioning cable. This enhances the moment capacity of the deck enabling a larger free span length.

Furthermore it is desirable to have a zero difference in rotation of the location of the two deck sections where they are welded together (at the location of zero bending at the supports), so a camber should be applied on each lifted prefabricated deck section in order to ensure that the

deck section is in horizontal position after self weight deflection between the temporary supports.
Another point of attention is the shear force during erection. The shear force in erection phase is much higher than in the situation of the continuous supported deck by the hangers. The maximum shear force in this case is determined by $V_{Ed} = ½ * q_{self\ weight} * l_{1;distance\ temp.supports.}$ The maximum shear force capacity of the cross section is determined by NEN-EN-1993-1-5:

$$V_{c,Rd} = \frac{f_{yw} h_w t}{\sqrt{3}\gamma_{M1}} \frac{355*3685*13*2}{\sqrt{3}} = 19637kN$$

The acting maximum shear force in the deck during this erection scheme is V_{Ed} = 13320 kN
So the shear force capacity is still sufficient in erection phase but remains an issue to be checked for erection phase of the bridge.

Points of attention
The main points of attention for this method are:

-Camber of deck sections. A lifted deck section of 144 metres requires a camber of about 780 mm in order to be in horizontal position after deflection and to be able to weld this section to other sections.
-Welding conditions at the temporary and permanent supports to connect the deck section.
-Reduction of the navigation channel to 55% involves risk of collision.
-Bending moment condition after hanger installation. Due to the simply supported condition between the temporary supports the bending moment distribution after hanger installation will deviate from the assumed condition as mentioned in §1.1.7.
-Prefabrication and transport of the large deck sections

5.3.2 Erecting as a continuous beam

In the finalized stage of the erection of the deck, when all sections are welded together, the deck can be considered as a continuous beam on temporary- and permanent supports. The sagging- and hogging bending moments due to self-weight in this situation determine the stress condition in the flanges of the box girder. The location of the zero moments can be utilized to divide the entire deck into several sections to be lifted. In that way the last section in the mid can be lifted between to canti-levered deck sections over the temporary supports, see Figure 106. The length of this section depends on the location of zero bending in the main span, see Figure 107.

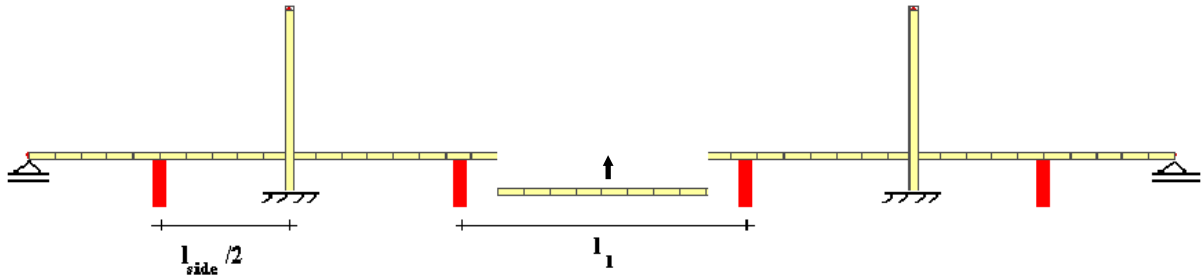

Figure 106 Canti levered deck sections

According to the given erection criteria given by the city council of Nijmegen, see §5.1, it is desirable to span at least 80 percent of the navigation width of the channel. This results in a required distance of the supports of approximately 210 metres.
The bending moments of a finalized erected deck under self weight loading on temporary supports with a distance of 210 metres is given in Figure 107.

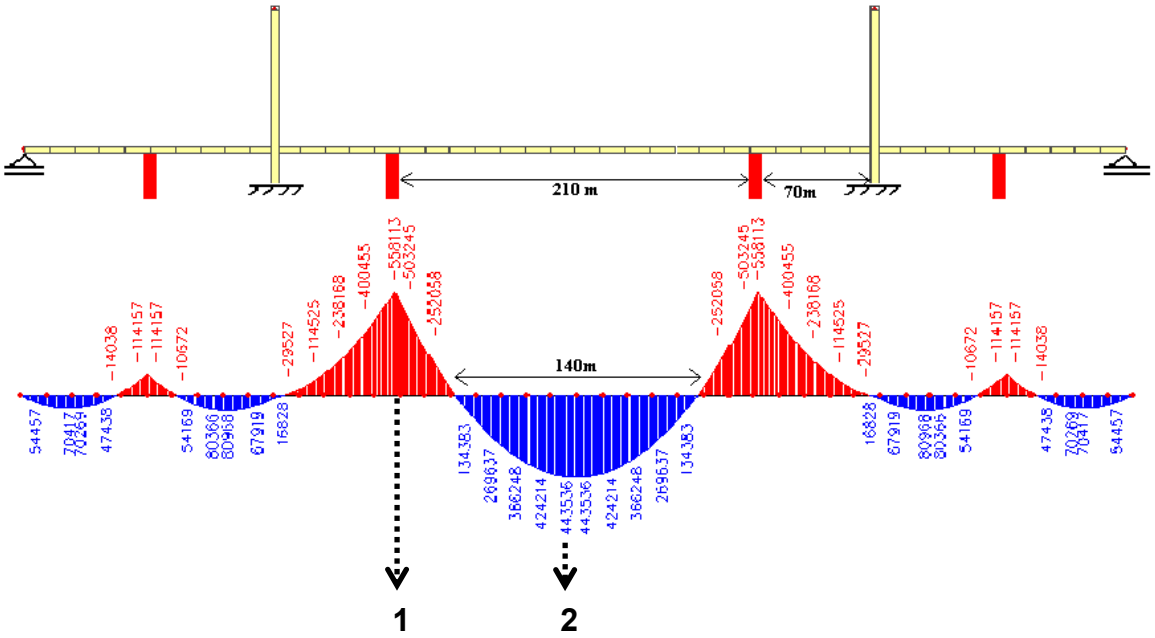

Figure 107 Bending moments [kNm] with temporary supports at 210m distance

This moment distribution reveals critical spots for the deck at two locations:

1. hogging moment at temporary supports in main span

2. sagging moment field location in the mid of the main span

Other locations along the length of the deck during erection will cause no problem due to the limited bending moments compared to location 1 and 2 mentioned above.

With girder properties as shown in Table 16 the stresses at these locations are:

Location 1.:

Table 23 Stresses box girder erection phase, location 1

Effective width	$\beta_{1;top\ flange}$	0,179	
	$\beta_{1;bottom\ flange}$	0,196	
Plate thickness flanges location 1	$t_{equivalent\ flange\ top}$	40	mm
	$t_{equivalent\ flange\ bottom}$	20	mm
Effective section modulus	$W_{eff;top}$	953303462	mm^3
	$W_{eff;bottom}$	604543040	mm^3
Stresses flanges	$\sigma_{top\ flange}$	586	N/mm^2
	$\sigma_{bottom\ flange}$	923	N/mm^2
Shear force	V_{Ed}	19079	kN
Shear force resistance	$V_{c,Rd}$	19637	kN

Location 2.:

Table 24 Stresses box girder erection phase location 2

Effective width	$\beta_{1;top\ flange}$	0,434	
	$\beta_{1;bottom\ flange}$	0,485	
Plate thickness	$t_{equivalent\ flange\ top}$	40	mm
	$t_{equivalent\ flange\ bottom}$	20	mm
Effective section modulus	$W_{eff;top}$	2265817108	mm^3
	$W_{eff;bottom}$	1361830242	mm^3
Stresses flanges	$\sigma_{top\ flange}$	196	N/mm^2
	$\sigma_{bottom\ flange}$	326	N/mm^2

The stresses in the flanges of the box girder at the location 1, see Table 23, are well above the acceptable yield strength. These peak stresses can be solved by an application of additional plate thicknesses in the flanges over a certain length near the temporary supports.

Tabel 25 Stresses at location 1 with additional plate thickness

Additional plate thickness location 1	$t_{equivalent\ flange\ top}$	75	mm
	$t_{equivalent\ flange\ bottom}$	60	mm
Effective width	$\beta_{1;top\ flange}$	0,179	
	$\beta_{1;bottom\ flange}$	0,196	
Effective section modulus	$W_{eff;top}$	1782264229	mm^3
	$W_{eff;bottom}$	1593873380	mm^3
Stresses flanges	$\sigma_{top\ flange}$	313	N/mm^2
	$\sigma_{bottom\ flange}$	350	N/mm^2

Tabel 25 shows that when additional plate thicknesses are applied in the box girder at the temporary support location, the stresses are reduced to acceptable levels. The additional plate thickness should be applied in the area where the bending moment, given in Figure 107, exceeds the moment capacity of the box girder with normal plate thicknesses i.e. $M_{y,Rd;box\ girder} = W_{eff;bottom} * f_y = 214613$ kNm. The extra required plate thicknesses are required over a length of about 53 metres near the temporary supports as shown in Figure 108.

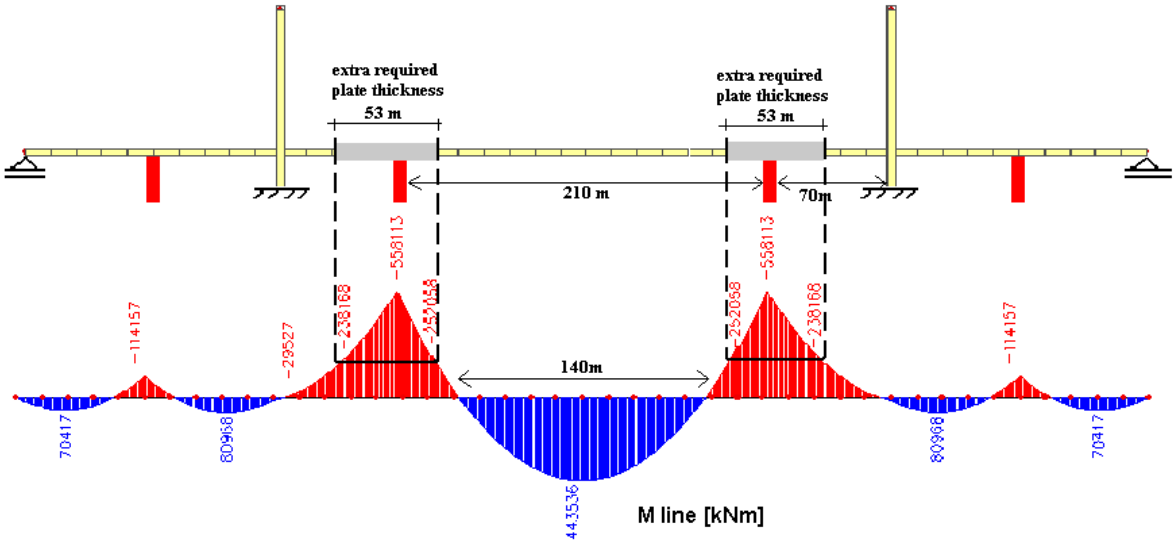

Figure 108 Required length for additional plate thicknesses

Other possibilities for reducing the hogging moment at the temporary supports, like support displacements of the temporary supports, are not discussed but can be worth considering. Lowering a support reduces the hogging moment but increases the sagging moment in the field.

Erection sequence of the deck
Based on the location of zero bending in each step, the deck can be divided in several section which have to be lifted individually in a certain sequence. The deck can be welded together at the zero bending location after each erection step as presented in Figure 109.

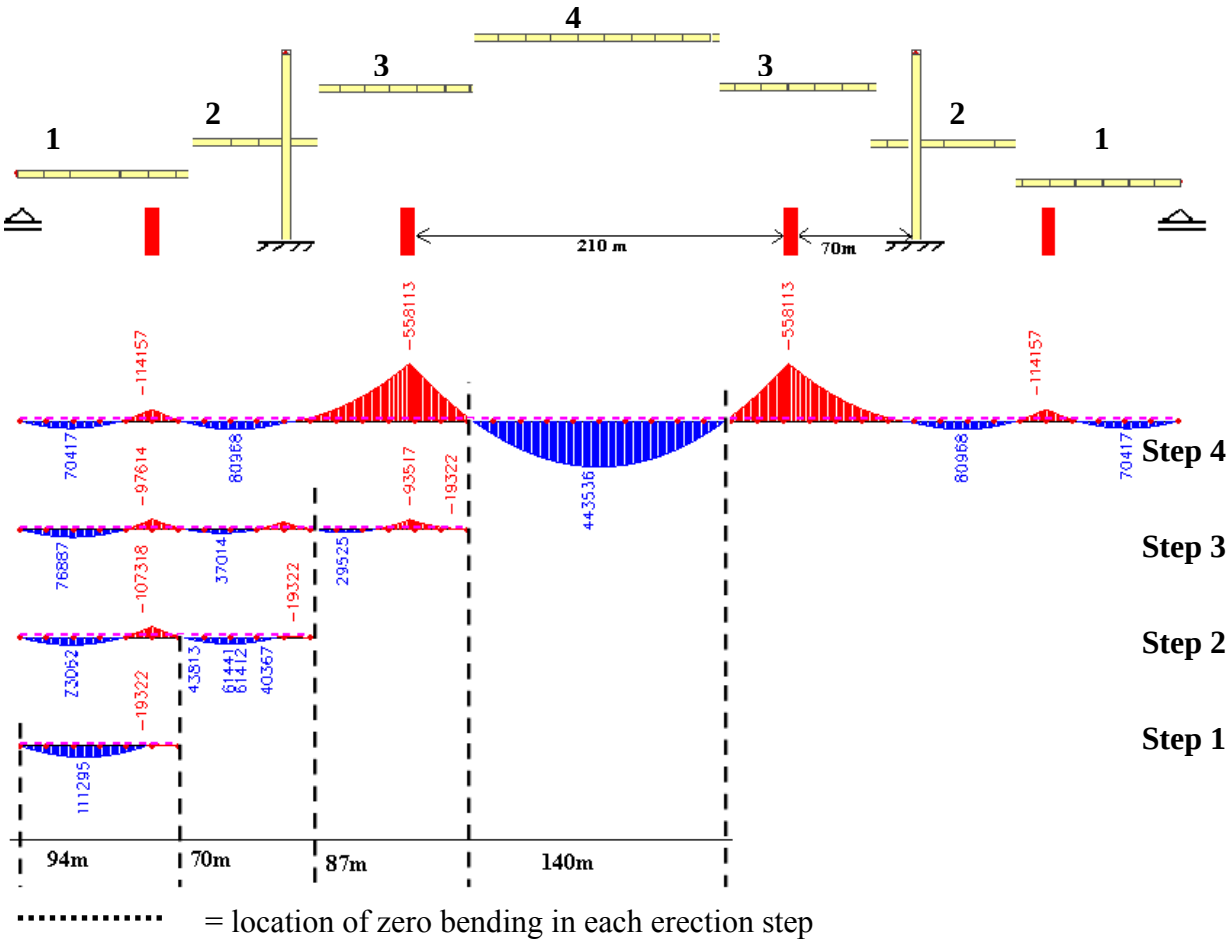

Figure 109 Lifting sequence of deck sections & zero bending locations in M line

Figure 109 shows the following erection steps:
Step 1: Lifting the a section of 94 metres on the permanent end support and a temporary support in the side span.
Step 2: Erecting a deck section of 70 metres on the canti levered part of section 1 and the permanent support near the pylon.
Step 3: Erecting a deck section of 87 metres on the permanent support near the pylon and the temporary support in the main span.
Step 4: Erecting the closing deck section of 140 metres between the two cantilever parts of section 3. This step will introduce the decisive bending moments and stress conditions in the deck during erection.

Points of attention

-Additional plate thicknesses in the flanges are required in the cross section of the box girder at the location of the temporary supports in main span.
-Other option to reduce the hogging moment situation at the temporary support is to apply a support displacement. This has both influence of the hogging moment at the support and the sagging moment in the field.

-Shear force condition. Table 23 shows that the shear force after step 4 in the erection sequence is becoming critical but still sufficient provided that enough longitudinal and transverse stiffeners are applied at this location.
-Production and erection of the temporary supports
-Prefabrication and transport of the large deck sections
-Navigation clearance underneath the deck during erection
-Collision risk of the temporary supports by shipping traffic

Erecting the deck on temporary supports introduces many problems and decisive stress conditions compared to the finalized stage of the bridge.

5.4 Constructing without temporary piers in the Waal river

Constructing without any temporary supports in the Waal river implies that temporary stay cables have to be used to erect and temporary support the deck. Using temporary stay cables can either be used without any- or in combination with some temporary supports. Some erection possibilities with temporary stays in combination with temporary supports are given in Figure 110 and Figure 111. Many variation to these configuration are possible.

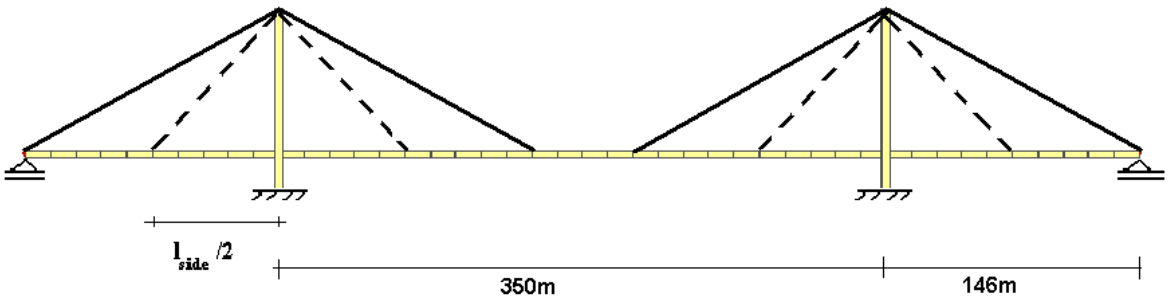

Figure 110 Erecting with temporary stay cables

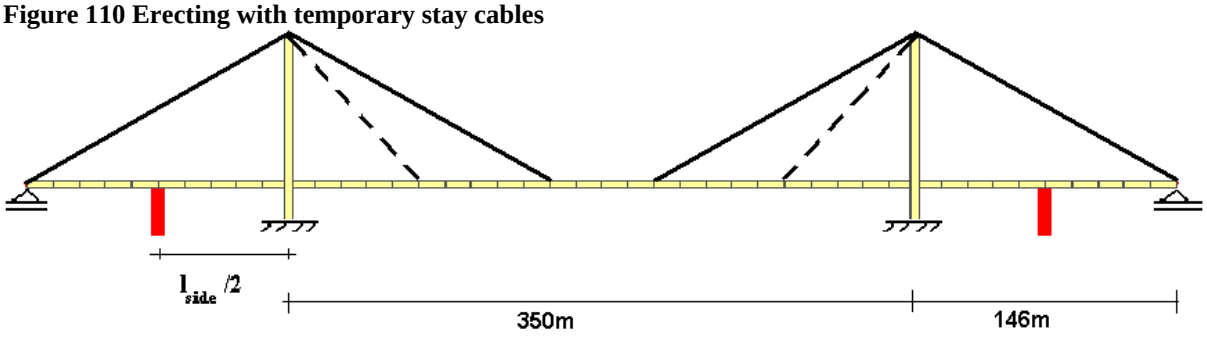

Figure 111 Erecting with temporary stays and temporary supports in the side span

Both methods imply the same bending moments in the deck, large hogging moments will occur at the location of the stay cables and supports.
The elimination of the temporary supports in the main span is a big advantage of this method. As shown in §5.3.2, large hogging moments require many provisions in the cross section of the box girder. By using more than two temporary stay cables in the main span, the hogging moment can be reduced which is favourable for the stress conditions in the box girder in this phase.

Erection sequence of deck
This erection method is similar to that of the erection of a cable stayed bridge. Two main erection sequences are known for this bridge type, see Figure 112 and Figure 113.

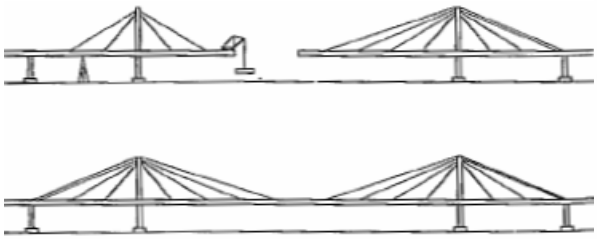

Figure 112 Erecting side span first

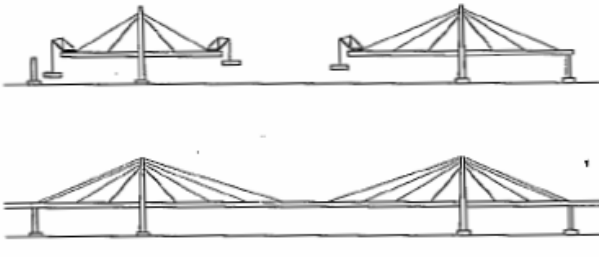

Figure 113 Cantilever process from pylon

Points of interest
Many issues are of importance for the evaluation of this method.

-Number of stay cables
-Properties of stay cable
-Vertical anchorage reaction at end support which can be decisive over the finalized situation of a parabolic main cable.
-Shear force condition in the deck
-Anchorage of the stay cables to the deck
-Conditions at cable saddle on the top of the pylon, placement of stay cables and parabolic main cable.
-Erection of the main cable and hangers and the removal of the temporary stays afterwards.
-Combination with use of temporary supports in the side span and/or partly in the main span
-Navigation clearance underneath the deck during erection

Many factors influence the feasibility of this erection method but in general when many stay cable are used the structural consequences for the deck can be less severe compared to the erection method solely on temporary supports as shown in §5.3.2. Another advantage is that smaller deck sections can be lifted which reduces the required lifting capacity of the crane or strand jacks.
A more detailed evaluation of this method is worth considering for the situation at Nijmegen city where a busy navigation channel makes it not desirable to apply temporary support in the main span. Reference is made to the erection methods used for cable stayed bridges.

5.5 Conclusions regarding erection

The brief exploration of an erection method for the new city bridge near Nijmegen city shows that in general the erection phase can cause a decisive stress situation for the deck compared to the finalized phase. During erection the deck is supported on a few temporary supports and permanent supports introducing large shear forces and sagging and hogging moments on locations which do not occur in a finalized situation of the deck where it is continuous supported by many hangers. The stress conditions in the box girder in erection phase can require a much stiffer deck than is required for the stress conditions and stability issues in finalized conditions of the bridge.

For the situation of Nijmegen city a reduction of the navigation width of 265 metres can be minimized to 80% (210 metres). But the consequences are that extra provisions have to be

made on the deck to be able to erect the deck on temporary supports with a distance of 210 metres.
It is clear that a further reduction of the distance between the temporary supports is desirable because it leads to less severe structural consequences for the deck during erection. The downside is off course that it gives more interference of the navigation channel.

The possibility of erecting without the use of temporary supports but stay cables is an attractive alternative in order to eliminate interference of the navigation channel. Other advantage is that the structural consequences can be less severe compared to the situation described in §5.3.1. But this method remains laborious and gives a justification for the application of a cable stayed bridge instead of a suspension bridge.

In general erecting a large self-anchored suspension bridge requires attention for:

- -Erecting large prefabricated deck sections
- -Required lifting capacity of a crane or strand jack are significant
- -Shear force condition during erection
- -Stress condition at temporary supports/ stay cables during erection in the box girder can require extra provisions
- -Welding procedure of the erected deck sections
- -Number of and distance between the temporary supports
- -Prefabrication and transport of the large deck sections
- -Interference of the navigation channel

6 Overall conclusions and recommendations

Based on this M.Sc. study to the structural behaviour and main span possibilities of a self-anchored suspension bridge, the following overall conclusions and recommendations can be made.

6.1 Conclusions

Structural behaviour

A parameter study on the structural behaviour of a self-anchored suspension bridge has revealed that for the global force distribution the ratio between the deck bending stiffness EI_{girder} and the axial stiffness $EA_{main\ cable}$ is an important aspect. The global stiffness of- and the maximum bending moment in the girder are greatly influenced by these bridge parameters. Regarding the global buckling of the stiffening girder it has been shown that the side span is decisive, the n-value for the upward buckling of side span is much lower than for the n-value of the downward buckling of the main span. A remark is made that these findings are based on the geometry ratio, of for instance side span to main span, that are made in this research. Adjustment of side span length can increase the resistance against buckling.
The overall conclusion of the parameter study into the structural behaviour is that on static strength, stiffness, frequency behaviour and the buckling stability of the box girder, a deck slenderness of the box girder of $\lambda = 1/100$ or even more slender is feasible.
Some local critical aspects in such a bridge are the support conditions of the girder at the pylon and the horizontal anchorage at the end support. Both location are imposed by locally high stresses which require attention for extra provisions in the cross section of the box girder.

Main span possibilities

The exploration of the span possibilities of a self-anchored suspension bridge has shown that it is technically feasible to achieve a main span length up to 500 metres. The expected problems regarding the buckling stability of the main girder has turned out to be feasible for span lengths up to 500 metres. Regarding static strength, stiffness, frequency behaviour and buckling stability, a girder slenderness of $\lambda = 1/100$ and even more slender is feasible. Even a main span beyond 500 metres is in technical view possible. An increasing main span up to 500 metres does show that the normal stresses in the box girder become dominant over the bending stresses, which can result in overall compressive stress conditions in the girder's flanges. Also the buckling stability of the girder becomes more critical for an increasing main span but still feasible. The so called n-value decreases from $n = 13$ for a span length of $L = 150$m to an n-value of $n = 6$ for a span length $L = 500$. This indicates that the buckling resistance at 500 metres is still sufficient but requires close attention in the design process.
The most limiting factor for the slenderness of the girder is the erection phase of the bridge. Depending on the number of- and distance between the temporary supports, the stress conditions during erection can easily govern the design of the cross section of stiffening girder. The choice for the construction method between erecting on temporary supports or temporary stays has influence on the extent of the required provisions for the box girder during erection.

Erection
The erection stage of a self-anchored suspension bridge remains the critical design issue. The deck encounters decisive stress conditions in this stage compared to the finalized stage of the bridge. An optimisation is to be found regarding the number of temporary supports allowed in the navigation channel and the structural consequences for the deck. A deck slenderness of about $\lambda = 1/100$ makes it possible to span at least 1/3 of the main during erection stage. In that way only two temporary supports are required in the main span.
.

6.2 Recommendations

- In the pre-design process of a suspension bridge in general, the ratio between the bending stiffness EI_{deck} of the deck and the axial stiffness of the main cable EA_{cable} should be evaluated. The maximum bending moment in the girder and global stiffness of the entire bridge is mainly determined by these two bridge parameters.

- The support conditions of the girder near the pylon introduce peak stresses due to the hogging moment and torsional effects by symmetric and asymmetric loading conditions. A detailed design should asses the required number of-, location of- and plate thicknesses of the longitudinal and transverse stiffeners to meet the local static strength and local stability issues.

- A similar recommendation can be made with respect to the main cable's anchorage to the deck. The introduction of the individual cable strands requires a detailed design of the box girder at this location. Many provisions like strand shoes, sockets, steel plates, stiffeners are to be situated in the cross section of the box girder. Local static strength and local stability issues of the steel plated elements should be assessed.
  A system like in the San Francisco bay bridge where the main cable is looped around the deck might me an interesting option to research into more detail.

- Regarding the material use, costs, structural behaviour and esthetical appearance of the bridge, it might be worth while to research the possibility to apply a more slender deck in the main than in the side span. On static strength, stability and dynamic issues the analyses in this study shows that the possibility exists for a deck slenderness beyond $\lambda = 1/100$.
  Also the possibility of the application of a truss girder as an alternative for the box girder might be interesting to investigate.

- As this research also has shown is that the erection stage causes static strength problems for the deck. The pre-design of the bridge should include a close and early assessment of the erection criteria determined by the local surrounding conditions and the client. Applying more than two temporary supports in the main span will reduce the decisive stress condition for the deck during erection. This is favourable for the possibility of applying a slender deck.

- A further research into of the buckling behaviour of the side span and main span in relation to the geometrical ratio like side span length to main span length can be interesting. This could reveal more closely the sensitivity of- and difference between the global buckling of the side span and main span and discover a more optimized geometrical ratio.

- In technical view this research revealed the possibility of self-anchored suspension bridge with a main span beyond 500 metres. The global research into the structural behaviour and span possibilities of this research could therefore be extended to a span range beyond 500 metres.

- No detailed assessment is made in this research into the fatigue strength issue. But as for every bridge type and cable supported bridges as well, a fatigue assessment should be made on bridge components like the deck, hanger connections to the deck, hangers, anchorage of the main cable to the deck, etcetera. From the fatigue strength point of view, the self-anchored suspension bridge has a similar approach as conventional suspension bridges. So no real restrictions are to be expected for large span self-anchored suspension bridges.

- The structural analyses of the self-anchored suspension bridge in this research has been performed with the FEM program ESA PT 6.0.185. At first sight no second order effects where visible in the geometrical non-linear analyses. But an alternative approach to this phenomena, as shown in this research, revealed that it is an issue that should be closely watched. The buckling stability of the deck is an issue that should be considered.

List of literature

Alsemgeest,D. *Rebuilding bridge Kanne, Suspension bridge-Static analyses- Check on strength, stiffness and stability*. Iv-Infra, October 2003

Chen, W. L.Duan. *Bridge Engineering Handbook*. CRC Press 2000

Cheng, J. et. al., *Nonlinear aerostatic stability analysis of Jiang Yin suspension bridge*. Engineering structures 24, 2002, pp 773-78.

Clemente,P. G. Nicolosi, A. Raithel. *Preliminary design of very long-span suspension bridges. Engineering structures 22 (2000)*, 1699-1706.

Gasparini,D. V. Gautam. *Geometrically Nonlinear Static behaviour of Cable Structures*. Journal of Structural Engineering, October 2002, pp 1317-1329.

Gimsing, N.J., *Cable supported Bridges*, Wiley&Sons, 1998

Habraken, A., Y. Ichimaru, Nesciobrug Amsterdam, *Met een slinger over het kanaal, Bouwen met Staal 193*, December 2006

Ichimaru, Y., Design *and engineering of 'Nescio' bridge-Amsterdam Rhine canal*. Arup

Overspannend staal, Rotterdam: Stichting Kennisoverdracht SG, Deel 3: *Construeren B*, 1996.

PvE Stadsbrug versie 1_0 20juni06.pdf, collected from the website: http://www2.nijmegen.nl/mmbase/attachments/359936/PvE_Stadsbrug_versie_1_0_20juni06.pdf

Ren, W. *Roebling suspension bridge. 1:Finite element model and free vibration response*, Journal of bridge engineering, March/April 2004, pp 110-118

Romeijn, A. *Examples of examination questions for Cable stayed bridges*. December 2005

Romeijn, A. *CT5125 Steel Bridges Part 1&2*. Faculty of Civil engineering and Geosciences

Thimmardy.E. et.al., New Carquinez bridge. *North America's Newest suspension bridge*. Steel bridge 2004 Millau.

Ulstrup, C., *Rating and preliminary analysis of suspension bridges*. Journal of structural engineering, Vol. 119, No.9. September 1993.

List of figures and tables

Tables:

Appendices

Content:

Appendix 1 Cable modelling

Deflections [mm] of model with cable elements

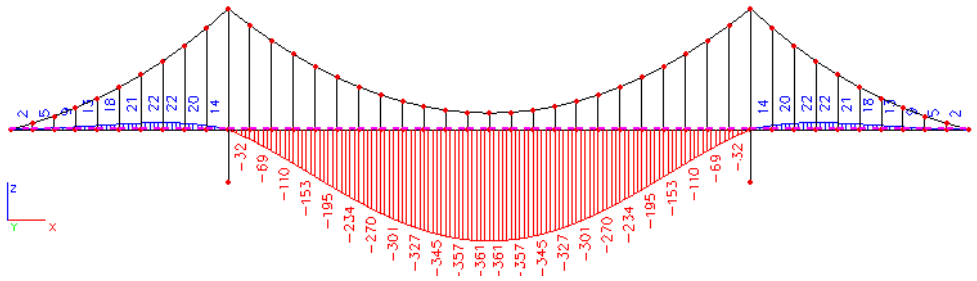

Deflections [mm] of model with a ‘chain’ as main cable

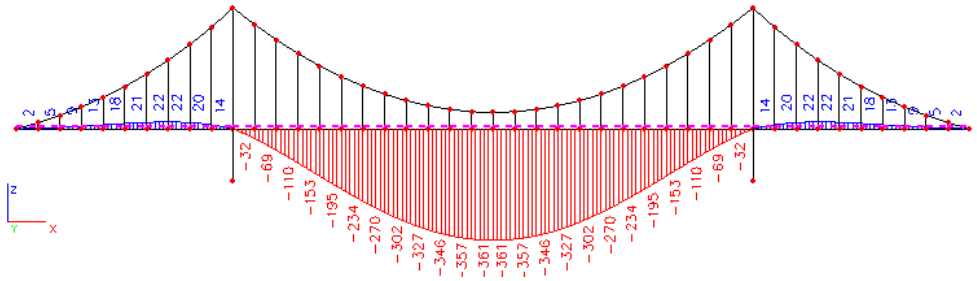

$M_{y;Ed}$ [kNm] of model with cable elements

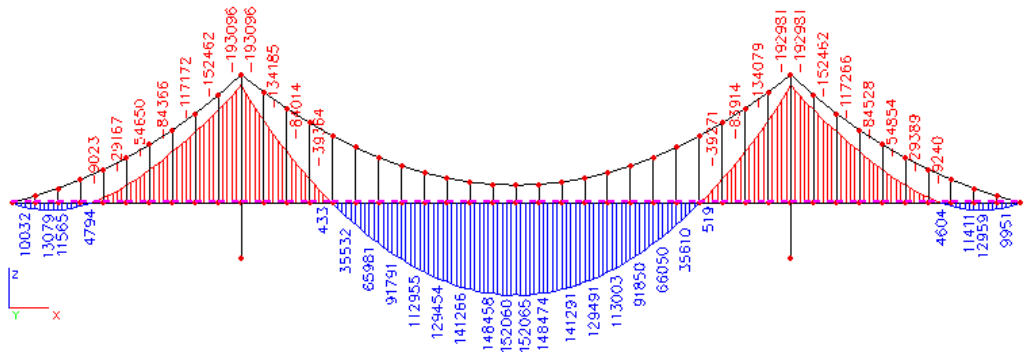

$M_{y;Ed}$ [kNm] of model with a ‘chain’ as main cable

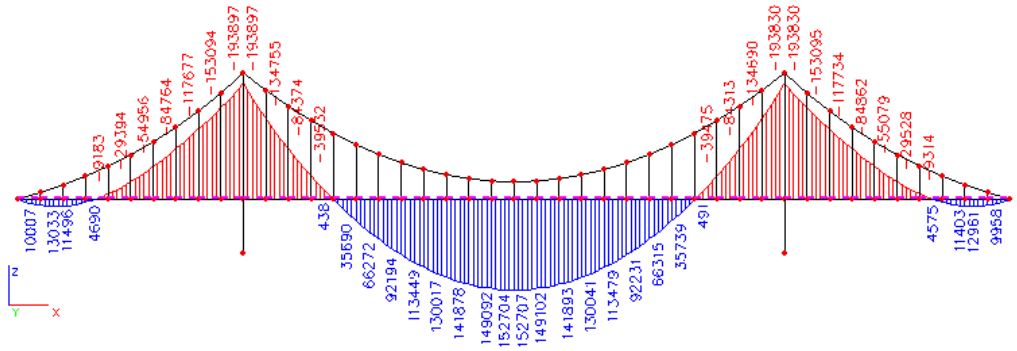

Appendix 2a Effective width at main and side span

Effective width of girder at main span

effective width

sagging bending

b eff bovenflens

$t\_eq := 40$

$t\_bovenflens := \frac{t\_eq}{1.65}$

$t\_bovenflens = 24.242 \quad mm$

$b0 := 35600 \quad mm$

$As1 := 0.65 \cdot t\_bovenflens \cdot b0$

$As1 = 5.61 \times 10^{5} \quad mm^{2}$

$\alpha 0 := \sqrt{1 + \frac{As1}{b0 \cdot t\_bovenflens}}$

$\alpha 0 = 1.285$

$L\_eff\_mainspan := 0.70 \cdot 150000 \quad mm$ $\qquad$ $L\_eff\_sidespan := 0.85 \cdot 62500 \quad mm$

$\kappa\_main := \alpha 0 \cdot \frac{b0}{L\_eff\_mainspan}$ $\qquad$ $\kappa\_side := \alpha 0 \cdot \frac{b0}{L\_eff\_sidespan}$

$\kappa\_main = 0.436$ $\qquad$ $\kappa\_side = 0.861$

$0.02 < \kappa \le 0.70$ than

$\beta 1\_main := \frac{1}{1 + 6.4 \cdot \kappa\_main^{2}}$ $\qquad$ $\beta 1\_main = 0.452$

$\beta 1\_side := \frac{1}{1 + 6.4 \cdot \kappa\_side^{2}}$ $\qquad$ $\beta 1\_side = 0.174$

$\kappa > 0.70$ than

$\beta 1\_main := \frac{1}{5.9 \cdot \kappa\_main}$ $\qquad$ $\beta 1\_main = 0.389$

$\beta 1\_side := \frac{1}{5.9 \cdot \kappa\_side}$ $\qquad$ $\beta 1\_side = 0.197$

$b\_eff\_mainspan := 0.452 \cdot b0$ $\qquad$ $b\_eff\_mainspan = 1.609 \times 10^{4}$ mm bovenflens main span

$b\_eff\_sidespan := 0.197 \cdot b0$ $\qquad$ $b\_eff\_sidespan = 7.013 \times 10^{3}$ mm bovenflens side span

b eff onderflens

$t\_eq := 20$

$t\_onderflens := \frac{t\_eq}{1.35}$

$t\_onderflens = 14.815 \quad mm$

$b0 := 35600 \quad mm$

$Asl\_onder := 0.35 \cdot t\_onderflens \cdot b0$

$Asl\_onder = 1.846 \times mm^2$

$\alpha 0 := \sqrt{1 + \frac{Asl\_onder}{b0 \cdot t\_onderflens}}$

$\alpha 0 = 1.162$

$L\_eff\_mainspan := 0.70 \cdot 150000 \quad mm$

$L\_eff\_sidespan := 0.85 \cdot 62500 \quad mm$

$\kappa\_main := \alpha 0 \cdot \frac{b0}{L\_eff\_mainspan}$

$\kappa\_side := \alpha 0 \cdot \frac{b0}{L\_eff\_sidespan}$

$\kappa\_main = 0.394$

$\kappa\_side = 0.779$

$0.02 < \kappa \leq 0.70$ than

$\beta 1\_main := \frac{1}{1 + 6.4 \cdot \kappa\_main^2}$ $\beta 1\_main = 0.502$

$\beta 1\_side := \frac{1}{1 + 6.4 \cdot \kappa\_side^2}$ $\beta 1\_side = 0.205$

$\kappa > 0.70$ than

$\beta 1\_main := \frac{1}{5.9 \cdot \kappa\_main}$ $\beta 1\_main = 0.43$

$\beta 1\_side := \frac{1}{5.9 \cdot \kappa\_side}$ $\beta 1\_side = 0.218$

$b\_eff\_mainspan := 0.502 \cdot b0$ $b\_eff\_mainspan = 1.787 \times 10^4$ mm onderflens

$b\_eff\_sidespan := 0.218 \cdot b0$ $b\_eff\_sidespan = 7.761 \times 10^3$ mm onderflens

Appendix 2b Effective width at support

Effective width of girder at support pylon

effective width

hogging bending

b eff bovenflens

$t\_eq := 40$

$t\_bovenflens := \frac{t\_eq}{1.65}$

$t\_bovenflens = 24.242 \quad mm$

$b0 := 35600 \quad mm$

$Asl := 0.65 \cdot t\_bovenflens \cdot b0$

$Asl = 5.61 \times 10^{5} \quad mm^{2}$

$\alpha 0 := \sqrt{1 + \frac{Asl}{b0 \cdot t\_bovenflens}}$

$\alpha 0 = 1.285$

$L\_eff := 0.25 \cdot (150000 + 62500) \qquad L\_eff = 5.313 \times 10^{4}$

$\kappa := \alpha 0 \cdot \frac{b0}{L\_eff}$

$\kappa = 0.861$

$0.02 < \kappa \leq 0.70$ than

$\beta 2 := \frac{1}{1 + 6.0 \cdot \left(\kappa - \frac{1}{2500 \cdot \kappa}\right) + 1.6\kappa^{2}} \qquad \beta 2 = 0.136$

$\kappa > 0.70$ than

$\beta 2 := \frac{1}{8.6 \cdot \kappa} \qquad \beta 2 = 0.135$

$b\_eff := 0.135 \cdot b0 \qquad b\_eff = 4.806 \times 10^{3} \quad mm \quad bovenflens$

b eff onderflens

$t\_eq := 20$

$t\_onderflens := \frac{t\_eq}{1.35}$

$t\_onderflens = 14.815 \quad mm$

$b0 := 35600 \quad mm$

$Asl\_onder := 0.35 \cdot t\_onderflens \cdot b0$

$Asl\_onder = 1.846 \times mm^2$

$\alpha 0 := \sqrt{1 + \frac{Asl\_onder}{b0 \cdot t\_onderflens}}$

$\alpha 0 = 1.162$

$L\_eff := 0.25 \cdot (150000 + 62500)$ $\quad L\_eff = 5.313 \times 10^4 \quad mm$

$\kappa := \alpha 0 \cdot \frac{b0}{L\_eff}$

$\kappa = 0.779$

$0.02 < \kappa \leq 0.70$ than

$\beta 2 := \frac{1}{1 + 6.0 \cdot \left(\kappa - \frac{1}{2500 \cdot \kappa}\right) + 1.6\kappa^3}$ $\quad \beta 2 = 0.156$

$\kappa > 0.70$ than

$\beta 2 := \frac{1}{8.6 \cdot \kappa}$ $\quad \beta 2 = 0.149$

$b\_eff := 0.149 \cdot b0$ $\quad b\_eff = 5.304 \times 10^3 \quad mm \quad$ bovenflens

Appendix 3a Girder influence

Iy box [m^4]	N deck	H cable	Rz	δ main 2nd	δ pylon 2nd	My main 2nd	My sup 2nd	1st fb	2nd fb	1st ft	2nd ft
1,10	35502	18159	6975	474	120	104641	137291	0,63	1,1	4,58	3,97
1,26	34935	17863	6822	453	115	113262	147528	0,65	1,16	4,71	4,02
1,42	34388	17576	6673	433	110	121618	157416	0,67	1,23	4,83	4,07
1,59	33863	17300	6530	414	105	129681	166928	0,68	1,29	4,94	4,11
1,77	33359	17036	6392	395	100	137455	176048	0,7	1,35	5,04	4,14
1,96	32878	16783	6260	377	95	144910	184711	0,72	1,41	5,13	4,19
2,16	32420	16542	6134	361	91	152065	193096	0,74	1,46	5,2	4,19
2,37	31983	16312	6014	345	87	158907	201026	0,76	1,52	5,31	4,21
2,59	31568	16094	5899	330	83	165448	208572	0,77	1,58	5,37	4,23
2,82	31174	15886	5789	315	79	171690	215744	0,79	1,63	5,44	4,24
3,06	30801	15690	5685	302	76	177658	222556	0,81	1,68	5,49	4,26
3,31	30447	15503	5586	289	73	183345	229023	0,83	1,73	5,55	4,27
3,57	30111	15326	5491	277	69	188779	235159	0,84	1,75	5,59	4,28
3,85	29793	15158	5401	265	67	193962	240982	0,86	1,83	5,63	4,29
4,13	29492	14999	5316	254	64	198908	246507	0,88	1,87	5,67	4,3
4,42	29206	14849	5234	244	61	203631	251751	0,89	1,92	5,71	4,31

*=Reference model

Appendix 3b Cable influence

E cable [N/mm^2]	N deck	H cable	Rz	δ main 2nd	δ pylon 2nd	My main 2nd	My sup 2nd	1st fb	2nd fb	1st ft	2nd ft
205000	32420	16542	6134	361	91	152065	193096	0,74	1,46	5,2	4,19
190000	31226	15977	5763	372	94	166998	211426	0,73	1,46	5,15	4,1
150000	27504	14219	4609	408	101	213485	268570	0,7	1,46	4,93	3,83
140000	26425	13711	4275	418	104	226931	285121	0,69	1,46	4,87	3,76

A cable [mm^2]	N deck	H cable	Rz	δ main 2nd	δ pylon 2nd	My main 2nd	My sup 2nd	1st fb	2nd fb	1st ft	2nd ft
7854	18125	9806	1746	498	119	324316	408532	0,65	1,48	4,53	3,59
11310	23381	12274	3353	447	110	262660	328974	0,68	1,47	4,88	3,85
15394	28174	14533	4826	401	100	203917	256745	0,71	1,47	5,11	4,05
17671	30367	15559	5502	380	95	177113	223824	0,72	1,47	5,17	4,13
20106	32420	16542	6134	361	91	152065	193096	0,74	1,46	5,2	4,19
22698	34334	17451	6725	342	87	128715	164500	0,75	1,46	5,26	4,23
25447	36116	18299	7274	326	83	107047	137987	0,77	1,46	5,25	4,26
28353	37771	19088	7785	310	79	86964	113452	0,78	1,46	5,19	4,27
31416	39307	19822	8259	296	75	68391	90785	0,8	1,45	5,15	4,27
34636	40733	20505	8698	282	73	51232	69860	0,81	1,45	5,09	4,25
38013	42056	21139	9105	270	70	35380	50556	0,82	1,45	5,03	4,22

*=Reference model

Appendix 3c Sag over span length influence

Sag/L	N deck	H cable	Rz	δ main 2nd	δ pylon 2nd	My main 2nd	My sup 2nd	1st fb	2nd fb	1st ft	2nd ft
1/5	32420	16542	6134	361	91	152065	193096	0,74	1,46	5,2	4,19
1/6	35545	18268	5739	400	83	186776	235639	0,71	1,47	5,82	4,74
1/7	37633	19491	5280	437	77	221178	277931	0,68	1,47	6,18	5,18
1/8	38934	20326	4808	471	73	253476	317643	0,66	1,47	6,4	5,52
1/9	39665	20871	4352	500	68	282937	353788	0,64	1,47	6,51	5,8

Appendix 3d Pylon influence

I pyloon [m^4]	N deck	H cable	Rz	δ main 2nd	δ pylon 2nd	My main 2nd	My sup 2nd	1st fb	2nd fb	1st ft	2nd ft
0,238	32624	16428	6295	366	94	155668	196633	0,73	1,46	4,95	4,06
0,278	32593	16451	6269	365	94	154945	195894	0,73	1,46	5,03	4,09
0,321	32558	16474	6240	364	93	154225	195172	0,73	1,46	5,1	4,12
0,368	32518	16497	6207	363	92	153507	194465	0,74	1,46	5,15	4,15
0,419	32474	16519	6172	362	92	152780	193771	0,74	1,46	5,18	4,17
0,474	32420	16542	6134	361	91	152065	193096	0,74	1,46	5,2	4,19
0,533	32362	16564	6093	359	90	151328	192414	0,74	1,46	5,21	4,21
0,596	32299	16586	6050	358	89	150593	191747	0,74	1,46	5,28	4,23
0,664	32232	16608	6003	357	89	149845	191088	0,74	1,47	5,3	4,25
0,735	32162	16631	5955	355	88	149106	190432	0,74	1,47	5,31	4,26
0,812	32082	16653	5903	354	87	148354	189786	0,75	1,47	5,32	4,28

Appendix 3e Number of hinges in girder

hinges	N deck	H cable	Rz	δ main 2nd	δ pylon 2nd	My main 2nd	My sup 2nd	1st fb	2nd fb	1st ft	2nd ft
0	32420	16542	6134	361	91	152065	193096	0,74	1,46	5,2	4,19
2	38278	19542	6269	472	120	162788	0	0,67	1,31	3,56	3,72

*=Reference model

Appendix 4 Comparable box girders

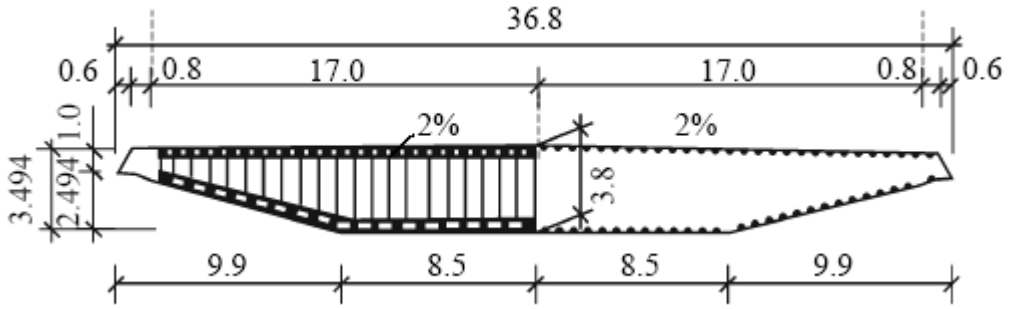

Table 1 The cross section and material properties of the bridge

Members	E (MPa)	A (m^2)	J_d (m^4)	Iz (m^4)	Iy (m^4)	M (kg/m^3)	Jm ($kg \cdot m^2/m$)
Girder	2.1×10^5	1.2481	5.034	1.9842	137.754	14732.0	1.852×10^6

Aerodynamic stability of cable-stayed-suspension hybrid bridges*

ZHANG Xin-jun (张新军)[†1], SUN Bing-nan (孙炳楠)[2]

(*[1]School of Civil Engineering and Architecture, Zhejiang University of Technology, Hangzhou 310014, China*)

(*[2]School of Civil Engineering and Architecture, Zhejiang University, Hangzhou 310027, China*)

[†]E-mail: xjzhang@zjut.edu.cn

Received Oct. 29, 2004; revision accepted Dec. 16, 2004

Bron: Dictaat Romeijn Stalen bruggen blz 84:

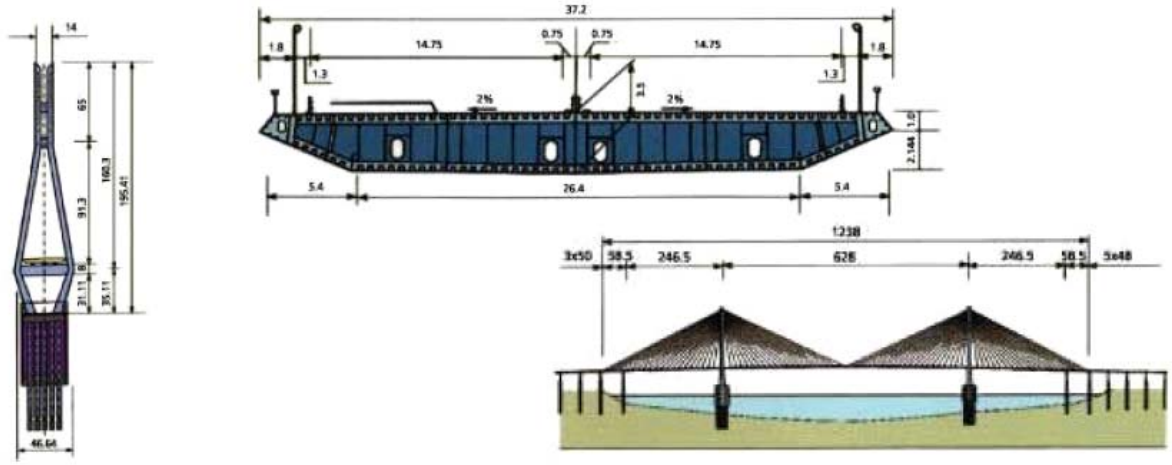

Appendix 5a Stability check reference model

$L := 62.5 \quad m$ side span

$\delta 2 := 235 \quad mm$

$N\_Ed := 37682 \quad kN$

$N\_cr := 551479 \quad kN$

$A := 2199600 \quad mm^2$

$f\_y := 355 \quad \frac{N}{mm^2}$

$$\lambda := \sqrt{A \cdot \frac{f\_y}{N\_cr \cdot 1000}}$$

$\lambda = 1.19$ Non dimensional slenderness

$\alpha := 0.34$

$\alpha = 0.34$ imperfection slenderness for buckling curve b

$$\phi := 0.5 \cdot \left[1 + \left[\alpha \cdot (\lambda - 0.2)\right] + \lambda^2\right]$$

$\phi = 1.376$

$$\chi := \frac{1}{\phi + \sqrt{\phi^2 - \lambda^2}}$$

$\chi = 0.484$ reduction factor for the relevant buckling mode

$Iy := 2.1651 \quad m^4$

$My := 54650 \quad kNm$ side span

$W\_eff := 581436314 \quad mm^3$

$My\_cr := 355 \cdot W\_eff$

$My\_cr = 2.064 \times 10^{11}$

$$\beta m := 1 + \left[\left[\frac{\left(3.14159^2 \cdot 210000 \cdot Iy \cdot 1000000000000 \cdot \delta 2\right)}{(L \cdot 1000)^2 \cdot My \cdot 1000000}\right] - 1\right] \cdot \frac{N\_Ed}{N\_cr}$$

$\beta m = 1.269$

Stabiliteits toets

$$UC\_stab := \left(\frac{N\_Ed}{\chi \cdot N\_cr} + \beta m \cdot \frac{My \cdot 1000000}{My\_cr}\right)$$

$UC\_stab = 0.477$

Appendix 5b Stability check Optimized model

$L := 62.5 \quad m$ side span

$\delta 2 := 529 \quad mm$

$N\_Ed := 37682 \quad kN$

$N\_cr := 504882 \quad kN$

$A := 2184600 \quad mm^2$

$f\_y := 355 \quad \frac{N}{mm^2}$

$$\lambda := \sqrt{A \cdot \frac{f\_y}{N\_cr \cdot 1000}}$$

$\lambda = 1.239$ Non dimensional slenderness

$\alpha := 0.34$

$\alpha = 0.34$ imperfection slenderness for buckling curve b

$$\phi := 0.5 \cdot \left[1 + \left[\alpha \cdot (\lambda - 0.2)\right] + \lambda^2\right]$$

$\phi = 1.445$

$$\chi := \frac{1}{\phi + \sqrt{\phi^2 - \lambda^2}}$$

$\chi = 0.457$ reduction factor for the relevant buckling mode

$Iy := 1.26 \quad m^4$

$My := 30582 \quad kNm$ side span

$W\_eff := 437850670 \quad mm^3$

$My\_cr := 355 \cdot W\_eff$

$My\_cr = 1.554 \times 10^{11}$

$$\beta m := 1 + \left[\left[\frac{\left(3.14159^2 \cdot 210000 \cdot Iy \cdot 1000000000000 \cdot \delta 2\right)}{(L \cdot 1000)^2 \cdot My \cdot 1000000}\right] - 1\right] \cdot \frac{N\_Ed}{N\_cr}$$

$\beta m = 1.788$

Stabiliteits toets

$$UC\_stab := \left(\frac{N\_Ed}{\chi \cdot N\_cr} + \beta m \cdot \frac{My \cdot 1000000}{My\_cr}\right)$$

$UC\_stab = 0.515$

Appendix 6 Design orthotropic steel box of the New Carquinez Bridge

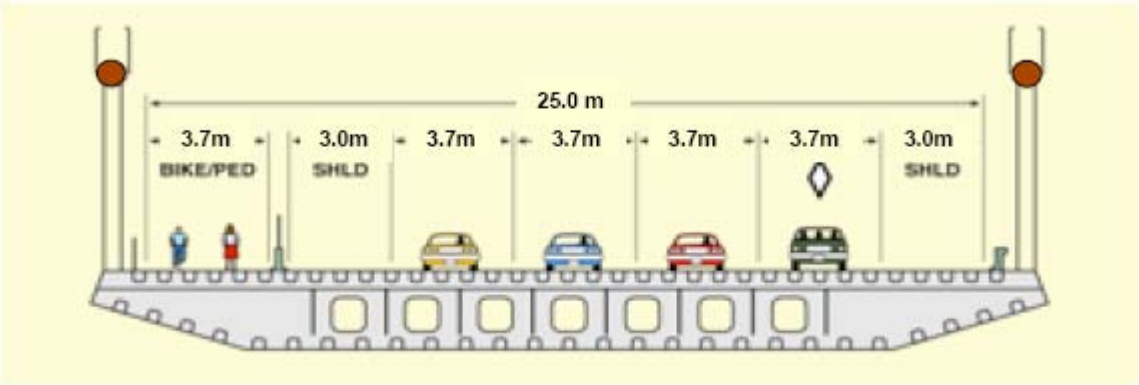

Figure 2 New Carquinez Bridge – Cross Section

4.3 Superstructure.

The suspended superstructure of the New Carquinez Bridge consists of a closed, orthotropic steel box girder continuous from the north anchorage to the transition pier at the south (Figure 15).

With a total length of 1056 m and unit weight of 10900 kg/m the total weight of the fabricated superstructure is 11 512 tons. A minimum grade of 345 MPa was specified for all structural steel of the main bridge components. The bridge has only two expansion joints at the ends of the suspension superstructure leading to improved maintenance and overall bridge performance. The closed box girder shape (Figure 2) provides enhanced torsional resistance. Improved dynamic behavior under wind and seismic loads has also been achieved.

As shown in Figure 2, the edge and side plates of the box girder are shaped to provide an aerodynamically stable cross section. The girder is supported along its 16 mm thick longitudinal bulkheads by suspenders located at the intersection of the vertical plane of the main cables with the transverse bulkheads uniformly distributed along the box girder at 12.4 m. Additionally, intermediate transverse bulkheads were provided at 6.2 m and intermediate transverse diaphragms at 3.1 m (Figure 16).

The orthotropic deck of the box girder consists of a 16 mm deck plate stiffened longitudinally by hermetically sealed trapezoidal ribs located 726 mm apart (Figure 16). The deck closed ribs are 305 mm deep and 8 mm thick. Similar closed ribs of 280 mm depth, located 940 mm apart were used for stiffening of the bottom and lower part of the side plate (Figure 16). The thickness of bottom, side and edge plates was 8 , 10 and 12 mm, respectively.

The stiffeners of this cross section can be expressed as a percentage of the area of the top flange, bottom flange and web:

$A_{\text{stiff. top flange}} = 65\% * A_{\text{top flange}}$

$A_{\text{stiff . bottom flange}} = 35\% * A_{\text{bottom flange}}$

$A_{\text{stiff. web}} = 15\ \% * A_{\text{web}}$

This estimation is retrieved from a similar box girder of the same dimensions: Thimmardy.E. et.al., *New Carquinez bridge. North America's Newest suspension bridge*. Steel bridge 2004 Millau.

Appendix 7 Stress calculation in reference model

b0	35600								
belastinggeval 1	**full length**								
Sagging									
main span			A_totaal	2199000	mm^2				
	boven flens		w_eff_boven	1322933567	mm^3	σ boven tgv M_Ed,y		114,9 N/mm2	compression
	β1	0,452	M_Ed,y =	152060	kNm	σ boven tgv N_Ed		14,8 N/mm2	compression
	b_eff_boven	16091,2 mm	N_Ed,y =	32491	kN		result	**129,7** N/mm2	**compression**
	onderflens		w_eff onder	776111587,2	mm^3	σ onder tgv M_Ed,y		195,9 N/mm2	tension
	β1	0,502	M_Ed,y	152060	kNm	σ boven tgv N_Ed		14,8 N/mm2	compression
	b_eff_onder	17871,2 mm					result	**181,2** N/mm2	**tension**
side span			A_totaal	2199000	mm^2				
	boven flens		w_eff_boven	581436314,4	mm^3	σ boven tgv M_Ed,y		50,2 N/mm2	compression
	β1	0,197	M_Ed,y	29167	kNm	σ boven tgv N_Ed		14,7 N/mm2	compression
	b_eff_boven	7013,2 mm	N_Ed,y	32420	kN		result	**64,9** N/mm2	**compression**
	onderflens		w_eff onder	354078229,5	mm^3	σ onder tgv M_Ed,y		82,4 N/mm2	tension
	β1	0,218	M_Ed,y	29167	kNm	σ boven tgv N_Ed		14,7 N/mm2	compression
	b_eff_onder	7760,8 mm					result	**67,6** N/mm2	**tension**
			A_totaal	2199000	mm^2				
Hogging	bovenflens		w_eff_boven	401761942,6	mm^3	σ boven tgv M_Ed,y		480,6 N/mm2	tension
	β2	0,135	M_Ed,y	193096	kNm	σ boven tgv N_Ed		14,8 N/mm2	compression
	b_eff_boven	4806 mm	N_Ed,y	32491	kN		result	**465,8** N/mm2	**tension**
	onderflens		w_eff onder	251302317,1	mm^3	σ boven tgv M_Ed,y		768,4 N/mm2	compression
	β2	0,149	M_Ed,y	193096	kNm	σ boven tgv N_Ed		14,8 N/mm2	compression
	b_eff_onder	5304,4 mm					result	**783,2** N/mm2	**compression**
end support			A_totaal	2199000	mm^2				
	bovenflens		w_eff_boven	1322933567	mm^3	σ boven tgv M_Ed,y		0,0 N/mm2	
	β 0	0,452	M_Ed,y	0	kNm	σ boven tgv N_Ed		14,8 N/mm2	compression
	b_eff_boven	16091,2 mm	N_Ed,y	32491	kN		result	**14,8** N/mm2	**compression**
	onderflens		w_eff onder	776111587,2	mm^3	σ boven tgv M_Ed,y		0,0 N/mm2	
	β 0	0,502	M_Ed,y	0	kNm	σ boven tgv N_Ed		14,8 N/mm2	compression
	b_eff_onder	17871,2 mm					result	**14,8** N/mm2	**compression**
belastinggeval 2	**midspan**								
Sagging									
main span			A_totaal	2199000	mm^2				
	boven flens		w_eff_boven	1322933567	mm^3	σ boven tgv M_Ed,y		124,3 N/mm2	compression
	β1	0,452	M_Ed,y =	164378	kNm	σ boven tgv N_Ed		14,9 N/mm2	compression
	b_eff_bove	16091,2 mm	N_Ed,y =	32827	kN		result	**139,2** N/mm2	**compression**
	onderflens		w_eff onder	776111587,2	mm^3	σ onder tgv M_Ed,y		211,8 N/mm2	tension
	β1	0,502	M_Ed,y	164378	kNm	σ boven tgv N_Ed		14,9 N/mm2	compression
	b_eff_onde	17871,2 mm					result	**196,9** N/mm2	**tension**
side span			A_totaal	2199000	mm^2				
	boven flens		w_eff_boven	581436314,4	mm^3	σ boven tgv M_Ed,y		191,6 N/mm2	tension
	β1	0,197	M_Ed,y	111377	kNm	σ boven tgv N_Ed		14,9 N/mm2	compression
	b_eff_bove	7013,2 mm	N_Ed,y	32827	kN		result	**206,5** N/mm2	**tension**
	onderflens		w_eff onder	354078229,5	mm^3	σ onder tgv M_Ed,y		314,6 N/mm2	compression
	β1	0,218	M_Ed,y	111377	kNm	σ boven tgv N_Ed		14,9 N/mm2	compression
	b_eff_onde	7760,8 mm					result	**329,5** N/mm2	**compression**
			A_totaal	2199000	mm^2				
Hogging	bovenflens		w_eff_boven	401761942,6	mm^3	σ boven tgv M_Ed,y		406,1 N/mm2	tension
	β2	0,135	M_Ed,y	163167	kNm	σ boven tgv N_Ed		14,9 N/mm2	compression
	b_eff_bove	4806 mm	N_Ed,y	32827	kN		result	**391,2** N/mm2	**tension**
	onderflens		w_eff onder	251302317,1	mm^3	σ boven tgv M_Ed,y		649,3 N/mm2	compression
	β2	0,149	M_Ed,y	163167	kNm	σ boven tgv N_Ed		14,9 N/mm2	compression
	b_eff_onde	5304,4 mm					result	**664,2** N/mm2	**compression**
end support			A_totaal	2199000	mm^2				
	bovenflens		w_eff_boven	1322933567	mm^3	σ boven tgv M_Ed,y		0,0 N/mm2	
	β 0	0,452	M_Ed,y	0	kNm	σ boven tgv N_Ed		14,9 N/mm2	compression
	b_eff_bove	16091,2 mm	N_Ed,y	32827	kN		result	**14,9** N/mm2	**compression**
	onderflens		w_eff onder	776111587,2	mm^3	σ boven tgv M_Ed,y		0,0 N/mm2	
	β 0	0,502	M_Ed,y	0	kNm	σ boven tgv N_Ed		14,9 N/mm2	compression
	b_eff_onde	17871,2 mm					result	**14,9** N/mm2	**compression**

belastinggeval 3	**sidespan**								
Sagging									
main span			A_totaal	2199000	mm^2				
	boven flens		w_eff_boven	1322933567	mm^3	σ boven tgv M_Ed,y	11,6	N/mm2	compression
	β1	0,452	M_Ed,y =	15352	kNm	σ boven tgv N_Ed	10,6	N/mm2	compression
	b_eff_bove	16091,2 mm	N_Ed,y =	23417	kN	result	**22,3**	N/mm2	**compression**
	onderflens		w_eff onder	776111587,2	mm^3	σ onder tgv M_Ed,y	19,8	N/mm2	tension
	β1	0,502	M_Ed,y	15352	kNm	σ boven tgv N_Ed	10,6	N/mm2	compression
	b_eff_onde	17871,2 mm				result	**-9,1**	N/mm2	**commpression**
side span			A_totaal	2199000	mm^2				
	boven flens		w_eff_boven	581436314,4	mm^3	σ boven tgv M_Ed,y	134,1	N/mm2	compression
	β1	0,197	M_Ed,y	77958	kNm	σ boven tgv N_Ed	10,6	N/mm2	compression
	b_eff_bove	7013,2 mm	N_Ed,y	23417	kN	result	**144,7**	N/mm2	**compression**
	onderflens		w_eff onder	354078229,5	mm^3	σ onder tgv M_Ed,y	220,2	N/mm2	tension
	β1	0,218	M_Ed,y	77958	kNm	σ boven tgv N_Ed	10,6	N/mm2	compression
	b_eff_onde	7760,8 mm				result	**209,5**	N/mm2	**tension**
			A_totaal	2199000	mm^2				
Hogging	bovenflens		w_eff_boven	401761942,6	mm^3	σ boven tgv M_Ed,y	166,0	N/mm2	tension
	β2	0,135	M_Ed,y	66698	kNm	σ boven tgv N_Ed	10,6	N/mm2	compression
	b_eff_bove	4806 mm	N_Ed,y	23417	kN	result	**155,4**	N/mm2	**tension**
	onderflens		w_eff onder	251302317,1	mm^3	σ boven tgv M_Ed,y	265,4	N/mm2	compression
	β2	0,149	M_Ed,y	66698	kNm	σ boven tgv N_Ed	10,6	N/mm2	compression
	b_eff_onde	5304,4 mm				result	**276,1**	N/mm2	**compression**
end support			A_totaal	2199000	mm^2				
	bovenflens		w_eff_boven	1322933567	mm^3	σ boven tgv M_Ed,y	0,0	N/mm2	
	β 0	0,452	M_Ed,y	0	kNm	σ boven tgv N_Ed	10,6	N/mm2	compression
	b_eff_bove	16091,2 mm	N_Ed,y	23417	kN	result	**10,6**	N/mm2	**compression**
	onderflens		w_eff onder	776111587,2	mm^3	σ boven tgv M_Ed,y	0,0	N/mm2	
	β 0	0,502	M_Ed,y	0	kNm	σ boven tgv N_Ed	10,6	N/mm2	compression
	b_eff_onde	17871,2 mm				result	**10,6**	N/mm2	**compression**

Toetsing sterkte

Girder
maatgevend Load case 2

					fy	UC
M_y,veld	164378 kNm	σ_top flange	139,2	compression	355	0,39
N_deck	32827 kN					
		σ_bottom flange	196,9	tension	355	0,55
M_y,side span	111377 kNm	σ_top flange	206,5	tension	355	0,58
		σ_bottom flange	329,5	compression	355	0,93
Maatgevend load case 1						
M_y,support	193096 kNm	σ_top flange	465,0	tension	355	1,31
		σ_bottom flange	783,0	compression	355	2,21
M_y, endsupport	0	σ_top flange	15,0	tension	355	0,04
		σ_bottom flange	15,0	compression	355	0,04

Cable
maatgevende load load case 2

		fu	
N_cable	21547 kN	1770	0,91
d	160 mm		
A cable	20106,19 mm2		

$$\frac{F_{Ed}}{F_{Rd}} = \frac{21547e3}{\frac{F_{uk}}{1.5\gamma_R}} = \frac{21547e3}{\frac{f_u * A_{main\_cable}}{1.5}} = \frac{21547e+3}{\frac{1770 * 20106}{1.5}} \leq 1$$

Hangers
maatgevende load case 1

		fu	
N_hanger	1254 kN	1770	0,45
d	55 mm		
A hanger	2375,829 mm2		

Pylon

M_Ed,y =	25040 kNm	Top flange	238,5771	compression	355	0,67
N_Ed,y =	28208 kN					
		Bottom flange	40,02047	compression	355	0,11

Toetsing stijfheid

Girder
maatgevend loadcase 2

		max	
deflection midspan	422 mm	430	0,98

pylon
maatgevend load case 2

displacement pylon	121 mm	170	0,71

Appendix 8a Erection of Konohana Bridge

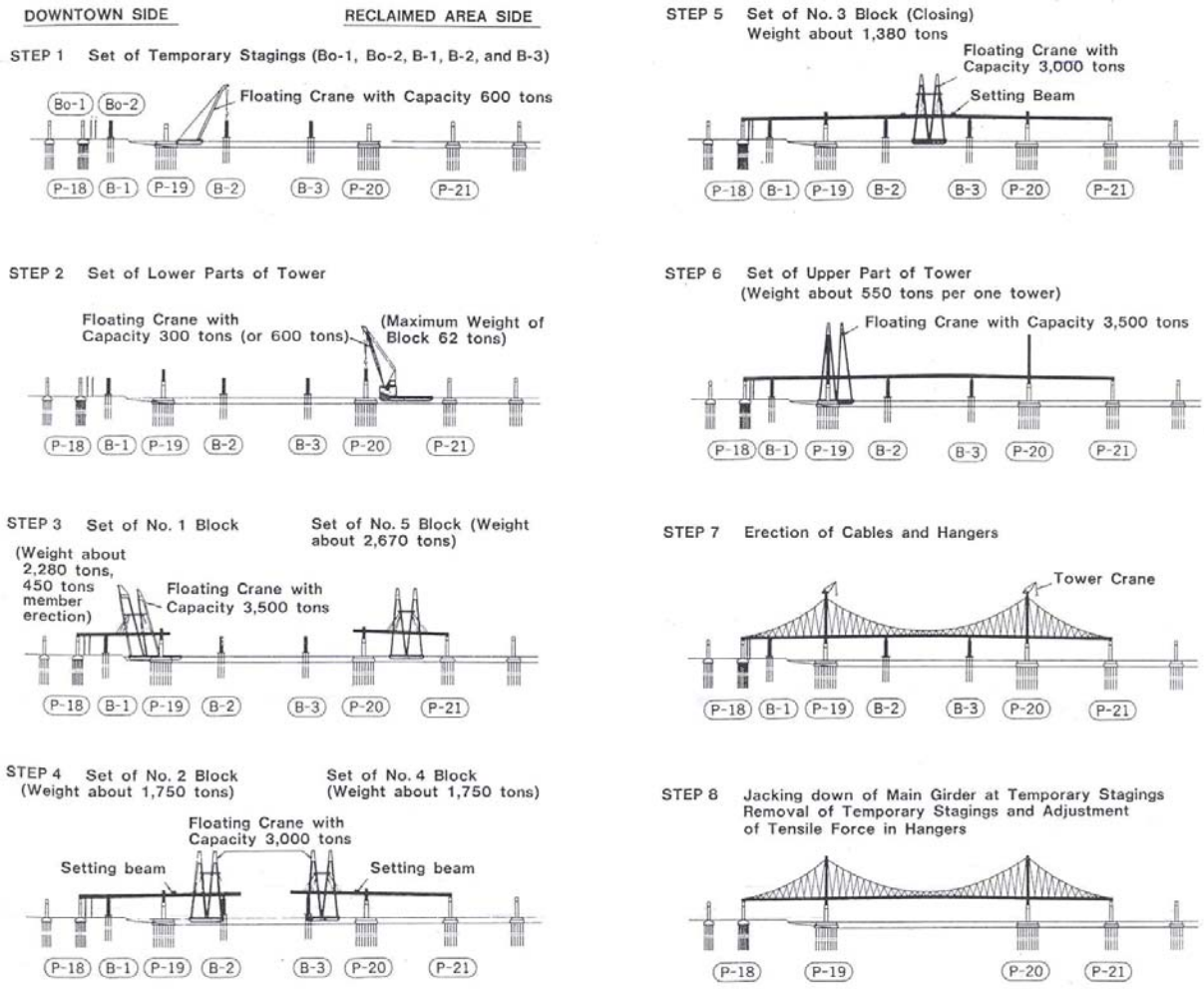

Appendix 8b Erection of Yeoungjong Grand Bridge

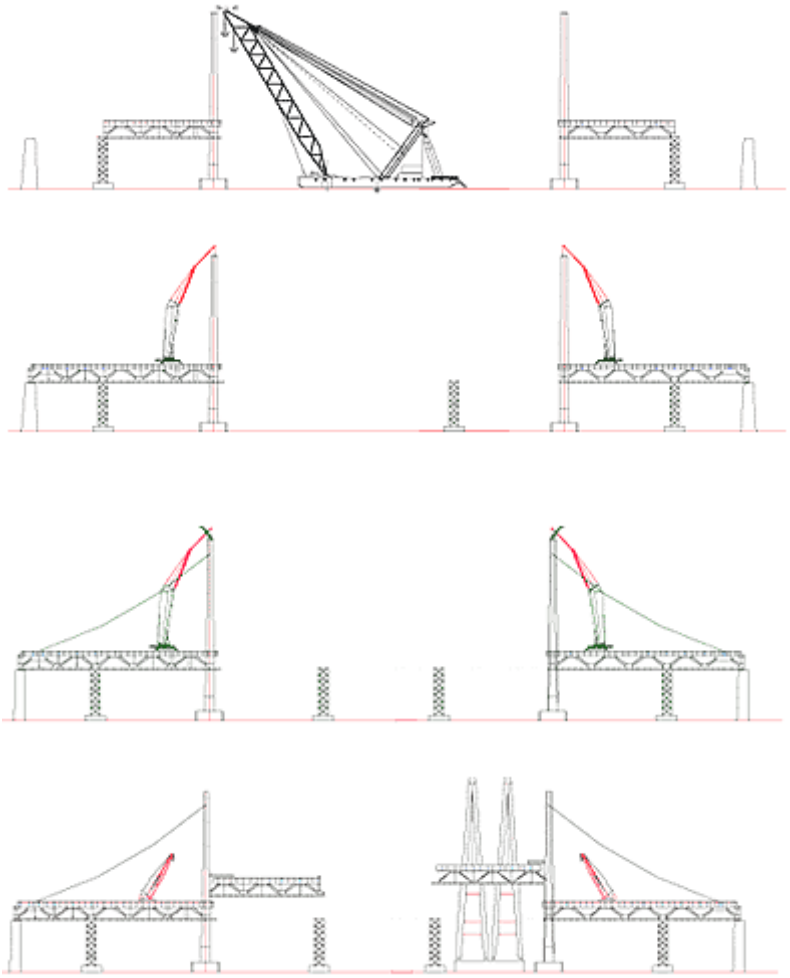

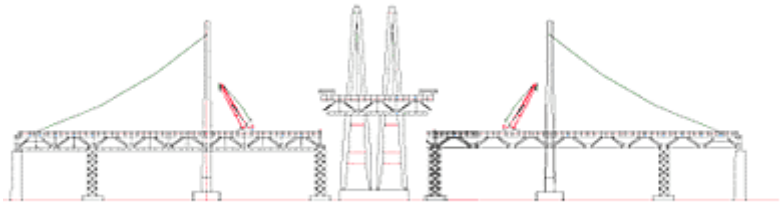

■BLOCK 분할 현황

구분		구간	연장(m)	중량(ton)	가설완료	비고
현수교 (550M)	G1	W2-B1	46	2,563	99-06-07	F/C
	G2	B1-W1	83	3,072	99-02-25	F/C
	G3	W1-B2	75	2,686	99-07-09	F/C
	G4	B2-B3	67	2,429	99-08-12	F/C(폐합블록)
	G5	B3-B4	75	2,600	99-08-11	F/C
	G6	B4-E1	75	2,685	99-07-11	F/C
	G7	E1-B5	83	3,072	99-03-02	F/C
	G8	B5-E2	46	2,563	99-06-09	F/C

Appendix 8c Erection of Nescio bridge